TARGETED METABOLOMICS REVEALED A KEY METABOLIC REPROGRAMMING IN CHOLESTEROL BIOSYNTHESIS PATHWAY UPON PTEN RE-EXPRESSION IN PTEN-NULL, METASTATIC AND CASTRATION-RESISTANT PROSTATE CANCER

A THESIS SUBMITTED TO

THE GRADUATE SCHOOL OF ENGINEERING AND SCIENCE

OF BILKENT UNIVERSITY

IN PARTIAL FULFILLMENT OF THE REQUIREMENTS FOR

THE DEGREE OF

MASTER OF SCIENCE

IN

MOLECULAR BIOLOGY AND GENETICS

By

Taha Buğra Güngül

June 2022

TARGETED METABOLOMICS REVEALED A KEY METABOLIC REPROGRAMMING IN CHOLESTEROL BIOSYNTHESIS PATHWAY UPON PTEN RE-EXPRESSION IN PTEN-NULL, METASTATIC AND CASTRATION-RESISTANT PROSTATE CANCER

By Taha Buğra Güngül
June 2022

We certify that we have read this thesis and that in our opinion it is fully adequate, in scope and in quality, as a thesis for the degree of Master of Science.

Asst. Prof. Onur Çizmecioğlu (Advisor)

Assoc. Prof. Özlen Konu Karakayalı

Assoc. Prof. Gülistan Meşe-Özçivici

Approved for the Graduate School of Engineering and Science:

Ezhan Karaşan

Director of the Graduate School

ABSTRACT

TARGETED METABOLOMICS
REVEALED A KEY METABOLIC REPROGRAMMING IN
CHOLESTEROL BIOSYNTHESIS PATHWAY
UPON PTEN RE-EXPRESSION IN PTEN-NULL, METASTATIC AND CASTRATION-RESISTANT PROSTATE CANCER

Taha Buğra Güngül

M.S. in Molecular Biology and Genetics

Advisor: Asst. Prof. Onur Çizmecioğlu

June 2022

Prostate cancer is the second most diagnosed type of cancer in males worldwide. Androgen signaling is a main driver of prostate cancers progression and androgen-deprivation therapies (ADT) are remained to be main treatment for preventing progression of the disease. Although ADT is effective at the first line and prolongs overall survival of the patients, eventually disease is recurred, develop resistance to castration and grow in an androgen-independent state, which completely eliminate ADT option. Metastatic and castration-resistant prostate cancers (mCPRC) are the most fatal type of the disease without any effective treatments currently, which is why, molecular drivers that contribute to emergence of castration-resistant phenotype need to be elucidated in order to develop efficient therapeutics against them. Metabolic reprogramming is one of the crucial hallmarks of cancer and loss-of tumor suppressor PTEN is an early and a frequent genetic alteration in prostate cancers, which leads to a hyperactivation of PI3K/Akt/mTOR axis and affects cellular metabolism widely. In this study, we aimed to unveil changes in the metabolome of C4-2 cells which are the type of mCRPC with a PTEN-null genetic background

and target metabolic vulnerabilities of these cells. In order to address the question, we employed high-throughput metabolomics assay and revealed changes on metabolome of the cells upon re-expression of PTEN. We found that PTEN re-expression impaired the sphingolipid and cholesterol biosynthesis pathways of C4-2 cells. Upon PTEN re-expression, metabolism of C4-2 cells had tendency to increase the level of anti-survival metabolite; ceramide, and decrease pro-survival metabolite; sphingosine-1-phosphate. In addition to that, PTEN re-expression significantly impaired and downregulated the cholesterol metabolism of these cells. To target these metabolic vulnerabilities, we combined inhibitors of sphingolipid and cholesterol metabolisms with FDA-approved androgen antagonist, MDV3100, to determine possible synergistic effects from the combination of drugs. MDV3100 single treatment had only cytostatic effect on viability of C4-2 cells and combination of simvastatin, cholesterol metabolism inhibitor, with MDV3100 significantly decreased the cellular viability and resulted in significant synergistic effects in inhibiting the growth of C4-2 cells. Thus targeting cholesterol pathway in combination with androgen-deprivation therapies would be a promising approach to develop new combinatorial therapies and combat mCRPC.

Keywords: Prostate cancer, mCRPC, PTEN-null, PI3K, metabolic reprogramming, sphingolipid metabolism, cholesterol metabolism, simvastatin, MDV3100

ÖZET

HEDEFLİ METABOLOMİKS YAKLAŞIMI İLE PTEN-NOKSAN, METASTATİK VE KASTRASYONA-DIRENÇLI PROSTAT KANSERİNDE PTEN'IN YENİDEN İFADESİ SONUCU KOLESTEROL METABOLİZMASINDAKİ ÖNEMLİ BIR METABOLİK YENİDEN PROGRAMLAMANIN AÇIĞA ÇIKARILMASI

Taha Buğra Güngül

Moleküler Biyoloji ve Genetik, Yüksek Lisans

Tez Danışmanı: Asst. Prof. Onur Çizmecioğlu

Haziran 2022

Prostat kanseri, dünya çapında erkeklerde en sık teşhis edilen ikinci kanser türüdür. Androjen sinyali, prostat kanserinin ilerlemesinde ana faktördür ve androjen-deprivasyon terapileri (ADT), hastalığın ilerlemesini önlemek için ana tedavi yöntemlerindendir. ADT hastaların genel sağkalımını uzatsa da, hastalık tekrarlar, kastrasyona direnç geliştirir ve ADT tedavi seçeneğini ortadan kaldıran androjen sinyalinden bağımsız olarak büyür. Metastatik ve kastrasyona dirençli prostat kanserleri (mCPRC), şu anda herhangi bir etkili tedavi olmaksızın hastalığın en ölümcül tipidir, bu nedenle, buna karşı etkili terapötikler geliştirmek için kastrasyona dirençli fenotipe katkıda bulunan moleküler faktörlerin açığa kavuşturulması gerekmektedir. Metabolik yeniden programlama, kanserin önemli özelliklerinden biridir ve PTEN kaybı, prostat kanserlerinde erken ve sık görülen bir genetik değişikliktir. PTEN kaybı PI3K/Akt/mTOR ekseninin hiperaktivasyonuna yol açar ve hücresel metabolizmayı geniş ölçüde etkiler. Bu çalışmada, PTEN-noksan genetik yapıya sahip mCRPC tipi C4-2 hücrelerinin metabolomlarındaki değişiklikleri ortaya çıkarmayı ve bu hücrelerin metabolik zafiyetlerini hedeflemeyi amaçladık. Soruyu ele

almak için, yüksek verimli metabolomik tahlil kullandık ve PTEN'in yeniden ekspresyonu üzerine hücrelerin metabolomundaki değişiklikleri ortaya çıkardık. PTEN'in yeniden ifadesinin, C4-2 hücrelerinin sfingolipid ve kolesterol biyosentez yollarını etkilediğini bulduk. C4-2 hücrelerinde PTEN'in yeniden ifadesi metabolizma üzerinde, apoptoz-indükleyici, seramid seviyesini artırma ve apoptoz-baskılayıcı metabolit Sfingosin-1-Fosfat'ı azaltma eğilimi gösterdiğini açığa çıkardık. Buna ek olarak, PTEN'in yeniden ifadesi, bu hücrelerde kolesterol sentezini önemli ölçüde azalttığını gördük. Daha sonra, ilaç kombinasyonundan kaynaklanan olası sinerjistik etkileri belirlemek için sfingolipid ve kolesterol metabolizması inhibitörlerini, FDA onaylı androjen antagonisti MDV3100 ile birleştirdik. MDV3100'ün tekli tedavisi, C4-2 hücrelerinin canlılığı üzerinde sitostatik etkiye sahipti ve kolesterol metabolizması inhibitörü olan simvastatinin MDV3100 ile kombinasyonu, hücresel canlılığı önemli ölçüde azalttı ve C4-2 hücrelerinin büyümesini inhibe etmede önemli sinerjistik etkilerle sonuçlandı. Bu nedenle, androjen-deprivasyon terapileri ile kombinasyon halinde kolesterol yolunu hedeflemek, yeni kombinatoryal terapiler geliştirmek ve mCRPC ile mücadele etmek için umut verici bir yaklaşım olacaktır.

Anahtar Sözcükler: Prostat kanseri, mCRPC, PTEN-noksan, PI3K, metabolik yeniden programlama, sfingolipid metabolizması, kolesterol metabolizması, simvastatin, MDV3100

To my nephews; Çınar & Tuna…

To the hope of all cancer patients…

ACKNOWLEDGEMENTS

I would to express my deepest and sincere gratitude to my advisor Asst. Prof. Onur Çizmecioğlu, who has been always kind, understanding and supporting. Beside his precious mentoring throughout the study, he was also a true role-model for me. This two-year of my master's period was full of joy thanks to him. It was a real pleasure and honor to learn from him and work under his wonderful guidance.

I would like to thank our collaboration group Asst. Prof. Berat Haznedaroğlu and his team at Boğaziçi University for mass spectrophotometry analysis of metabolomics experiment.

I would like to thank Assoc. Prof. Gülistan Meşe-Özçivici for her supports and guidance since my Bachelor's. She has milestone impacts on my education and it was a privilege to work with her during my Bachelor's period. I also would like thank Prof. Dr. Ferda Soyer for her guidance and supports in shaping my future career during my Bachelor's period. Also, I would like to express my gratitude to Asst. Prof. Deniz Uğur who supervised me during her PhD years and she taught me most of the wet-lab experiments that I am able to perform now. I would like to thank Assoc. Prof. Ali D. Güler for his helps and supports to plan my future education.

I would like to thank my colleagues at Çizmecioğlu Lab and Bilkent MBG family for their fun friendships and helps. I would like to offer my deepest appreciation to my project-mate and lifelong friend Irmak Kaysudu. She is an amazing friend one can could ever have. She has been always supportive and cheerful. I would like to thank for her valuable contributions, critical discussions and belief to this study.

I would like to thank my friends Zehra Elif Günyüz and Ahmet Kasapçopur. They were always available and willing to help me whenever I needed them. Their contributions and friendships are indispensable for me. I also would like to thank Ayşe Bengisu Gelmez, Melisa Cetinkaya and Olcay Uraz Aslan for their friendships and supports. I am so lucky to have them in my life.

Additionally, I would like to thank my dearest friends Kübra Çalısır and Serdar Baysal for their friendships and contributions. We have spent amazing days together filled with fun and these are the days that I will always remember happily. It is very fortunate to have caring and lovely friends as them. Also, I would like to thank Sultan Turan for her fun conversations and being always caring. She was always eager to help me whenever I needed her.

I would like to express my respect and gratitude to my mom Sema Güngül, my sisters Şule Hubup and Şeyma Şahin, and my brothers-in-law Cemal Hubup and Hakan Şahin without them I would not be achieving what I have done so far. They are always super motivative and supportive. I am the luckiest person to have this lovely family.

Finally, I would like to thank TUBITAK for BIDEB-2210/A scholarship and this project is funded by TUBITAK grant project with a project number 118Z976.

Table of Contents

LIST OF FIGURES

LIST OF TABLES

ABBREVIATIONS

PCa Prostate Cancer

PTEN Phosphatase and Tensin Homolog

AR Androgen Receptor

mCRPC Metastatic and Castration Resistant Prostate Cancer

ADT Androgen Deprivation Therapy

PI3K Phosphoinositide-3-Kinase

AKT Serine/Theronine Kinase

mTOR Mammalian Target of Rapamycin

MVD Mevalonate-5-pyrophosphate Decarboxylase

PH Pleckstrin Homology

PIP_3 Phosphatidylinositol-3,4,5-triphosphate

SREBP-2 Sterol Regulatory Element-Binding Protein-2

SQLE Squalene Epoxidase

SPT Serine Palmitoyltransferase

Des1 Dihydroceramide desaturase

S1P Sphingosine-1-Phosphate

BTK Bruton's Tyrosine Kinase

GFP Green Fluorescent Protein

CE Cholesterol Ester

PC Phosphatidylcholines

PC-O Glycerophosphocholines

SM Sphingomyelins

ASAH 1 N-acylsphingosine amidohydrolase 1

Cerk Ceramide Kinase

CHAPTER 1

1. INTRODUCTION

1.1. Prostate Cancer

The prostate gland is a reproductive male organ which is responsible for production of fluid that is necessary for nourishment and transportation of sperm. The cells residing in the prostate gland might transform themselves into tumorigenic phenotypes, constitute tumors and results in prostate cancer, especially in the mid-to-late ages of men [1]. Prostate cancer (PCa) is the second leading cause of cancer-related death among males after lung cancer. Every year, approximately 1.3 million men are diagnosed with this disease, and it causes more than 350.000 deaths annually[2]. There are many factors associated with the oncogenesis of PCa including genetic background, accumulation of somatic gene mutations, inherited susceptibility of germline and environmental factors. PCa cells that are localized mostly harbor many foci that have different kinds of alterations in their genetic makeup, along with their capacity for metastasis and resistance to treatments [3]. Although there are developments in PCa treatment, the ability of PCa cells to metastasize and develop resistance mechanisms makes the disease incurable [4].

1.1.1. Genomic Alterations in Prostate Cancer

Typically, in early PCa large-scale rearrangements in chromosome structures and copy number alterations are more common than single nucleotide polymorphisms . In early stages of the disease, fusion of TMPRSS2-ERG genes, loss-of-function mutations, and gain-of-function mutations in SPOP and FOXA1 genes are observable respectively. Large chromosomal deletions in PTEN and mutations in TP53 are found in 10-20% of patients with localized PCa and this rate increases to

more than 50% in patients having advanced PCa [3]. Almost every third PCa has genetic alterations and instability, including changes in copy number, gene hypermutations in localized regions, chromosome shattering, structural rearrangements of genes and all these alterations result in relapse of the disease [3,4]. Additionally, combination of genetic instability and some factors in the tumor microenvironment such as intratumoral hypoxia makes disease highly aggressive and results in relapse following local treatment [3].

1.1.2. Androgen Signaling in Prostate Cancer

Androgen is a steroid hormone which is responsible for regulation, maintenance and development of male characteristics. Androgen and androgen receptor (AR) mediates androgen signaling which has a key role in PCa's pathogenesis. AR transcription factor is a member of the nuclear receptor superfamily and its structure is similar to that of estrogen receptor and progesterone receptors [5]. It has a ligand-binding domain so that testosterone and dihydrotestosterone (DHT) can bind it in the cytoplasm, resulting in a change in the conformation of AR and releasing it from its inhibitory heat-shock proteins. Following ligand binding, translocation of AR into the nucleolus and dimer formation occurs. Then, through its DNA-binding domain (DBD), in the chromatin, AR binds to androgen-response elements (AREs). As a result of this binding, chromatin remodeling complexes, coactivators and finally RNA polymerase II are recruited. After recruitment of all these proteins, chromatin is remodeled and transcription initiation factors are assembled **(Figure 1.1)** [5,6].
There are many target genes in the downstream of the androgen-response element that have roles in many cellular events including proliferation, differentiation, migration and apoptosis [6].

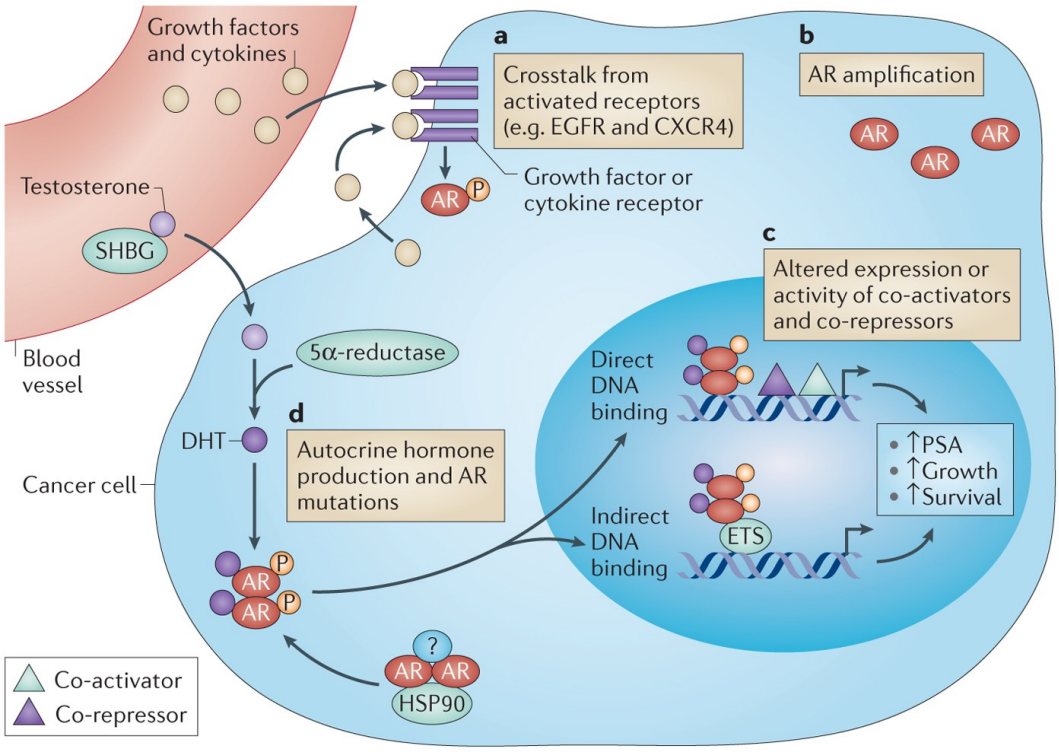

Figure 1.1. Androgen receptor signaling in CRPCs. AKR1C3 catalyzes the synthesis of testosterone and DHT and binding of these ligands to AR initiates AR signaling. After ligand binding, AR is translocated to nucleus where it interacts with AREs in the chromatin and transcription of target genes are initiated [88].

In healthy prostate, secretory proteins such as prostate-specific antigen (PSA) are upregulated by AR and AR found in stromal cells, which are the surrounding epithelial cells of prostate tissue, promote the growth of prostate. However, in prostate cancer, due to accumulation of different mutations, AR acquires novel activities including PSA synthesis, controlling lipid metabolism, inducing growth and many other functions [7]. MDV3100 (Enzalutamide) is an FDA-approved oral drug that is used in treatment of advanced PCa and AR signaling is targeted by enzalutamide in three different steps. It can inhibit binding interaction between androgen and androgen receptors,

prevent translocation of AR into nucleus after ligand binding and in the nucleus also it can prevent binding of AR to chromatin. However, high heterogenicity of prostate cancer allows it to develop complex and multiple resistance mechanisms against treatments and cause transformation of PCa into Castration-Resistant Prostate Cancer (CRPC) [7,8].

1.1.3. Castration-Resistant Prostate Cancer (CRPC)

So far, the most effective treatment method for metastatic PCa is androgen deprivation therapy (ADT) which lowers the androgen level in male body by either medicines such as drug called Enzalutamide or surgery. However, recurrence of PCa is very frequent after depletion of androgen, PCa that is recurred after androgen deprivation therapy is known as castration-resistant prostate cancer (CRPC) [8,9]. The average time of development of CRPC after ADT treatments is usually between 2-3 years. Interestingly, despite the fact that systemic androgen levels are significantly reduced following ADT, CRPCs still maintain AR signaling [10]. There are many studies which aim to reveal this sustained AR signaling in CRPC and they have shown that overexpression/amplification of AR in CRPC is one of the main reasons for ADT failure. Also, AR antagonists that are used in ADT, induces mutations in AR and these mutant ARs get activated by additional ligands which cannot activate wild-type AR. Splice variants of AR (AR-Vs) have been identified in prostate cancer cell lines as well as in CRPC patient-derived tumors which contribute to the development of CRPC [9,11]. In addition to mutations and splice variants, other important signaling pathways have crosstalk and feedback regulation with AR signaling in CRPC such as PI3K/Akt/mTOR pathway [11]. Other mechanistic explanations for continued AR signaling in CRPC is sufficiency of reduced level of testosterone and DHT in the prostate tissue for AR activation and *de novo* androgen synthesis by using cholesterol precursor in the prostate

tissue. All these mechanisms cause PCa to transform into CRPC, which eliminate treatment options and result in a dramatically reduced survival rate [12].

1.2. Phosphoinositide 3-Kinase (PI3K) Signaling Pathway

Phosphoinostide-3-kinase (PI3K) signaling pathway have wide range of functions in metabolism, proliferation, growth and survival of cells. Activation of this highly conserved pathway is a multi-step process and as its name implies, it is activated by PI3Ks [13]. These PI3Ks are associated with plasma membrane and they function as lipid kinases. They are classified into three groups according to their structure which are Class I, Class II and Class III PI3Ks **(Figure 1.2)** [14]. Class I PI3Ks are the most-studied and characterized class and they are composed of two subgroups which are Class IA and Class IB. p110α, p110β, and p110δ belong to Class IA and p110γ belongs to Class IB. Amongst all classes, Class II PI3Ks, which are composed of PI3K-C2α, PI3K-C2β, PI3K-C2γ, is the least understood one. The last class of PI3Ks, Class III, has only one member which is vacuolar protein sorting 34 (Vps34) and this is the only type of PI3Ks that is expressed in all eukaryotic organisms [14,15]. Regulatory subunit and catalytic subunit of Class I PI3Ks form heterodimers in cells. Regulatory subunit and catalytic subunit of Class I PI3Ks form heterodimers in cells. They can be activated by G protein-coupled receptors (GPCRs), Receptor Tyrosine Kinases (RTKs) or RAS. Binding of growth factors to GPCRs or RTKs activates these receptors and this activation allows interaction of regulatory subunit of PI3K with intracellular part of the receptor and then catalytic subunit is activated [16].

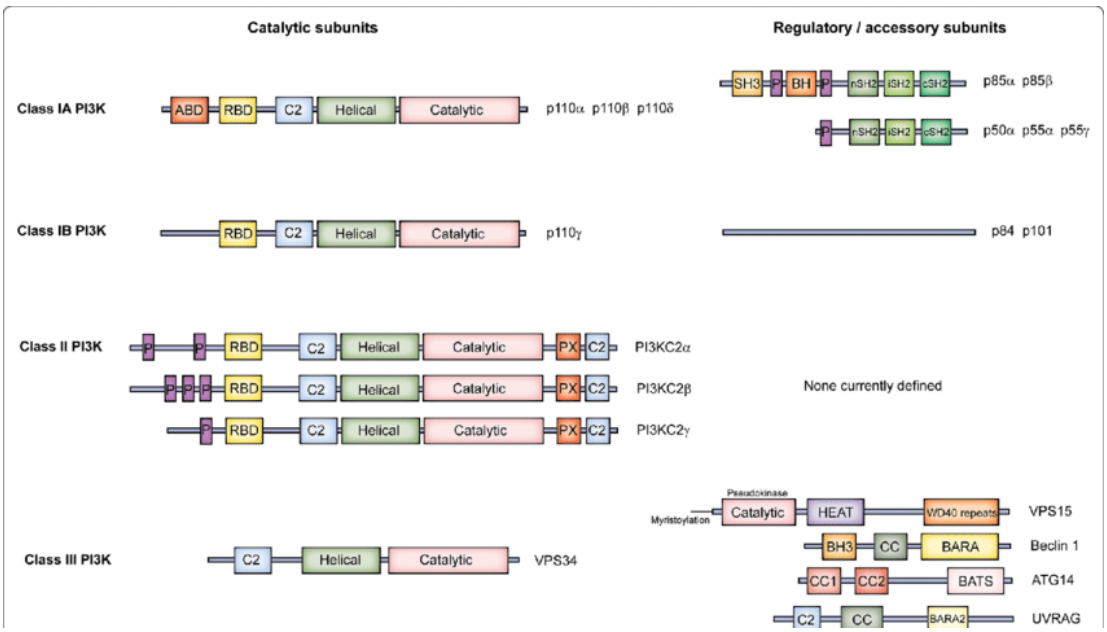

Figure 1.2. **Catalytic and regulatory subunits of different PI3K classes.** Three classes of PI3Ks exist which are Class IA, Class IB, Class II and Class III PI3Ks. Class IA PI3Ks are consisted of p110α, p110β, and p110δ isoforms; Class IB PI3K is consisted of only p110γ; Class II PI3Ks are consisted of PI3K-C2α, PI3K-C2β, PI3K-C2γ isoforms and Class III PI3K is consisted of Vps34 isoform [14].

Activated PI3Ks phosphorylate membrane-bound lipid phosphatidylinositol (4,5)-biphosphate (PIP_2) and turn it into a crucial second-messenger phosphatidylinositol (3,4,5)-triphosphate (PIP_3) and PIP_3 is considered as a main mediator of the activity of Class I PI3Ks [16,17]. It is serves as a docking site for proteins that have pleckstrin homology (PH) domain, including Protein Kinase B (PKB/Akt) and Phosphoinositide-dependent kinase-1 (PDK1). After binding of PDK1 to PIP_3 on the cellular membrane, Akt is phosphorylated by PDK1 at its T308 position and this leads to partial activation of Akt. Second phosphorylation of Akt is performed by mTOR Complex 2 (mTORC2) at S473 position and this leads to the fully activation of Akt **Figure (1.3)** [16,18].

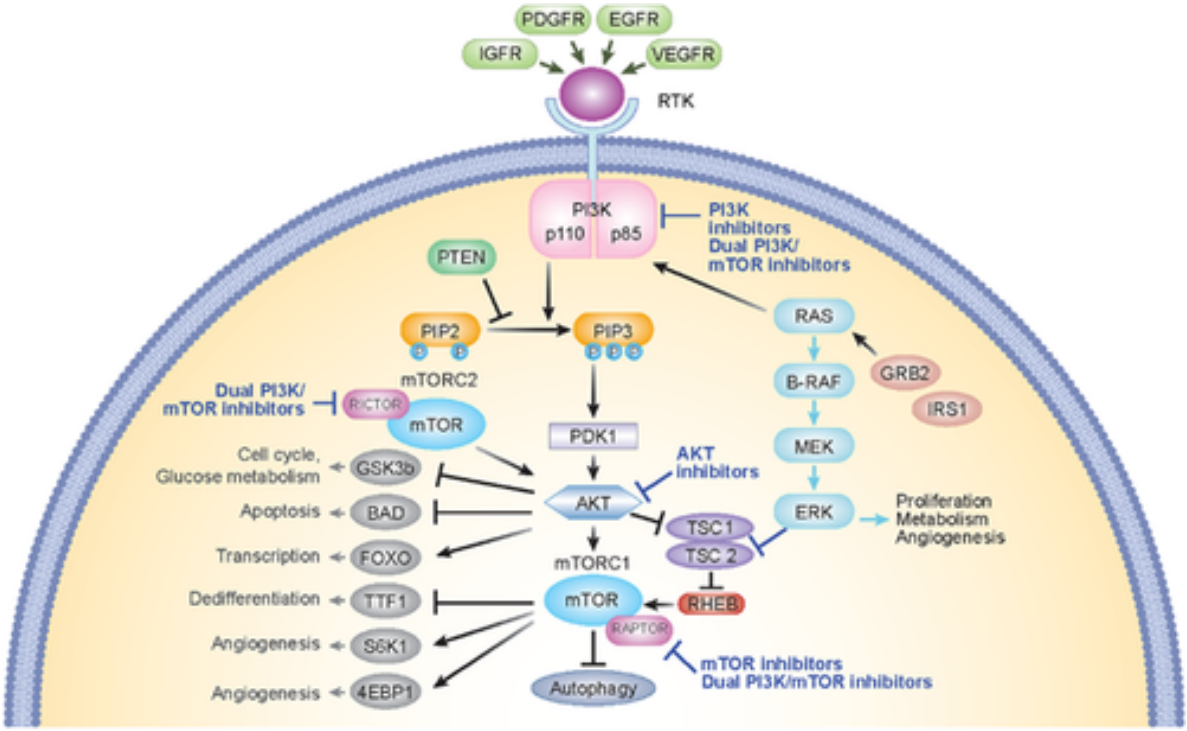

Figure 1.3. PI3K/Akt/mTOR Signaling Axis. PI3K pathway is activated binding of ligands to either GPCRs or RTKs. Once activated PI3Ks initiate signaling through secondary messenger PIP3. Akt is the major downstream effector protein of the PI3K pathway and it initiates the downstream signaling events which ends up with activation of proteins responsible for cell proliferation, growth and metabolism [91].

Once activated, Akt acts as a downstream effector protein of PI3Ks and it is able to initiate wide range of cellular signaling and responses which control diverse events in cells including cell growth, death, metabolism and motility [17]. Fully activated Akt can activate mTOR Complex 1 (mTORC1) and in turn, activated mTORC1 can activate Ribosomal protein S6 kinase beta-1 (S6K1) and inhibit 4E (eIF4E)-binding protein 1 (4EBP1), which in turn results in initiation of protein synthesis and cell growth [16,18]. Proapoptotic proteins including Bax and BID proteins

are negatively regulated by Akt so that PI3K-Akt axis promotes cell survival [19]. PI3K pathway is negatively controlled by its antagonist named as Phosphatase and Tensin Homolog (PTEN) [13].

1.2.1. Phosphatase and Tensin Homolog (PTEN)

PTEN is a potent and haploinsufficient tumor suppressor and loss of function mutations in PTEN gene, such as loss of function mutation, is a very frequent event in most of the cancers [20]. It regulates a variety of biological functions in the cell such as cell survival, proliferation, metabolism, migration and also it maintains the stability of genome. PTEN is a dual-phosphatase which can dephosphorylate its lipid and protein substrates and all biological functions of PTEN are attributed to both its phosphatase function and its phosphatase-independent function [21]. Changes in the expression level and activities of PTEN such as subtle decrease in its expression is enough to make cells susceptible to gain tumorigenic phenotypes and also it expedites tumor progression [22]. Thus, especially in past few decades research studies trying to understand PTEN biology have gained more attention and revealing the regulations and functions of PTEN are considered as ways to develop new therapeutics against cancer [20].

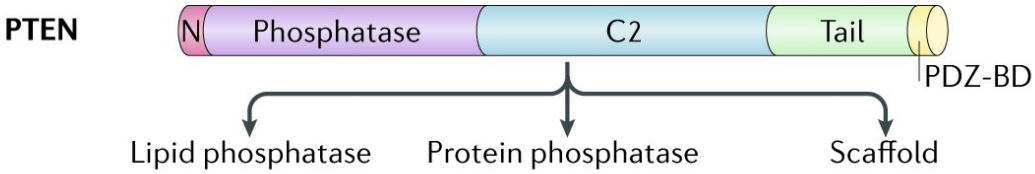

Figure 1.4. PTEN structure and its domains. PTEN perform its tumor-suppressor and other biological functions in phosphatase dependent or scaffold (phosphatase-independent) ways. It has phosphatase domain, C2 domain, C-terminal tail, PIP_2-binding domain and PDZ domain [20].

PTEN has five domains which are PIP_2-binding domain (PBD), C2 domains which is for membrane or lipid binding, a phosphatase domain which perform its catalytic function, C terminal tail which has motifs of Thr, Ser, Pro, Glu (PEST) sequences and PDZ domain **(Figure 1.4)** [23]. PIP_3 is one of the major substrates of PTEN. It is dephosphorylated by PTEN and converted back to PIP_2 by which PI3K-AKT-mTOR signaling is downregulated [24]. Lipid phosphatase function of PTEN in cells are is more prominent than its protein phosphatase function but it can also dephosphorylate its protein substrates at Tyr, Thr and Ser residues *in vitro*, which is why PTEN is known as dual-phosphatase [25]. Besides its phosphatase function, PTEN has crucial non-canonical functions, for example; it has been revealed that in the nucleus PTEN functions as scaffold protein which has influences on protection of genomic stability and regulation of cell cycle [24,25]. Additionally, it has been shown by several research groups that more aggressive cancers exhibit no PTEN or significantly downregulated level of PTEN which indicates nuclear functions of PTEN also important for its tumor suppressor roles in the cell [26]. PTEN is located at position 10q23.3 in human chromosome and this locus is highly prone to aberrant alterations of genetic sequence in cancer cells [27]. Mutations in the PTEN gene is very frequent in many cancer types including prostate cancer with 20% frequency, breast cancer and glioblastoma and these mutations include point mutations, heterozygous or homozygous large chromosomal deletions of PTEN gene [27,28]. Cowden disease (CD) is one of the well-known examples of PTEN hamartoma tumor syndromes (PHTS) which is caused by germline mutations of PTEN [29]. So far, number of cancer-associated mutations on PTEN gene have been identified such as G129E and Y138L point mutations which diminish the lipid phosphatase and protein phosphatase activities of PTEN respectively. Additionally, C124S point mutation completely abolishes the both protein and lipid phosphatase functions of PTEN and makes PTEN catalytically inactive [30]. Identification of these

mutations have allowed and contributed to the research studies that aim to characterize and understand PTEN lipid and protein functions independently in biological processes [28,30].

1.2.1.1. PTEN and Cell Metabolism

Metabolic reprogramming is one of the crucial hallmarks of cancer cells by which rapid cell proliferation and growth are sustained [31]. One of the well-known examples of this metabolic reprogramming is Warburg effect in which cancer cells skip oxidative phosphorylation step and produce energy from glycolysis step, independent of the presence of oxygen in the environment. With the help of Warburg effect, cancer cells produce high quantity of intermediates that are required for synthesis of macromolecules to support their rapid proliferation and growth [32]. This metabolic reprogramming is mostly due to oncogenic activation or mutations in tumor suppressor genes. In this context, PI3K-AKT-mTOR pathway activation as a result of some mutations in key components of the pathway, such as gain-of function mutations in PI3Ks or loss of PTEN promotes this metabolic reprogramming [33]. Loss of PTEN has a significant impact on metabolism of cancer cells due to overactivation of PI3K pathway. For example, 4EBP1 and p70S6 proteins expression are upregulated when PTEN is deficient and this results in elevated protein synthesis [34]. Also, PI3K-AKT-mTOR axis regulates the metabolic responses coming from insulin signaling. Loss of PTEN cause hypersensitivity to insulin and as a result uptake of glucose is increased [32]. Moreover, sterol regulatory element-binding proteins (SREBPs) control the enzymes required for biosynthesis of lipids and SREBPs expression are increased when PI3K-Akt pathway is overactivated which results in accumulation of lipids to fuel fast growth of cancer cells [35]. Recent studies demonstrated that in mice, elevation of PTEN expression systemically limits the rate of glycolysis and oxidative phosphorylation increases which shows that elevation in PTEN

level shows anti-Warburg effect *in vivo*. Healthy metabolism was observed in these mice and they were protected from risk of cancer and some metabolic disorders. All these observations align with PTEN's tumor suppressor role in the cell [36].

Frequency of PTEN deletion in human PCa is very high and loss of PTEN induce crucial carcinogenesis events in these cancers including metabolic reprogramming [37]. There are many metabolic changes in PCa that are associated with loss of PTEN such as increase in the level of metabolites related with glutaminolysis and glycolysis or increase in the de novo synthesis of fatty acids [38]. Hence, loss of PTEN induces severe changes in the cells associated with carcinogenesis and amongst all these changes metabolic reprogramming is key for cancer cells. Hence, understanding the metabolic changes and vulnerabilities due to loss of PTEN gene is considered as a way to target cancer cells and develop new therapeutics against them [39].

1.3. Sphingolipid Metabolism

Sphingolipids are class of eukaryotic lipids characterized by their eighteen carbon length backbones with sphingoid base and amino-alcohol groups [40]. They are one of the constituent lipids of cell membrane with diverse biological functions in the cells from proliferation and growth to migration and metastasis [41]. Serine and palmitoyl CoA condensation is the first step in sphingolipids biosynthesis and this reaction is catalyzed by an enzyme named serine palmitoyltransferase (SPT) which is also a rate-limiting enzyme [42]. This condensation reaction leads to sphinganine formation and by acylation reaction dihydroceramide is formed from sphinganine by the action of sphingosine N-acyltransferase (CERS) enzyme. Through desaturation reactions catalyzed by dihydroceramide desaturase (Des1), dihydroceramide is turned into ceramide [43]. All these reactions from serine and palmitoyl CoA to ceramide are carried out in

the endoplasmic reticulum and following reactions are carried out in the Golgi complex, once ceramide is produced and transported **(Figure 1.5)** [44].

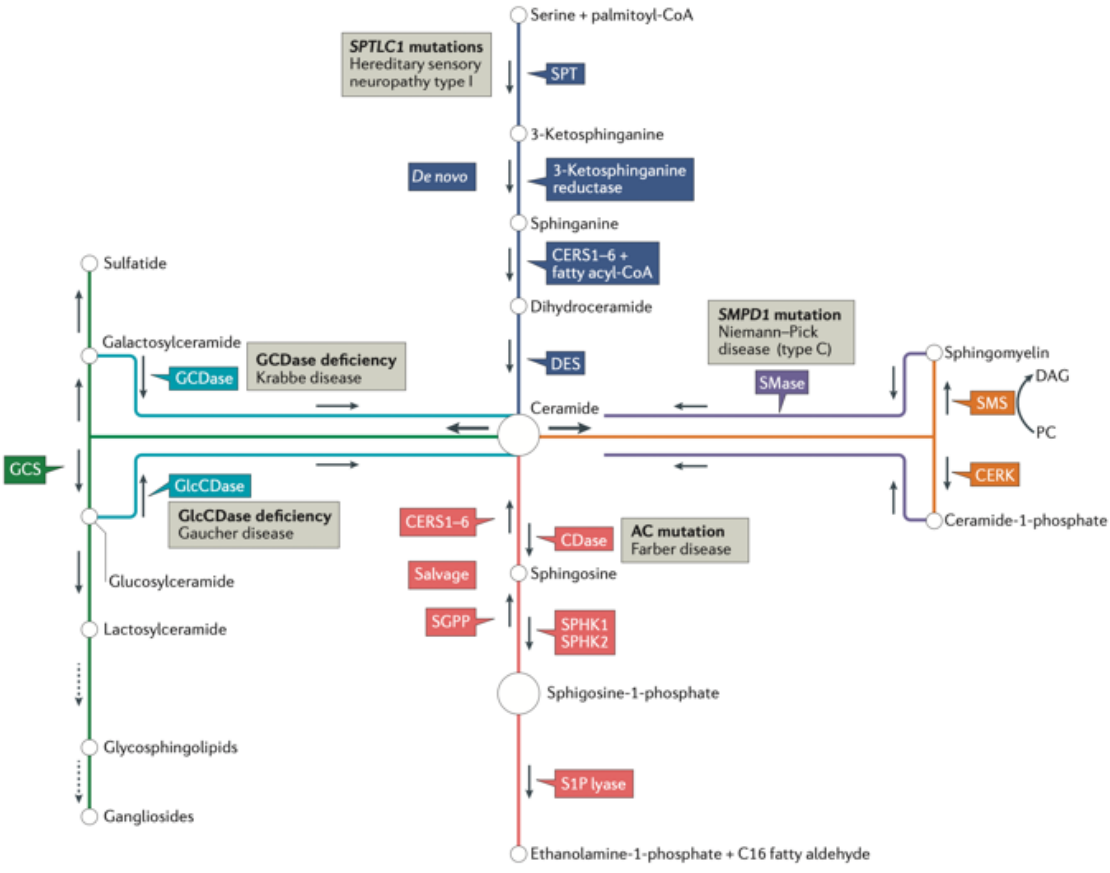

Figure 1.5. Sphingolipid biosynthesis pathway and key enzymes of the pathway [41].

Ceramide is used as substrate in the Golgi complex for further reactions to synthesize complex sphingolipids, by adding variety of head of groups to ceramide, such as glycosphingolipids. Once these complex sphingolipids are formed, they are transported to different parts of the cell by vesicular transport where they perform their distinct functions [45].

1.3.1. Sphingolipids in Cancer Metabolism

Sphingolipids have broad range of functions in cancers by affecting cell survival, death and also it is known that they might contribute to the development of resistance mechanisms against cancer therapies. They are thought to have a context-dependent roles in cancer biology [46]. For instance, it has been implicated that a central intermediate of sphingolipid biosynthesis, a ceramide, have anti-tumorigenic functions such as antiproliferative effects on cancer cells including breast, head and neck and prostate cancers. On the other hand, sphingosine-1-phosphate (S1P) which is known as a signaling sphingolipid has some pro-tumorigenic functions by promoting survival of cancer cells including prostate, ovarian and breast cancers and invasion, angiogenesis as well as chemotherapy resistance [46,47]. Thus, recent research studies have been aiming to develop some therapies against cancer by increasing synthesis of ceramide and downregulating or inhibiting the expression of S1P. [48]. Cancer cell death that is induced by induction of ceramide synthesis induction or its accumulation might be mediated by different mechanisms including apoptosis, mitophagy or necroptosis. Endogenous ceramides which are synthesized *de novo* might regulate these cellular events in cancer cells. Subcellular localization, transportation and target protein interactions of ceramides mainly regulate cell death effect of ceramides in the downstream pathways of cancer cells [47,49] However, synthesis of S1P from ceramide promotes survival of cancer cells either by oncogenic signaling from G-protein-coupled S1P receptor (S1PR) or via independent mechanisms [50]. Effects of S1P in cancer cells is mediated by communication between cancer cell and tumor stroma via protein spinster homologue 2 (SPNS2) which induce lymphatic endothelial cells to secrete S1P. Consequently, accumulation of S1P results in migration and metastasis of cancer cells [50,51]. According to certain studies, androgen-deprivation in hormone-naïve human prostate cancer cell line, LnCaP, resulted in pro-apoptotic phenotypes in

these cells such as cell cycle arrest with a C_{16}-ceramide upregulation [52]. Also, sphingolipids accumulation including ceramides that have pro-apoptotic functions were observed after treatments with inhibitors of AR-signaling or after some cancer therapies such as radiation in prostate cancer [53]. All in all, targeting sphingolipid metabolism is considered as a novel strategy in order to develop new cancer therapeutics and targeting of this metabolic pathway is mainly focuses on inducing ceramide signaling which is considered as pro-apoptotic signaling, or downregulating-inhibiting S1P signaling which is considered as pro-survival signaling [54].

1.4. Cholesterol Metabolism

Cholesterol is an organic molecule that is found and synthesized by all cells in animal body. It is a sterol and an essential constituent of the cellular membrane. Also, it serves as a precursor in biosynthesis of many complex molecules in the cells including steroids, bile acids and Vitamin D [55]. Once cholesterol is synthesized in the cell, it is largely located at the cell membrane, where it controls the structural properties of the membrane such as permeability, fluidity and rigidity. In addition to its structural functions on the membrane, it also influences conformations of transmembrane proteins by interacting with them [55,56]. Cholesterol trafficking and its distribution in the cell is regulated by interaction between different sterol transport proteins and cholesterol [57]. Biosynthesis of cholesterol takes place in cytosol and endoplasmic reticulum. Acetyl-CoA is a starting molecule in cholesterol biosynthesis pathway which is converted to HMG-CoA by condensation reactions in the cytosol. In next step, mevalonate is synthesized from HMG-CoA by the action of first rate-limiting enzyme of the pathway, HMG-CoA reductase

enzyme (HMGCR). After that, sterols precursor farnesyl pyrophosphate (FFP) is synthesized from mevalonate which is followed by condensation reactions to squalene from FFP.

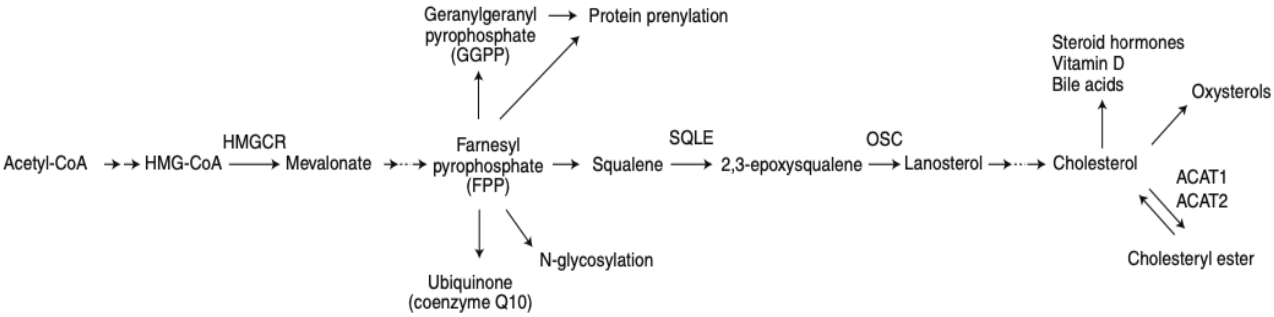

Figure 1.6. Cholesterol biosynthesis pathway and key enzymes of the pathway [58]

In addition to squalene, geranylgeranyl pyrophosphate (GGPP) can be synthesized from FFP [58]. These two molecules, FFP and GGPP, can perform post-translational modifications on proteins which is called prenylation and this modification might result in activation of some proteins such as Ras oncoprotein [59]. After synthesis of squalene, oxidation reaction takes places in order to oxidize squalene and produce 2,3-epoxysqualene. Oxidation of squalene is performed by squalene epoxidase (SQLE) enzyme which is a rate-limiting enzyme. After that, lanostreol is produced and finally cholesterol is synthesized from it. From cholesterol different molecules can be synthesized such as steroid hormones, oxysterols or cholesterol esters **(Figure 1.6)** [55, 60].

1.4.1. Cholesterol in Cancer Metabolism

Cholesterol metabolism is involved in cancer progression by contributing the proliferation, migration and also invasion of cancer cells. As a result of uncontrolled and fast proliferation, cancer cells require increased cholesterol level in order to maintain their biogenesis of membrane as well as for other cellular functions of cholesterol [61]. Beside structural function of cholesterol in membrane, it is also essential precursor of steroid hormone and bile acids, which is why upregulation in cholesterol level promotes the tumorigenesis of hormone-dependent cancers such as prostate cancer and breast cancer [62]. Cholesterol levels are tightly regulated in the cell by two master transcription factors which are liver X receptors (LXRs) and sterol regulatory element-binding protein-2 (SREBP2). Once cholesterol accumulates in the cell, SREBP-2 is inactivated by the action of insulin-induced gene (INSIG) which inhibits SREBP-cleavage activating protein (SCAP). In order to be functional, SREBP-2 must be forming a complex with SCAP first and retention of SCAP by INSIG inhibits the SREBP-2 activity, as a results, cholesterol biosynthesis is downregulated. Meanwhile, LXRs can be activated by precursors of cholesterol and some end products of cholesterol biosynthesis pathway such as oxysterols which results in increased expression of genes involved in efflux of cholesterol including ATP-binding cassette subfamily A member 1 (ABCA1) [63, 64]. These pathways that control metabolism and transport of cholesterol is often altered in many cancer types including prostate cancer. Prostate cancer cells, exhibit almost two-fold increased cholesterol level compared to healthy prostate cells [65]. SREPB2 mRNA expression substantially increases from normal prostate cells to localized PCa and CRPC and decreased survival rate of patients as wells as poor clinical outcome are often associated with higher SREBP2 expression [66]. Expression level of rate-limiting enzymes of cholesterol biosynthesis pathway are altered during the progression of PCa. For example, increase in the

expression of two rate-limiting enzymes of cholesterol metabolism, SQLE and HMGCR, are frequently observed especially in metastatic CRPC [67]. Recently, it has been shown that upon PTEN-loss PCa cells exhibited increased level of cholesterol esters as a consequence of upregulation in PI3K/AKT/mTOR signaling pathway and SREBP2 and as well as low-density lipoprotein receptor (LDRr) and targeting esterification of cholesterol in these cells, resulted in suppression of tumorigenesis [68]. Due to aberrant alteration in cholesterol metabolism related genes, targeting cholesterol biosynthesis with cholesterol-lowering drugs such as statins, in cancer cells is considered as a way to suppress progression of cancer cells, which has potential to overcome the resistance to other anti-cancer drugs [61].

1.5. Aim of the Study

Metabolic reprogramming is one of the hallmarks of cancer and in order to maintain their aggressive proliferation and high demand of energy, cancer cells undergo metabolic reprogramming. PI3K/Akt/mTOR signaling pathway is essential for growth and metabolism of cells and this pathway is often altered in cancer cells due to aberrant mutations in the pathway components. Deletion of tumor suppressor gene PTEN, a negative regulator of PI3K pathway, is a very frequent and early event in many types of cancer including prostate cancers, which leads to upregulation of PI3K/Akt/mTOR pathway and affects cancer metabolism widely. In this study, we wanted to reveal changes in metabolome of metastatic castration-resistant prostate cancer cells, which is a type of prostate cancer without any effective treatment currently, caused by loss of PTEN. In order to address this question, we employed PTEN-null castration-resistant prostate cancer cells and by Tet-on gene expression system, WT and different functional mutant forms of PTEN were expressed in these cells. Generation of Tet-inducible PTEN expression in our cellular models allowed us to profile acute and dynamic changes in transcriptome and metabolome of these cells. According to these data, we wanted to highlight and validate genes that are responsible for biosynthesis of key metabolites which have their levels changed after PTEN expression. Finally, we wanted to target these metabolic pathways and examine the effects of combining metabolic vulnerabilities of these cells with an FDA-approved androgen receptor antagonist drug that our advanced prostate cancer cellular models have resistance to it, named MDV3100.

Main aims of this project are;

- Identification of metabolic differences caused by PTEN loss-of-function mutations in metastatic and castration-resistant prostate cancer models
- Determination of effects of specific enzymatic functions (protein and lipid phosphatase functions) of PTEN tumor suppressor on prostate cancer's metabolism.
- Identification of genes involved in the anabolism and catabolism of metabolites whose levels are determined to be regulated by different enzymatic functions of PTEN in advanced prostate cancer models.
- Determination of the possible synergistic effects of targeting the determined metabolic pathways in combination with FDA-approved androgen receptor antagonist MDV3100 (Enzalutamide) on metastatic and castration-resistant prostate cancers.

CHAPTER 2

2. MATERIALS AND METHODS

2.1. MATERIALS

2.1.1. Buffers and Solutions

Solutions	Ingredients
1X Cell Lysis Buffer	1X RIPA 1X Protease inhibitor 1X Phosphatase inhibitor mix 1 μM DTT 1 mM Na3VO4
10X Western Blotting Running Buffer	30 g Trizma-Base 144 g Glycine 10 g SDS Complete volume up to 1 liter with ddH_2O
10X Western Blotting Transfer Buffer	30.3 g Trizma-Base 144.1 Glycine Complete Volume up to 1 liter with ddH_2O
1X Western Blotting Transfer Buffer	100 mL 10X Transfer buffer 200 mL Methanol 700 mL ddH_2O
10X TBS	80 g NaCl 2 g KCl

	30 g Trizma-Base pH adjusted 7.4 with HCl Complete volume up to 1 liter with ddH_2O
1X TBS-T	1 mL Tween-20 1 liter 1X TBS
Resolving Gel Buffer (pH=8.8)	187 g Trizma-Base pH adjusted to 8.8 with HCl Complete volume up to 1 liter with ddH_2O
Stacking Gel Buffer (pH=6.8)	60.5 g Trizma-Base pH adjusted to 6.8 with HCl Complete volume up to 1 liter with ddH_2O
Cell Fixation Solution	4% Paraformaldehyde (PFA) dissolved in 1X PBS
Crystal Violet Staining Solution	0.4% crystal violet powder 20% Ethanol complete to desired volume with ddH_2O
Destaining Solution	10% Acetic Acid 0.5% SDS complete to desired volume with ddH_2O
50X TAE	242 g Trizma-base 57.1 mL acetic acid 100 mL 0.5M EDTA

2.1.2. Cell Culture Reagents

Catalog Number	Product Name	Brand
P04-17500	RPMI	Pan-Biotech, Germany
41966-029	DMEM	Gibco, US
S1810-500	Fetal Bovine Serum (FBS)	Biowest, US
S181T-500	Tetracycline-Free FBS	Biowest, US
15140-122	Penicillin-Streptomycin	Gibco,US
25300-054	Trypsin-EDTA (0.05%)	Gibco,US
L3000-008	Lipofectamine 3000	Thermo Scientific, US
631455	Retro-X Concentrator	Takara Bio, US
AB-101L	Nourseothricin (NAT)	Jena Bioscience, Germany
10131-035	Geneticin (G418 Sulfate)	Gibco, US
A111138-03	Puromycin	Gibco, US
D9891-1G	Doxycycline Hyclate	Sigma-Aldrich, US
S1250	Enzalutamide (MDV3100)	Selleckchem, US
S1792	Simvastatin	Selleckchem, US
10011619	Terbinafine (Hydrochloride)	Cayman Chemical, US
1H72652	PBS, 10X pH 7.4	BioShop, Canada
P36931	ProLong Gold Antifade reagent with DAPI	Invitrogen, US
5100-0001	Mr. Frosty Freezing Container	Thermo Scientific, US

2.1.3. Cell Lines and Their Growth Medium Ingredients

Cell Line	Growth Medium
C4-2 (Parental)	RPMI-1640; 8% FBS; 1% P/S
C4-2 PTEN (Tet-On PTEN expressing cells)	RPMI-1640; 8% Tet-Free FBS; 1% P/S
PC3 (Parental)	RPMI-1640; 8% FBS; 1% P/S
PC3 PTEN (Tet-ON PTEN expressing cells)	RPMI-1640; 8% Tet-Free FBS; 1% P/S
HEK293	DMEM; 8%FBS; 1% P/S

2.1.4. Western Blotting Reagents

Catalog Number	Product Name	Brand
161-0747	Laemli Sample Buffer (4x)	Bio-Rad, US
10688.01	Acrylamide/Bisacrylamide Solution (30w/v)	Serva, Germany
K-12045-D20	WesternBright ECL kit	Advansta, US
11930.03	Albumin Bovine Fraction V, pH 7.0	Serva, Germany
773301	Prime-Step Protein Ladder	BioLegend, US
23391. 02	Glycine	Serva, Germany
39055.01	Phosphatase Inhibitor Mix	Serva, Germany
P0758S	Sodium Orthovanadate	New England Biolabs, US
11836153001	cOmplete, Mini Protease Inhibitor Cocktail	Merck, Germany

2502	ReBlot Plus Mild Stripping Solution, 10x	Merck, Germany
2504	ReBlot Plus Strong Stripping Solution, 10x	Merck, Germany
GE10600003	Nitrocellulose Blotting Membrane	Merck, Germany
23225	Pierce™ BCA Protein Assay Kit	Thermo Scientific, US

2.1.5. Western Blotting Antibodies

Catalog Number	Product Name	Brand
2118S	GAPDH (14C10) Rabbit mAb	Cell Signaling Technology, US
9559S	PTEN (138G6) Rabbit mAb	Cell Signaling Technology, US
9272S	Akt Rabbit mAb	Cell Signaling Technology, US
9018P	Phospho-Akt1 (Ser473) Rabbit mAb	Cell Signaling Technology, US
4056S	Phospho-Akt (Thr308) Rabbit mAB	Cell Signaling Technology, US
2072S	mTOR Rabbit mAb	Cell Signaling Technology, US
2971S	Phospho-mTOR (Ser2448) Rabbit mAb	Cell Signaling Technology, US
2317S	S6 Ribosomal Protein Mouse mAb	Cell Signaling Technology, US

2215S	Phospho-S6 Ribosomal Protein (Ser240/244) Rabbit mAb	Cell Signaling Technology, US
4858S	Phospho-S6 Ribosomal Protein (Ser235/236) Rabbit mAb	Cell Signaling Technology, US
9452S	4E-BP1 Rabbit mAb	Cell Signaling Technology, US
9451S	Phospho-4E-BP1 (Ser65) Rabbit mAb	Cell Signaling Technology, US
40695S	SQLE Rabbit mAb	Cell Signaling Technology, US
42201S	HMGCS1 Rabbit mAb	Cell Signaling Technology, US
SC-271616	SREBP2 Mouse mAb	Santa Cruz Biotechnology, US
7076S	Anti-Mouse IgG, HRP-linked	Cell Signaling Technology, US
7074S	Anti-Rabbit IgG, HRP-linked	Cell Signaling Technology, US

2.1.6. Kits

Catalog Number	**Product Name**	**Brand**
169014875	Plasmid Midi Kit	Qiagen, Germany
11922402	NucleoSpin RNA Isolation Kit	Macherey-Nagel, Germany
00627493	GeneJET Gel Extraction Kit	Thermo Scientific, US
00789174	GeneJET Plasmid Miniprep Kit	Thermo Scientific, US
21071	SMART BCA Protein Assay Kit	Intron Biotechnology, South Korea

E-BC-K004-M	Free Cholesterol (FC) Colorimetric Assay Kit	Elabscience, US

2.1.7. Vectors and reagents used in cloning experiment

Catalog Number	Product Name	Brand
M0202S	T4 DNA Ligase	New England Biolabs, US
R3101S	EcoRI-High Fidelity Restriction Enzyme	New England Biolabs, US
R0103S	HincII Restriction Enzyme	New England Biolabs, US
N3232L	1kb DNA Ladder	New England Biolabs, US
M0371L	Alkaline Phosphatase Enzyme	New England Biolabs, US
C3040I	NEB Stable Competent *E. coli*	New England Biolabs, US
48501.01	LB Medium	Serva, Germany
10835269001	Ampicillin	Roche Life Sciences, US
51463	PH-Btk-GFP vector	Addgene, US
1764	pBABE-puro retroviral vector	Addgene, US

2.1.8. qPCR Reagents

Catalog Number	Product Name	Brand
15596025	TriZol Reagent	Invitrogen, US
170-8891	iScript cDNA Synthesis Kit	Bio-Rad, US
L003037B	SSoAdvanced Universal IT SYBR Green Supermix	Bio-Rad, US
04729692001	LightCycler 480 Multiwell Plate 96, White	Roche Life Sciences, US

2.1.9. Primer sequences of human genes used in qPCR experiments

Gene Name	**Forward Primer**	**Reverse Primer**
HMGCS	5’GGGCAGGGCATTATTAGGCTAT3’	5’TTAGGTTGTCAGCCTCTATGTTGAA3'
HMGCR	GGACCCCTTTGCTTAGATGAAA	CCACCAAGACCTATTGCTCTG
MVD	TGAACTCCGCGTGCTCATC	CGGTACTGCCTGTCAGCTTCT
MVK	TGGACCTCAGCTTACCCAACA	GACTGAAGCCTGGCCACATC
PMVK	CCGCGTGTCTCACCCTTT	GACCGTGCCCTCAGCTCAT

SGMS2	CTTAGCCCTCCACTCCC	CAGAATCTGCGTCCCAC
CERK	CACCTTAGCCTCCATCACCACTG	AACATACCATCTCCGCCGACAC
DES1	CTATGCGTTTGGCAGTTGCA	CAGTTGCCAAAGGCAGCATT
SPTLC1	CAGAACCTCTTGTTCCTCCTGTC	TTTTGTGGCTTGGAGGGC
CERS2	AGATCATCCACCATGTGGCC	TGATTAGAGTCCCAGCTCGGA
ASAH1	AGTTGCGTCGCCTTAGTCCT	TGCACCTCTGTACGTTGGTC
GAPDH	GCCCAATACGACCAAATCC	AGCCACATCGCTCAGACAC

2.1.10. Equipments

Mini-Protean Tetra Cell	Bio-Rad, US
Amersham Imager 600	GE Healthcare, US
Centrifuges	Hettich, Germany, Nuve, Turkey
Cell Culture Hood	Nuaire, US
CO_2 Incubator	Thermo Scientific, US
Nanodrop one	Thermo Scientific, US
Synergy HT Microplate Reader	Biotek, US
LightCycler 96 Sytem for qPCR	Roche Life Sciences, US
Thermocycler for PCR	Bio-Rad, US
Fluorescence Microscope AX10 Imager.A1	Zeiss, Germany

2.2. METHODS

2.2.1. Maintenance of C4-2 and PC3 Cell Lines

In this study, C4-2 and PC3 human prostate cancer cell lines were used. Cells were split when they reached around 80% confluency. For splitting, cells were washed with 3-4 mL 1X PBS and incubated with 0.05% Trypsin/EDTA for 5 minutes, at 37°C and 5% CO_2. After trypsin incubation, detachment of cells from petri-dish was confirmed under the microscope and 3-4 mL growth media were added. Cells were collected into 15 mL falcon tubes and pelleted by centrifugation at 1000 rpm, RT for 5 minutes. Then, supernatant was discarded and cells seeded into new petri-dish with 1:5-1:6 splitting ratio. For C4-2 cells 1:5 and for PC3 cells 1:6 splitting ratios were used. They were incubated in cell culture incubator providing 37°C and 5% CO_2 atmosphere.

2.2.2. Freezing and Thawing of Cells

Cells were frozen when they were in their log growth phase. For freezing procedure, same protocol was employed as splitting of cells. After centrifugation, supernatant was discarded and cells were resuspended in freezing medium (40% RPMI, 50% FBS, 10% DMSO) and transferred into cryovials. For efficient freezing, cryovials were placed into Mr. Frosty Freezing Container and it was incubated at -80°C overnight. Then, cryovials were placed into liquid nitrogen tank for long-term storage. For thawing procedure, cryovial was taken from liquid nitrogen tank and incubated in water bath at 37°C until it dissolves completely. After that, thawn cell suspension was transferred into 15 mL falcons and centrifuged at 1000 rpm, for 5 minutes. Then, supernatant was discarded completely and pellet was resuspended with 4 mL thawing medium (90% RPMI, 10% DMSO, without P/S). Finally, suspended cells were seeded into 6-cm petri-dish.

2.2.3. Subcloning of PH-Btk-GFP into pBABE-puro retroviral vector

PH-Btk-GFP mammalian expression vector and pBabe-puro retroviral vector were double digested by EcoRI-HF and HincII restriction enzymes at 37°C for 1 hour at thermocycler. Digestion reactions were set up as indicated in Table 2.1. Digestion reaction was loaded to 1% agarose gel and run at 90V for 40 minutes. Then, digested PH-Btk-GFP band which is insert (1411 bp) and pBABE-puro band which is vector (5086 bp) were cut from agarose gel. By using GeneJet Gel Extractions kit insert and vector were extracted from agarose gel according to manufacturer's protocol. DNA concentrations were measured by Nanodrop and from both samples 1 µl were loaded to an agarose gel and run as a confirmation of gel extraction procedure

Table 2.1. Double digestion reaction conditions

Reagent	Concentration or Volume
EcoRI-HF Restriction Enzyme	1 µL
HincII Restriction Enzyme	1 µL
Cut-Smart Reaction Buffer	1X
DNA	2 µg

Ligation of PH-Btk-GFP insert into digested pBABE-puro vector was done by 3:1 molar ratio which is insert DNA:vector DNA, according to NEBioCalculator. Ligation reaction was set up as indicated in Table 2.2 and reaction was incubated at 16°C, overnight in thermocycler machine.

Table 2.2. Ligation reaction conditions

Reagent	Concentration or Volume
T4 DNA Ligase	1 µL
T4 DNA Ligase Buffer	1 µL
Vector DNA	0.020 pmol
Insert DNA	0.060 pmol

For transformation, 25 µL *E. coli DH5-alpha* competent cells were thawed on ice and gently mixed with 1 µL ligation reaction sample. It was incubated on ice for 30 minutes, following heat shock was done at 42°C for 30 seconds in waterbath. 1 mL SOC-medium was added into competent cells-vector mixture and incubated in shaker (200 rpm) at 37°C for an hour. After incubation, it was centrifuged at 12,000 rpm for 2 minutes and 800 µL of supernatant was discarded. Pellet was resuspended with 200 µL leftover supernatant and resuspension was spread into LB-agar plate containing appropriate antibiotic (ampicillin) and incubated at 37°C overnight. Next day, single colony was selected and inoculated into 3-4 mL LB-medium and incubated overnight at 37°C on shaker. After overnight incubation, miniprep was done according to the manufacturer's protocol. In order to confirm cloning, cloned plasmid was double digested by the same restriction enzymes used in cloning. After confirmation, starter culture was inoculated into big culture according to Midiprep kit protocol and midiprep was done to isolate plasmid in a high quantity and to use in downstream processes.

2.2.4. Retroviral Transduction of Mammalian Cells

C4-2 human prostate cancer cells were stably transduced with pRXTN PTEN WT, pRXTN PTEN YL, pRXTN CS, pRXTN PTEN GE and pBabe-PH-Btk-GFP retroviral plasmids separately. For production of viral particles containing DNA-of-interest, Lipofectamine 3000 reagent was used according to manufacturer's protocol. In brief, the day before the transfection, $2x10^5$ HEK293 cells were seeded into 6-well plates including control wells. Next day, a triple transfection was done with 1μg envelope plasmid (VSV-G), 1 μg packaging plasmid (Gag-Pole) and 2 μg plasmid-transduced-to-be. First, DNA mix was prepared in 1.5 mL Eppendorf tube containing 125 μL serum-free DMEM, plus plasmids and 6 μL P3000 reagent. Then, second lipofectamine3000 tube mix was prepared in 1.5 mL Eppendorf tube containing 3.75 μL lipofectamine3000 plus 125 μL serum-free DMEM for per well of 6-well plate. Both tubes were mixed gently by up and down the tube and DNA mix was added into lipofectamine3000 tube mix and incubated at RT for 20 minutes. After incubation, media of HEK293 cells were changed with 1.75 mL fresh growth medium and 250 μL lipofectamine-DNA mixture were given drop-by drop and mixed gently by back and forth. After overnight incubation, medium was changed with fresh growth medium and at 48 hour of transfection supernatant was collected into 50 mL falcon tubes and new growth medium was given. This procedure was repeated at 72 hours as well. Then, supernatant was filtered through 0.45 micron filters and Retro-X-Concentrator was added with 1:3 ratio (Concentrator:Supernatant) and mixed thoroughly, covered with aluminum foil and left for overnight incubation at 4°C. Then, supernatant-concentrator mixture was centrifuged at 1500 g, +4°C for 45 minutes to pellet down the viral particles. After centrifugation, supernatant was discarded and pellet was resuspended in proper amount of growth medium and given to the cells transduced-to-be along with 10 ug/mL polybrene. Cells were incubated for overnight with viral

particles and after that, medium was changed with fresh growth medium and antibiotic selection was started. Selection was done until all control well cells died. For pRXTN plasmids selection Nourseothricin (NAT) was used with a final concentration of 250 µg/mL and for pBabe-puro-PH-Btk-GFP plasmid selection, Puromycin was used with a final concentration of 1.1 µg/mL in C4-2 cells.

2.2.5. Crystal Violet Cellular Proliferation Assay

Cellular proliferation assay was done in either 6-well or 12-well plates. $1x10^4$ and $3x10^4$ C4-2 cells were seeded into per well of 12-well and 6-well plates respectively and $5x10^3$ and $1.5x10^4$ PC3 cells were seeded into per well of 12-well and 6-well plates respectively. After seeding cells with their fresh growth medium, they were left for overnight incubation. Next day, their growth medium was replaced with medium containing 4% FBS and inhibitor and incubated for 5 days. For doxycycline treatment, cells were incubated with proper concentration of doxycycline for 3 days. After incubation was done, media of cells were discarded and they were washed with 2 mL 1X PBS once. Then, cells were fixed with 4% PFA at 4°C for overnight, 500 µL fixation solution for per well of 12-well and 1 mL fixation solution for per well of 6-well plate was used. Next day, fixation solution was removed and cells washed with 2 mL 1X PBS and cells were stained with crystal violet stain for 1 hour at RT, 500 µL crystal violet stain for per well of 12-well and 1 mL crystal violet stain for per well of 6-well plate was used. After incubation, crystal violet stain was discarded and cells were washed extensively twice with tap water and left for air dry under the fume food. When they dried, photo of each well was taken and destaining solution was added to the each well and incubated for 30 minutes on the shaker with mild agitation, 1 mL destaining solution for per well of 12-well and 2 mL destaining solution for per well of 6-well plate was used. Finally, 10 µL solution was taken from each destained well and mixed with 190 µL destaining

solution (1:20 dilution) in 96-well plate and absorbance was measured as triplicates by spectrophotometer at 595 nm. Absorbance values of samples were normalized by subtracting the blank absorbance values from average of samples absorbance values.

2.2.6. Immunofluorescence Analysis

$2x10^5$ C4-2 cells were seeded into coverslips in 6-well plates with growth medium including control wells. Next day, medium of cells was changed with 4% FBS medium and proper amount of doxycycline was introduced to treatment wells and left for three days incubation. At the end of three days, cells were washed with 1X PBS once and fixed with 1 mL 4% PFA for per well at RT, for 15 minutes. After that, cells were washed again once with 1X PBS and dipped into ddH_2O and was dried. Then, coverslip containing fixed cells was mounted with 15 µL mounting medium (ProLong Gold Antifade reagent with DAPI) to slide. Mounted slide was incubated in dark overnight, at RT, to get solidified. Finally, images were taken under the Zeiss AX10 fluorescence microscope and images were analyzed by Image J tool.

2.2.7. Immunoblotting Analysis

2.2.7.1. Cell Harvest and Cell Lysis

Cells were washed with 1X cold PBS on ice. After that 2 mL 1X cold PBS was added onto cells and they were lifted by cell-scraper. Then, cell suspension was transferred to 2 mL Eppendorf tube and centrifuged at 4000 rpm, +4°C for 15 minutes. After centrifugation, supernatant was removed and cells were lysed. For lysis of the cells, freshly prepared 1X cell lysis buffer (recipe is shown at materials 2.2.1) was used. Volume of lysis buffer was determined as three times the volume of the cell pellet. After addition of the lysis buffer, cells were resuspended by pipetting several times and incubated on ice for 30 minutes. During incubation, every 10 minutes, cells were vortexed. Next, cells were centrifuged at 14000 rpm, +4°C for 40 minutes. Then, supernatant which contains

proteins was transferred into new 1.5 mL eppendorf. If they are not going to use immediately, they were snap-frozen in liquid nitrogen and stored at -80°C.

2.2.7.2. Protein Concentration Determination by BCA Assay

For determination of protein concentration, Pierce™ BCA Protein Assay Kit was used according to manufacturer's protocol. In brief, standards of albumin were prepared in 0-1-3-5-7-10-13-15 µg as indicated in Table 2.3. in 96-well plate. From working solution, 200 µL was added to each well and for sample wells 1 µL unknown protein sample was added and rest was completed to 25 µL with ddH_2O. Thus, each well contained 225 uL mix as triplicates.

Table 2.3. Protein standards preparation

Standard Concentration (µg/µL)	**Bovine Serum Albumin (BSA) (2µg/µL)**	**ddH_2O**
0	0 µL	25 µL
3	1.5 µL	23.5 µL
5	2.5 µL	22.5 µL
7	3.5 µL	21.5 µL
10	5 µL	20 µL
13	6.5 µL	18.5 µL
15	7.5 µL	15 µL

All wells were mixed well by pipetting and incubated at 37°C for 30 minutes. After incubation was done, absorbance was measured by spectrophotometer at 562 nm. Protein concentration was calculated according to the equation obtained from standard proteins.

2.2.7.3. Immunoblotting

10% resolving SDS gel and 4% stacking SDS gel were prepared according to formula shown in Table 2.4 which is for two gels.

Table 2.4. Resolving and Stacking Gel Formula

	Resolving Gel (10%)	**Stacking Gel (4%)**
Acrylamide/bisacrylamide (30w/v)	3.3 mL	660 µL
TEMED	5 µL	5 µL
10% APS	50 µL	25 µL
Resolving Gel Buffer (pH=8.8)	2.5 mL	-
Stacking Gel Buffer (pH=6.8)	-	1.26 mL
ddH_2O	4.1 mL	3 mL
Total Volume	10 mL	5 mL

In most of the experiments, 10-20 µg proteins were loaded and run on an SDS-PAGE. For running samples, they were denatured at 95°C with 10% β-mercaptoethanol-90% Laemmli Sample Buffer mix for 10 minutes. After denaturation, protein samples were loaded and run at 70 volt for 30 minutes. Then, voltage was increased to 90 volt and run for approximately 60-70 minutes. After running was done, wet-transfer method was employed to transfer proteins into nitrocellulose membrane. Transfer was done either at 250 mA for 150 minutes or overnight at 90 mA at 4°C. In order to confirm successful transfer, membrane was stained with Ponceau S after transfer and

Ponceau S was destained from membrane by washing with ddH_2O. For total proteins, 5% skim milk solution was prepared in 1X TBS-T buffer for blocking and if protein of interest is a phospho-protein, 5% BSA solution was prepared in 1X TBS-T buffer. Blocking was done at RT for 1-2 hours. After blocking, membranes were incubated in corresponding primary antibodies for overnight at 4°C. When primary antibody incubation was done, membranes were washed with 1X TBS-T buffer for three times and 5 minutes intervals. Then, membranes were incubated in HRP-conjugated secondary antibodies at RT, for 1-2 hour. After secondary antibody incubation, membranes were washed again with 1X TBS-T buffer for three times and 5-minute intervals. Then, membranes were soaked in ddH_2O and ECL solution was prepared according to manufacturer's protocol. After incubation of membranes with ECL solution, membranes were developed and visualized by Amersham Imager 600. Analysis of immunoblotting results were performed by ImageJ 1.53k. Normalization of phosphor-proteins were done by first normalization phosphor-protein and its total protein to loading control and then, phosphor-proteins were further normalized to its normalized total protein.

2.2.8. RT-qPCR Experiment for mRNA Expression Analysis

2.2.8.1.RNA Isolation

Before starting RNA isolation, work bench and equipment were cleaned with RNAse ZAP in order to prevent any RNase contamination. Cells were washed with cold 1X PBS once. After that, 2 mL cold 1X PBS were added and cells were lifted by cell scraper and transferred into 2 mL Eppendorf tubes. They were centrifuged at 4000 rpm, 4°C for 15 minutes. Then, total RNA isolation was performed by NucleoSpin RNA Isolation Kit according to manufacturer's protocol.

Concentrations of RNA were measured with Nanodrop. Then, they were snap-frozen in liquid nitrogen and stored at -80°C.

2.2.8.2. cDNA Synthesis

cDNA synthesis reaction was set up with 1 µg total RNA using BioRad iScript cDNA Synthesis Kit according to manufacturer's protocol. The reaction condition for cDNA synthesis is shown at Table 2.5.

Table 2.5. Reaction conditions of cDNA synthesis

Reagent	Volume or Concentration
5X Reaction Mix	4 µL
Reverse Transcriptase	1 µL
RNA	1 µg
DEPC-water	Up to 20 µL

2.2.8.3.qPCR

cDNA samples were prepared according to Table 2.6 for qPCR reaction. Amplification conditions of cDNA samples in qPCR reactions was shown in Table 2.7 Reaction was set up in 96-well plates as triplicates.

Table 2.6. Reaction conditions for qPCR

Reagent	Volume or Concentration
Syber Green Mix (2X)	5 µL
Forward Primer	250 nM
Reverse Primer	250 nM
cDNA Template	30 ng
DEPC-water	Up to 10 µL

Table 2.7. Cycles for qPCR reaction

Step	Temperature	Duration	Cycle Number
Preincubation	98°C	150 s	1
2 Step Amplification	98°C	10 s	40
	60°C	30 s	
Melting	65°C	10 s	1
	95°C	300s	

Cycle time (Ct) values of gene of interests were normalized to housekeeping gene (GAPDH) Ct values. $2^{-\Delta\Delta CT}$ method was used for calculation of fold changes.

2.2.9. Targeted Metabolomics Analysis

2.2.9.1.Sample Preparation for Targeted Metabolomics Analysis

Cells were seeded with 60-70% confluency with their growth medium. Next day, their media were replaced with 2% FBS containing medium and 1µg/mL doxycycline was given to cells. They were incubated for three days and at the end of three days, cells were washed with 1X ice-cold PBS

once and they were scraped and collected into 2 mL eppendorfs. After that, they were centrifuged at 1500 rpm, +4°C for 10 mins. Then, supernatant was discarded and pellets were snap frozen with liquid nitrogen and stored at -80°C. In total, 5 biological replicates were prepared from each cell line and each variant and in order to do metabolites normalization $5x10^6$ cells were analyzed from each cell line.

2.2.9.2.Mass Spectrophotometry Analysis of Metabolites

Targeted metabolomics experiments were performed in collaboration with Dr. Berat Z. Haznedaroglu's group at Bogazici University, Institute of Environmental Sciences. Absolute*IDQ* p400 HR (Biocrates, Austria) kit was utilized on a Thermo Q Exactive™ mass spectrometer for the targeted metabolomics approach. Kit provides standards for each metabolite groups and either LC-MS/MS or FIA-MS/MS methods were employed according to set of metabolites and concentration of metabolites in the samples were calculated either quantitative or relative quantitative in μM concentrations.

2.2.10. Free Cholesterol Assay

C4-2 Empty vector and WT PTEN cells were induced with 0.02 - 1 μg/mL range of doxycycline for three days. Cells were harvested and counted and experiment was performed with the same number of cells for each comparison groups. Free cholesterol concentration of cells was measured by using Free Cholesterol (FC) Colorimetric Assay Kit (E-BC-K004-M, Elabscience, US) according to manufacturer's protocol.

2.2.11. Statistical Analysis

For statistical analysis and generation of graphs GraphPad Prism 8 was used. In order to determine and show statistical differences between comparison of two groups two-tailed student's t-test was used.

Analysis of metabolomics data was performed by using online web-tool MetaboAnalyst 5.0. Fold Change (FC) value was set to 1.5 and p value was set to 0.05 for indication of significant changes on the metabolite levels between comparison of two groups. Quantitative metabolite set enrichment analysis was performed by using MetaboAnalyst 5.0 with metabolite pathways for human from KEGG database.

Coefficient Drug Interaction (CDI) was used to evaluate synergistic effect in drugs combination experiments according to formula; CDI = AB/(AxB) where AB is the absorbance ratio of combined drugs group to control absorbance value, A and B are the single drug treatment absorbance ratios to control absorbance value.

CHAPTER 3

3. RESULTS

3.1. Generation of Tet-On System for Dox-Inducible PTEN expression in mCRPC cells

In order to investigate impacts of PTEN-loss on metabolome of metastatic castration-resistant prostate cancer (mCRPC) cellular models, C4-2 and PC-3 cell lines were selected. Tet-On (doxycycline-inducible) gene expression system was utilized to re-introduce PTEN into these cells. Both of the cell lines have a PTEN-null background so that endogenous PTEN expression is completely abolished. Tet-On system enables inducible expression of a gene of interest by doxycycline introduction at a certain concentration to the culture media [69]. Cells were transduced with the Tet-On system components, rtTA and pRXTN-PTEN vectors separately for each PTEN variant. After rtTA transduction, cells were selected with G418 (Geneticin) antibiotic as it is a selection marker for rtTA plasmid and selected cells were transduced with pRXTN-PTEN vectors for each PTEN variants **(Table 3.1)** separately and selected with NAT (Nourseothricin) antibiotic.

Table 3.1. PTEN variants and their catalytic properties

PTEN Variants	**Phenotype**
Empty Vector	Negative Control
Wild Type (WT) PTEN	WT PTEN
Y138L PTEN	Lipid phosphatase function active PTEN (protein phosphatase function inactive)
G129E PTEN	Protein phosphatase function active PTEN (lipid phosphatase function inactive)
C124S PTEN	Catalytically inactive PTEN

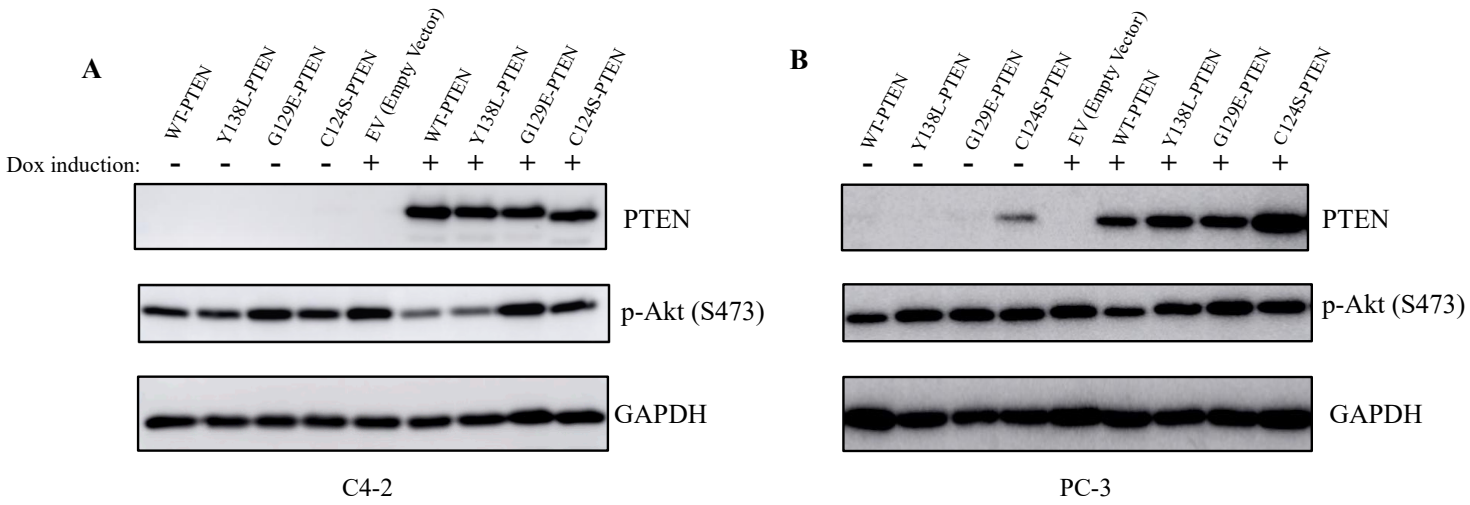

Figure 3.1. WT and mutants PTEN expression levels in PTEN-null mCRPC cells after establishing Tet-On gene expression system. C4-2 cells upon reintroduction of PTEN variants **B)** PC-3 cells upon reintroduction of PTEN variants. Cells were induced with 0.02 - 1 µg/mL range of doxycycline. Cells were harvested and immunoblotting was done for determination of PTEN and p-Akt (S473) levels. GAPDH was used as a loading control.

After Tet-On gene expression system was established for WT and mutant PTEN genes in C4-2 and PC-3 cells, they were induced with doxycycline and immunoblotting was performed to observe PTEN levels **(Figure 3.1)**. All PTEN variants have relatively similar PTEN expression level in C4-2 cells. Additionally, in uninduced (-dox) cells, no PTEN expression was detected. Tet-on system is prone to leakage especially when trace amount of doxycycline is present in the medium, which is why having no expression in uninduced cells is important. Akt is one of the very first effectors in the PI3K pahway and its phosphorylation status at Threonine 308 and Serine 473 are downregulated by lipid phosphatase function of PTEN, which makes Akt phosphorylation an essential marker for PTEN functionality. Expression of WT PTEN and, Y138L PTEN, which are lipid phosphatase proficient, resulted in downregulation in p-Akt (S473) compared to empty vector

and uninduced counterparts. Since they do not have intact lipid phosphatase function, expression of G129E PTEN and C124S PTEN mutants, did not affect Akt phosphorylation **(Figure 3.1A)**. PC-3 PTEN variants also had similar level PTEN expression after doxycycline induction. Although, some level of downregulation in p-Akt (S473) was observed upon WT PTEN expression compared to empty vector, downregulation is not that much prominent compared to C4-2 cells. Additionally, Y138L PTEN expression did not result in downregulation in p-Akt (S473) level and expression of G129E and C124S PTEN, did not lead to a change in p-Akt levels of PC-3 cells as well **(Figure 3.1B)**.

3.2. Analysis and confirmation of PTEN functionality on mCRPC cells

PIP_3 is the main target of PTEN which is dephosphorylated and converted back to PIP_2 by the lipid phosphatase function of PTEN, so effects of PTEN can be directly checked by inspecting PIP_3 levels in a cell. Proteins having PH- domains can bind various membrane lipids including PIP_3 on the cellular membrane. Bruton's Tyrosine Kinase (BTK) protein has a PH domain and its PH domain can serve as a bona fide PIP_3 biosensor. [70]. We used a construct where its PH domain was tagged with Green Fluorescent Protein (GFP) which is denoted as PH^{BTK}-GFP. C4-2 WT PTEN and C124S PTEN cells were transduced with PH^{BTK}-GFP plasmid and immunofluorescence experiments were done with these cells in the presence and absence of WT and C124S PTEN expressions **(Figure 3.2A)**.

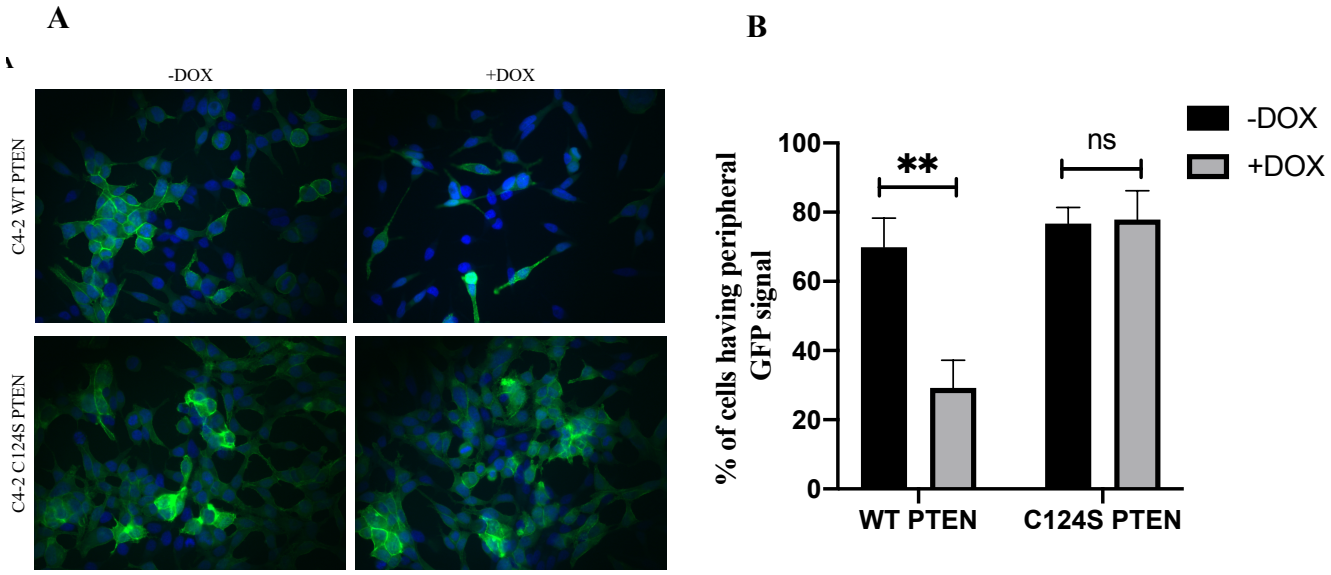

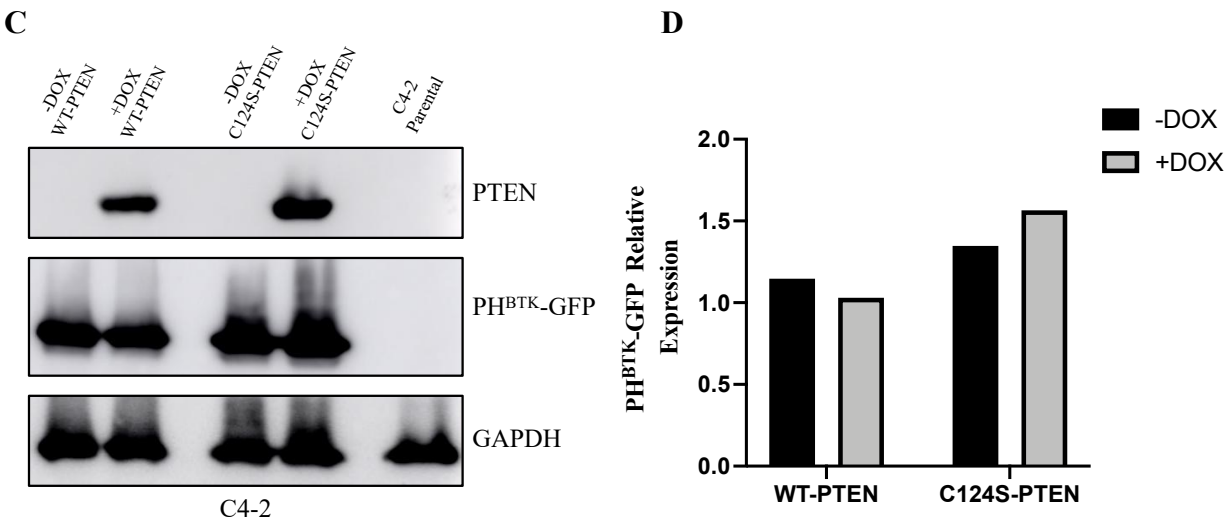

Figure 3.2. Reduction in the PIP_3 associated signal upon WT-PTEN but not upon C124S-PTEN expression in C4-2 cells. A) Immunofluorescence images of C4-2 cells expressing PIP_3 biosensor PH^{BTK}-GFP with or without WT and C124S PTEN expression. Blue color depicts cellular nuclei and, green represents the PH^{BTK}-GFP fusion protein. **B)** Quantification of cells having peripheral GFP signal over total GFP signal (n=3, **p<0.01). **C)** Immunoblotting for determination of PH^{BTK}-GFP fusion protein expression levels with or without WT and C124S PTEN expression. GAPDH was used as a loading control. **D)** Quantification of PH^{BTK}-GFP protein levels in C4-2 cells. PH^{BTK}-GFP fusion protein expression levels with or without WT and C124S PTEN expression. GAPDH was used as a loading control.

GFP signal was reduced upon WT PTEN expression compared to uninduced cells and also GFP signal localized to the cell periphery indicative of PIP_3 binding by the fusion protein. However, following WT PTEN expression, GFP signal was reduced around the cell periphery and became a fuzzy-diffused signal in most cells. These observations confirm that the active lipid phosphatase

function of PTEN reduced PIP_3 levels on the membrane. Meanwhile, expression of catalytically inactive mutant C124S PTEN, which served as a negative control, did not affect the localization and the strength of the GFP signal **(Figure 3.2-A)**. GFP positive cells were analyzed for the localized peripheral versus diffused GFP signals and quantification of the percentage of the localized GFP signal was performed. This quantification showed that in uninduced (-dox) WT PTEN C4-2 cells, peripheral GFP signal was significantly higher than induced (+dox) WT PTEN cells (**$p<0.01$) and there is no significant difference in peripheral GFP signal between induced and uninduced C124S PTEN C4-2 cells **(Figure 3.2-B).** Next, we wanted to make sure doxycycline induction does not affect GFP expression level in these cells and reduced GFP signal is not due to a change in the total GFP levels. For this purpose, immunoblotting was performed to see GFP expression by anti-GFP antibodies and we observed that GFP expression level did not change upon doxycycline induction in these cells **(Figure 3.2C)**. C4-2 parental cells (do not have PH^{BTK}-GFP) was used as a negative control to confirm antibody does not have non-specific binding. Both C4-2 WT PTEN and C124S PTEN cells have relatively similar PH^{BTK}-GFP expression before and after PTEN expression **(Figure 3.2D)**. Thus, it was confirmed that GFP signal differences observed induced and uninduced WT PTEN cells is due to phosphatase function of PTEN which restrains the PI3K pathway.

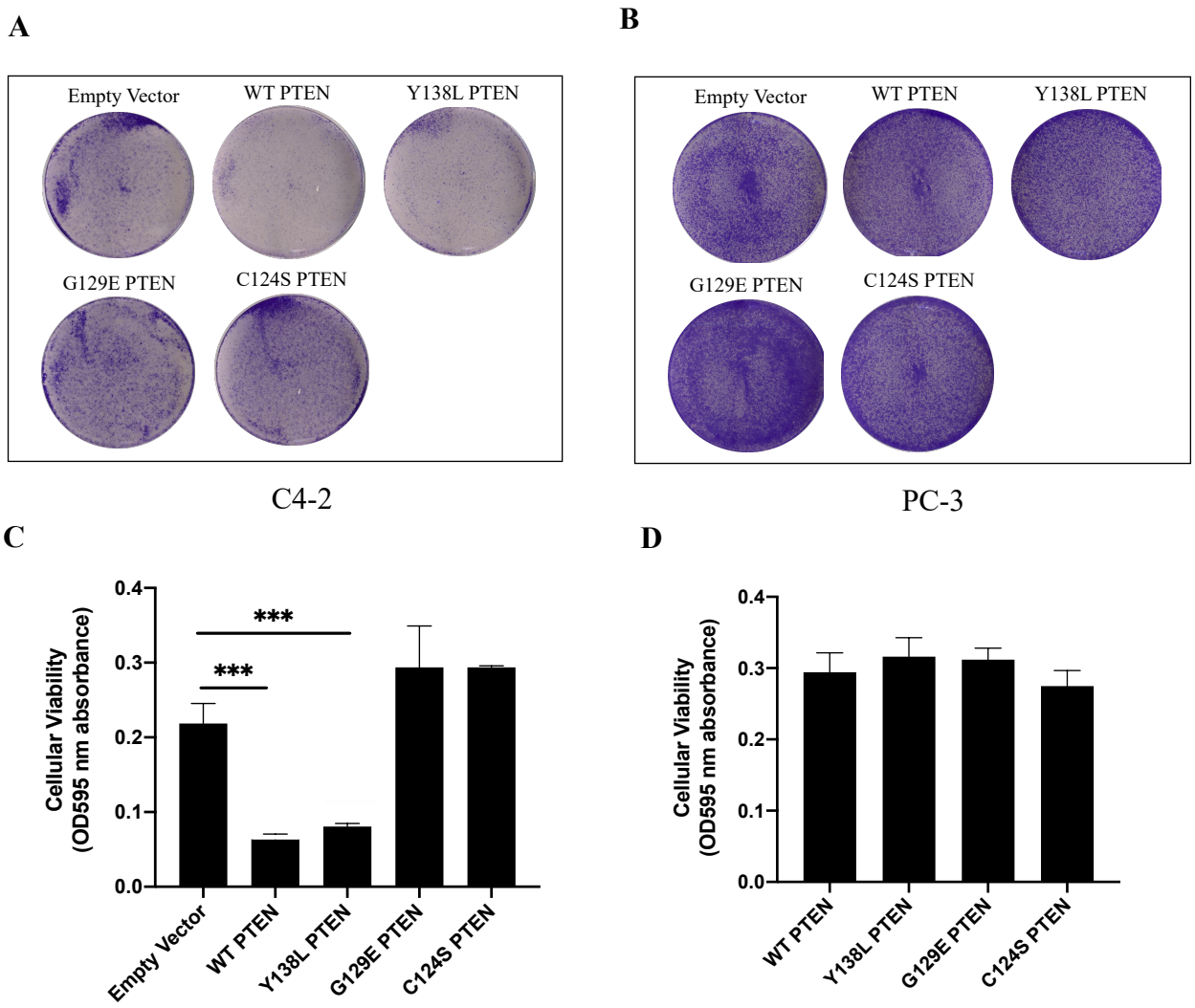

Figure 3.3. Expression of WT and Y138L PTEN expression compromised viability of C4-2 cells but did not affect viability of PC-3 cells. Representative image of crystal violet cellular viability assays of empty vector and different PTEN variants expressing **A)** C4-2 cells, **B)** PC-3 cells. Quantification of crystal violet assay of **C)** C4-2 cells, **D)** PC-3 cells (n=3 for each experiment, ***$p<0.001$). Error bars display S.D.

PI3K pathway directly controls the proliferation and viability of cells. In order to see effects of WT and mutants PTEN expression on cellular viability, crystal violet cellular viability assay was performed on C4-2 and PC-3 cells after doxycycline induction for PTEN expression **(Figure 3.3)**. Expression of WT PTEN and Y138L PTEN significantly reduced the viability of C4-2 cells compared to empty vector (***$p<0.001$). Additionally, expression of lipid phosphate function diminished G129E PTEN and C124S PTEN did not reduce the viability of C4-2 cells **(Figure 3.3-A&C)**. Expression of either WT PTEN or mutant forms of PTEN did not affect the viability of PC-3 cells, which suggests that PC-3 cells did not respond the PTEN re-expression **(Figure 3.3-B&D).** Thus, with cellular viability assay, we showed that lipid phosphatase function of PTEN compromised proliferation of C4-2 cells, which is not the case for G129E PTEN and C124S PTEN. Also, integrity of Tet-on gene expression system and functions of PTEN was confirmed on C4-2 cells which aligns with Figure 3.2 results.

3.3. Characterization of mCRPC cells upon WT PTEN and different mutant forms of PTEN expression for PI3K/Akt/mTOR pathway

Next, we aimed to characterize C4-2 and PC-3 cells for PI3K/Akt/mTOR signaling pathway components following WT and mutants PTEN expression by immunoblotting experiments and wanted to see changes on the phosphorylation level of key effector proteins of PI3K pathway.

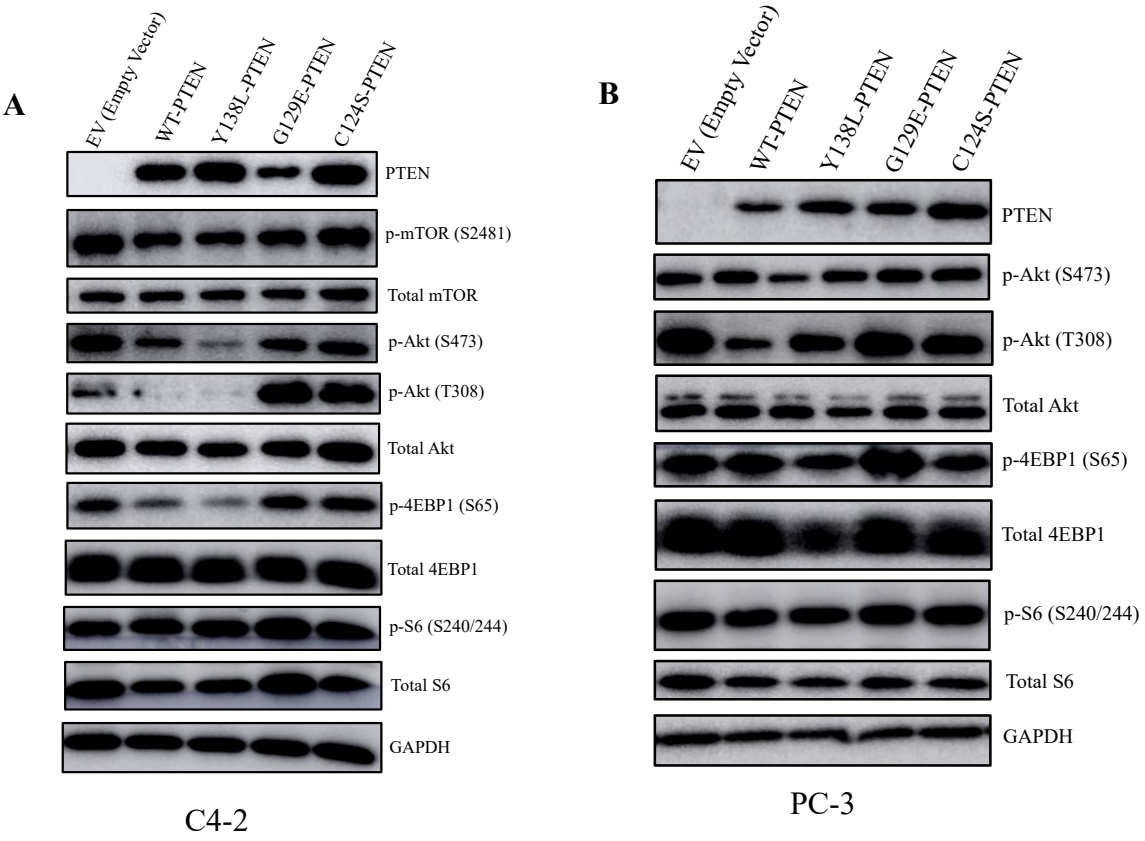
A
EV (Empty Vector)
WT-PTEN
Y138L-PTEN
G129E-PTEN
C124S-PTEN
PTEN
p-mTOR (S2481)
Total mTOR
p-Akt (S473)
p-Akt (T308)
Total Akt
p-4EBP1 (S65)
Total 4EBP1
p-S6 (S240/244)
Total S6
GAPDH
C4-2
B
EV (Empty Vector)
WT-PTEN
Y138L-PTEN
G129E-PTEN
C124S-PTEN
PTEN
p-Akt (S473)
p-Akt (T308)
Total Akt
p-4EBP1 (S65)
Total 4EBP1
p-S6 (S240/244)
Total S6
GAPDH
PC-3

C

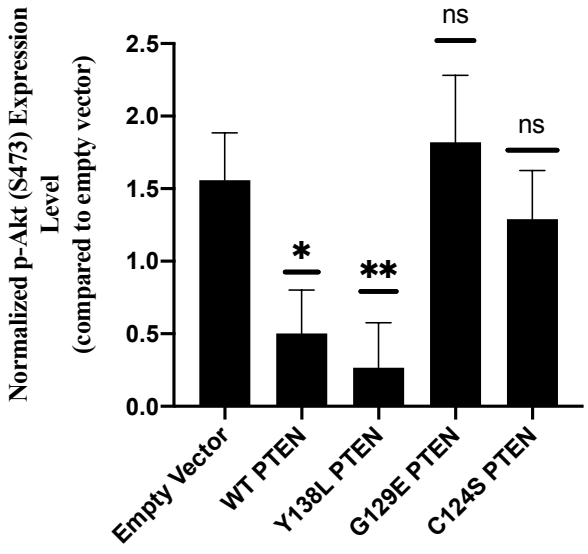
Normalized p-Akt (S473) Expression Level (compared to empty vector)
2.5
2.0
1.5
1.0
0.5
0.0
*
**
ns
ns
Empty Vector
WT PTEN
Y138L PTEN
G129E PTEN
C124S PTEN

Figure 3.4. PI3K pathway characterization of mCRPC cells following WT and different mutant forms of PTEN expression. A) C4-2 cells, **B)** PC-3 cells were induced with 0.02 - 1 μg/mL range of doxycycline for 72 hours. They were harvested and immunoblotting was performed with indicated antibodies. GAPDH was used as a loading control. **C)** Quantification of p-Akt(S473) protein levels in C4-2 cells (n=3, *p<0.05, **p<0.01). Error bars display S.D.

PTEN expression significantly downregulated the phosphorylation of Akt, main effector protein of PI3K pathway, at both T308 and S473 compared to empty vector ($p<0.05$, $p<0.01$ respectively) and no downregulation in phosphorylation of Akt was observed following G129E PTEN and C124S PTEN expressions **(Figure 3.4-C)**. Also, compared to empty vector, expression of WT PTEN and Y138L PTEN decreased p-mTOR (S2481) levels and phosphorylation level of 4EBP1, one of the main substrates of mTOR, dramatically decreased upon WT PTEN and Y138L PTEN expressions. Levels of p-S6 (Ser65) was not affected by any PTEN expression which signifies the crosstalk and feedback signals from other signaling pathways impinging on S6 protein **(Figure 3.4-A)**. In the light of immunoblotting results, WT PTEN and Y138L PTEN expressions antagonized the PI3K pathway by downregulating phosphorylation of effector proteins of the pathway. Antagonizing PI3K pathway by lipid phosphatase intact PTEN also explains the significantly downregulated viability of C4-2 cells after WT PTEN and Y138L PTEN (Figure 3.3C) which is a consequence of PI3K pathway downregulation by lipid phosphatase function of PTEN. The expression of G129E PTEN and C124S PTEN did not result in downregulation of phosphorylation of PI3K effector proteins. This implies that functions of PTEN in the PI3K pathway is mainly controlled by its lipid phosphatase rather than its protein phosphatase function.

According to the immunoblotting results of PC-3 cells **Figure (3.4-B)**, some level of downregulation in p-Akt (T308) and p-Akt (S473) level, following WT PTEN and Y138L PTEN respectively, was observed compared to empty vector. However, downregulation was not as prominent as the one exhibited by C4-2 cells. Additionally, phosphorylation of other downstream components of the pathway, e.g. p-4EBP1 and p-S6, were not reduced significantly in comparison to empty vector control. These results also explain the reason that why we did not observe any significant differences in viabilities of PC-3 cells upon WT PTEN and Y138L PTEN expressions (Figure 3.3-B&C). PC-3 cells developed some level of resistance to expressions of WT PTEN and Y138L PTEN so that the PI3K pathway and their proliferative potential were partially restrained. This might be due to baseline level of PTEN expression leakage without doxycycline induction in PC-3 cells allows them to receive feedbacks from other related signaling pathways and eliminate PTEN effects after culturing of them for a while. All in all, effects of WT PTEN and Y138L PTEN expressions were dramatic on PI3K pathway in C4-2 cells, as opposed to PC-3 cells, which is why we did not further continue experiments with PC-3 cells.

3.4. Targeted metabolomics analysis of C4-2 cells upon expression of PTEN and its variants

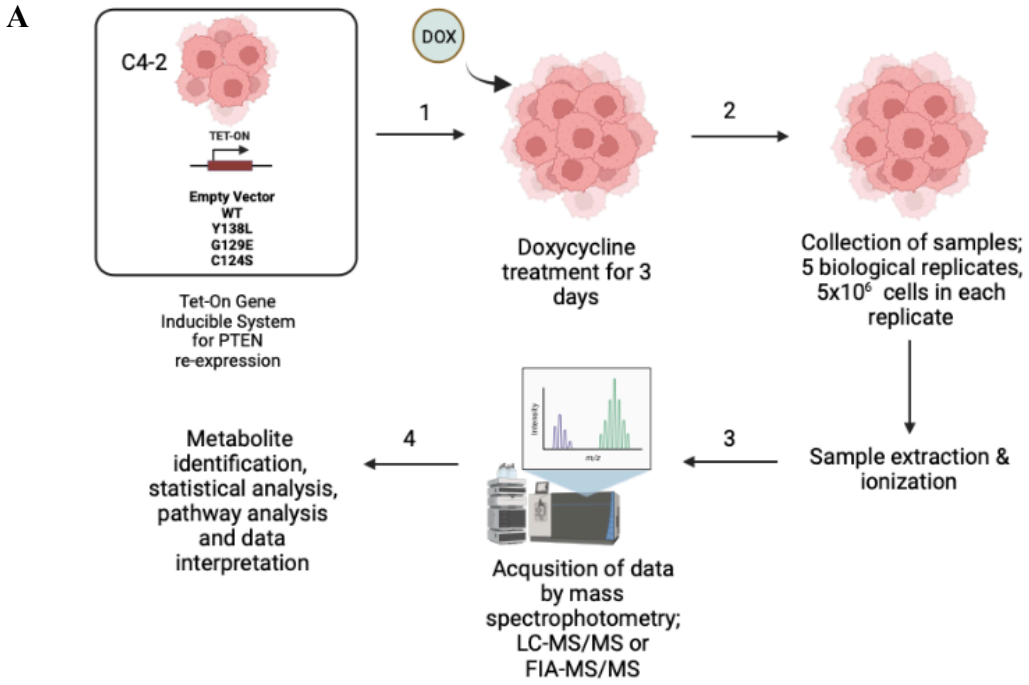

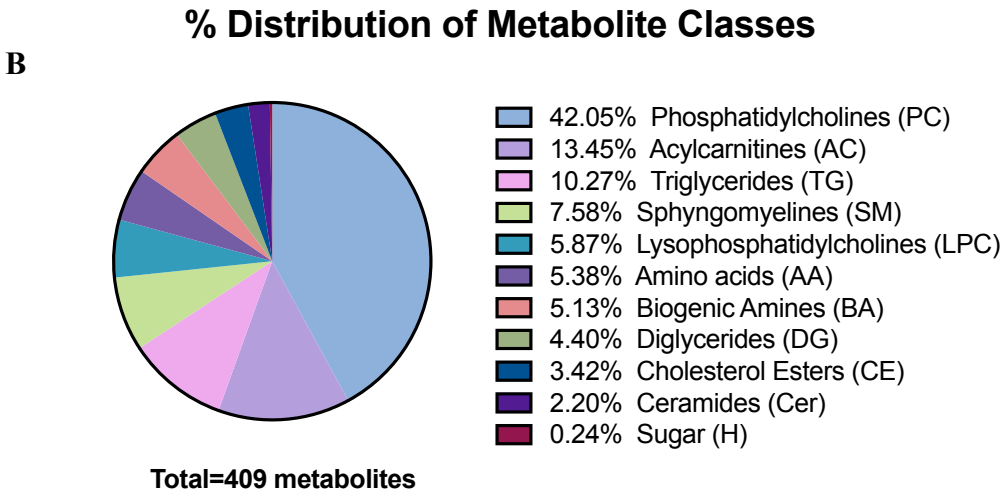

Figure 3.5. Targeted metabolomics approach. A) Workflow of targeted metabolomics analysis of C4-2 cells upon empty vector control and expression of WT and mutant PTEN versions. **B)** Classes and percentages of metabolites quantified in the analysis.

In order to reveal the systemic impact of PTEN loss in mCRPC, changes in the metabolome of C4-2 cells were analysed upon empty vector, WT and mutant PTEN expressions in a targeted metabolomics assay using Absolute*IDQ* p400HR metabolomics kit. For the analysis, we prepared 5 biological replicates and each replicate was counted to have the same number of cells ($5x10^6$ cells in each biological replicate) to enable metabolite normalization between samples. After, sample extraction and ionization, mass spectrometry analysis was done according to the metabolite groups in which either liquid chromatography mass spectrophotometry (LC-MS/MS) or flow injection analysis mass spectrophotometry (FIA-MS/MS) were used **(Figure 3.5-A).** This targeted metabolomics analysis allowed us to quantify 409 metabolites from the central metabolic pathways from 11 different classes. Percentages show the ratio of specific metabolite set amongst total 409 metabolites. **(Figure 3.5-B).**

3.5. Changes in the lipid metabolism of C4-2 cells upon expression of PTEN and its variants

A

Metabolites	C4-2			
	WT PTEN	Y138L PTEN	G129E PTEN	C124S PTEN
PC(42:7)	2.66	1.85	n.s	1.89
PC(42:6)	2.23	1.58	n.s	1.8
PC(42:5)	2.17	n.s	n.s	1.65
PC(40:4)	2.49	1.80	n.s	1.76
PC(40:3)	2.76	1.90	n.s	n.s
PC(40:2)	1.92	1.84	n.s	2.15
PC(32:2)	n.s.	0.59	1.70	n.s
PC(32:1)	n.s.	0.67	n.s	n.s
PC(31:2)	n.s.	0.59	n.s	n.s
PC(30:1)	n.s	n.s	1.73	n.s
PC(30:0)	n.s	n.s	1.51	n.s
PC(42:4)	2.29	n.s	n.s	1.86
PC(40:9)	2.54	2.51	2.44	3.19
PC(40:8)	1.51	n.s	n.s	n.s
PC(40:7)	2.00	n.s	n.s	n.s
PC(40:6)	1.92	n.s	n.s	n.s
PC(40:5)	2.81	n.s	n.s	n.s
PC(38:7)	1.75	0.63	n.s	1.58
PC(38:4)	1.55	1.67	n.s	1.93
PC(38:2)	2.08	1.75	n.s	1.89
PC(37:4)	1.95	1.64	n.s	n.s
PC(37:2)	1.65	n.s	n.s	n.s
PC(36:6)	n.s.	0.55	n.s	n.s
PC(36:1)	1.71	1.64	n.s	1.76
PC(34:5)	n.s.	0.62	1.82	n.s
PC(34:4)	n.s.	0.65	n.s	n.s
PC(34:3)	n.s.	0.59	1.89	n.s
PC(33:3)	0.57	n.s	n.s	n.s
PC(32:4)	n.s	n.s	1.77	2.06
PC(32:3)	n.s.	1.81	1.67	2.22
LPC(20:1)	n.s	1.63	n.s	n.s
LPC(16:1)	0.56	0.57	n.s	n.s
LPC(15:0)	0.58	n.s	n.s	n.s

Phosphatidylcholines

B

Metabolites	C4-2			
	WT PTEN	Y138L PTEN	G129E PTEN	C124S PTEN
PC-O(34:3)	n.s	0.60	n.s	n.s
PC-O(34:2)	n.s	0.63	n.s	n.s
PC-O(34:1)	0.56	0.50	n.s	n.s
PC-O(32:3)	n.s.	0.64	1.60	n.s
PC-O(32:2)	n.s.	0.61	n.s	n.s
PC-O(32:1)	0.51	0.41	1.54	n.s
PC-O(30:0)	0.43	0.47	1.54	n.s
PC-O (38:6)	1.84	n.s	n.s	n.s
PC-O (38:3)	n.s	n.s	n.s	1.53
PC-O (36:6)	n.s	0.65	n.s	n.s
PC-O(36:5)	n.s	0.51	0.54	0.55
PC-O(36:4)	n.s	0.61	1.88	n.s
PC-O(34:4)	n.s	0.39	n.s	n.s
PC-O(33:3)	0.66	0.55	n.s	n.s

Glycerophosphocholines

C

Metabolites	C4-2			
	WT PTEN	Y138L PTEN	G129E PTEN	C124S PTEN
SM(40:1)	1.67	3.13	n.s	2.12
SM(38:2)	1.90	2.29	n.s	n.s
SM(38:1)	2.31	4.14	n.s	1.83
SM (36:1)	n.s	1.60	n.s	n.s
SM(34:2)	0.64	n.s	n.s	n.s
SM(34:1)	0.66	n.s	n.s	n.s
SM(32:1)	0.62	n.s	n.s	n.s

Sphingomyelins

Figure 3.6. Effects of WT PTEN and its variants expression on lipid metabolism of C4-2 cells

Quantifications of targeted metabolomics data for selected metabolites; **A)** Phosphatidylcholines, **B)** Glycerophosphocholines and **C)** Sphingomyelins for C4-2 cells upon WT PTEN and mutants-PTEN expression. Tables depict metabolic changes in C4-2 cells for each PTEN variant and fold change (FC) values relative to empty vector levels were displayed. Colored cells indicate significant differences (FC>1.5 and $p<0.05$). Blue represents the downregulation, red represents the upregulation of metabolite, and n.s. represents non-significant fold changes of metabolites compared to empty vector. Each sample has at least three biological replicates.

Lipid metabolism has diverse effects on prostate cancers and dysregulation in lipid metabolism is a very a frequent consequence of reprogrammed metabolism in tumor cells [31]. Our targeted metabolomics analysis revealed changes in several lipid species in C4-2 cells upon WT or mutant PTEN re-expression **(Figure 3.6)**. Although most of the phosphatidylcholines (PC) inspected increased upon WT PTEN and Y138L PTEN expressions, some PCs were found to be decreased. PC (42:7), PC (42:6), PC (40:4) and PC (40:3) metabolite levels increased after WT PTEN and Y138L PTEN expressions compared to empty vector. Levels of these metabolites were significantly upregulated (FC > 1.5 and $p<0.05$) in either WT PTEN or Y138L PTEN expressing C4-2 cells. Also, expression of G129E PTEN (lipid phosphatase inactive) did not result in any significant difference in these metabolites, whereas expression of catalytically inactive PTEN (C124S) expression mostly resulted in increase, which indicates lipid phosphatase function of PTEN and also phosphatase-independent functions of PTEN were implied on biosynthesis of these metabolites **(Figure 3.6A)**. PC (32:2), PC (32:1) and PC (31:2) were significantly downregulated (FC<1.5 and $p<0.05$) by Y138L PTEN expression compared to empty vector but their levels did not change by the expression of WT and other mutants of PTEN, except for PC (32:2) whose level increased by G129E PTEN expression. This shows that lipid phosphatase function of PTEN influenced synthesis of these metabolites and protein phosphatase function of PTEN might compensate effects of lipid phosphatase function, since WT PTEN expression did not alter levels of these metabolites but G129E PTEN, protein phosphatase function intact, increased PC (32:2) level. Thus, on these three metabolites sets of phosphatidylcholines protein phosphatase and lipid phosphatase functions of PTEN showed opposite effects **(Figure 3.6A)**. Concordantly, PC (34:5) levels also did not change by WT PTEN expression, but its level decreased by Y138L PTEN expression and increased by G129E PTEN expressions. Thus, lipid phosphatase and protein

phosphatase functions of PTEN differentially regulates metabolic production of certain phosphatidylcholine species **(Figure 3.6A)**. Lysophosphatidylcholines (LPC) are also phosphatidylcholine derivatives which are produced by the action of an enzyme called phospholipase A. One fatty acid group removal by phospholipase A converts phosphatidylcholines to lysophosphatidylcholines (LPC) [71]. Levels of LPC (16:1) and LPC (15:0) had decrease upon WT PTEN expression and LPC (16:1) level showed decrease by both WT PTEN and Y138L PTEN expression compared to empty vector and levels of these LPCs were not affected by expression of G129E PTEN and C124S PTEN expressions. This implicates that lipid phosphatase function of PTEN had some impact on production of LPCs, whereas protein phosphatase and phosphatase independent functions of PTEN did not alter the levels of these two LPCs **(Figure 3.6A)**. Lastly, sphingomyelins were quantified as lipid metabolites. Sphingolipids are also crucial functions in the context of cancer biology. SM (40:1), SM (38:2) and SM (38:1) levels had significant increases in their fold changes upon WT PTEN and Y138L PTEN expression, compared to empty vector (FC>1.5) and amongst them SM (38:2) showed significant increase (FC>1.5 $p<0.05$) in its level by WT PTEN and Y138L PTEN. None of these three metabolites showed significant fold differences by G129E PTEN expression and expression of C124S PTEN resulted in upregulation of both SM (40:1) and SM (38:1) **(Figure 3.6C)** Thus, lipid phosphatase function of PTEN had significant impacts on regulation of these metabolites and phosphatase-independent functions of PTEN had some impacts on regulation of these metabolites but it is not that prominent as lipid phosphatase function of PTEN. In addition to these, protein phosphatase function of PTEN did not have influence on levels of these three sphingomyelin metabolites. On the other hand, levels of SM (34:2), SM (34:1) and SM (32:1) levels had significant fold change differences compared to empty vector by WT PTEN expression which causes downregulation of levels of these

metabolites. However, protein phosphatase and phosphatase-independent mutants of PTEN did not affect regulation of these metabolites **(Figure 3.6C)**.

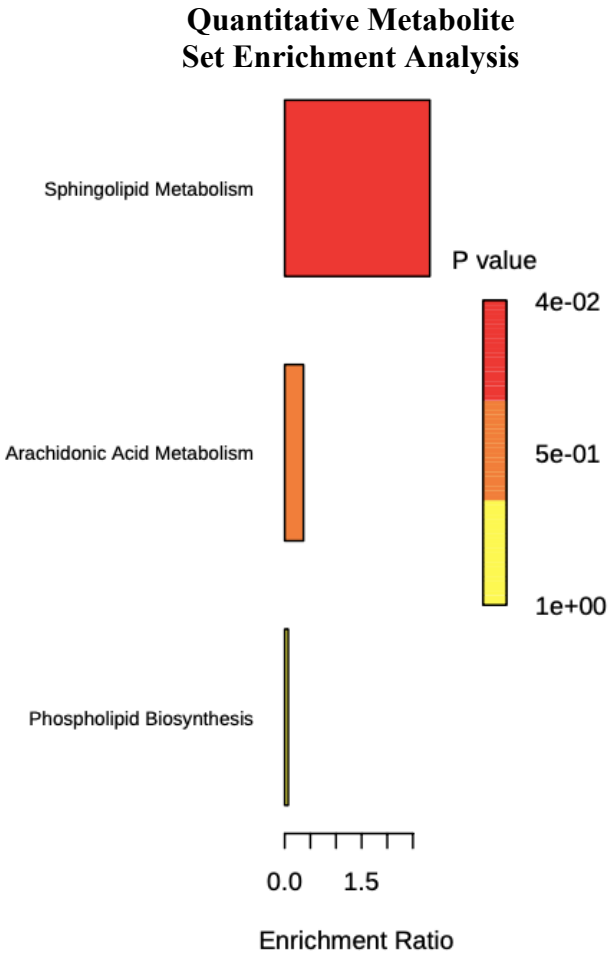

Figure 3.7. **Expression of WT PTEN and Y138L PTEN resulted in enrichment of sphingolipid metabolism of C4-2 cells.** Quantitative metabolite set enrichment analysis was done for lipid metabolites of C4-2 cells expressing WT PTEN and Y138L PTEN. Each sample has at least three biological replicates.

Since, we observed most of the differences, upregulations and downregulations, in lipid metabolites levels of C4-2 cells following WT PTEN and Y138L PTEN expressions, we analyzed metabolite set enrichment of these cells. Enrichment analysis revealed that sphingolipid metabolisms of WT PTEN and Y138L PTEN expressing C4-2 cells significantly enriched compared to empty vector ($p<0.05$) **(Figure 3.7)**.

Sphingolipids have broad range of functions on tumor cells by regulating their growth, death, inflammation and as well as angiogenesis. Ceramide, a central molecule of sphingolipid metabolisms, is known to have anti-proliferative effects on tumor cells by inducing apoptosis. Whereas, sphingosine-1-phosphate (S1P) has pro-survival functions on tumor cells. Thus, balance of ceramide: S1P level is critical for the fate of tumor cells. Sphingosine is produced from ceramide by the action of acid ceramidase enzyme named ASAH1. Sphingosine is further phosphorylated to produce S1P. Sphingosine kinase 1 and 2 are the enzymes catalyzing phosphorylation reactions of sphingosine to produce S1P [72]. According to targeted metabolomics analysis and enrichment analysis, sphingolipids metabolism of C4-2 cells enriched upon lipid phosphatase intact PTEN expressions, which is why we wanted to analyze mRNA expression level of genes that encode key enzymes involved in sphingolipid biosynthesis. WT PTEN C4-2 cells and Empty Vector C4-2 cells were induced with doxycycline for three days and RT-qPCR experiment was performed **(Figure 3.8)**.

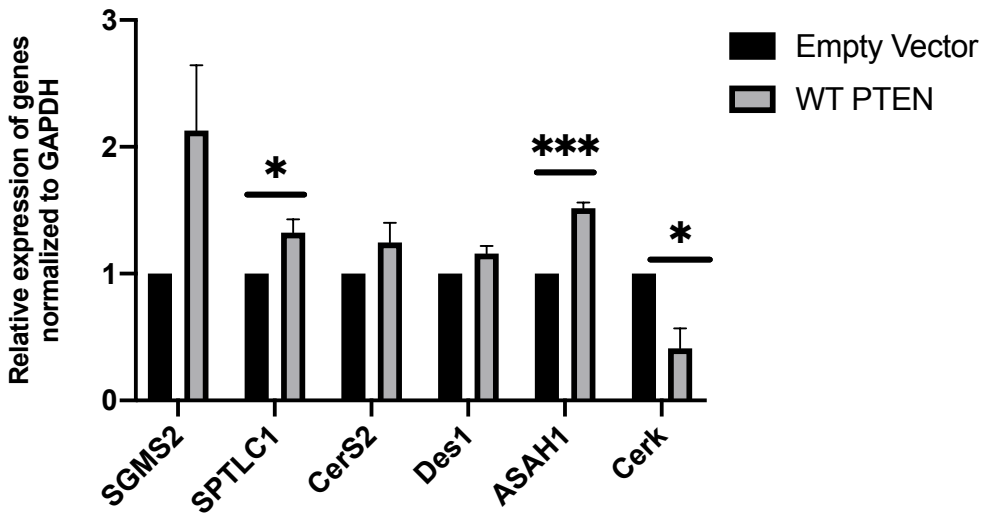

Figure 3.8. Relative mRNA expression levels of genes involved in sphingolipid metabolism upon WT PTEN expression. RT-qPCR experiment was performed following three days of doxycycline induction of C4-2 cells and fold differences of genes were quantified compared to empty vector. GAPDH was used as a housekeeping gene. (n=3 ***$p<0.001$, *$p<0.05$). Error bars display SEM.

According to RT-qPCR result, except for Cerk gene, mRNA expression levels all other genes had an increasing trend compared to empty vector. mRNA level of SPTLC1 gene which is the first enzyme in sphingolipid biosynthesis significantly upregulated upon WT PTEN expression ($p<0.05$). Additionally, acid ceramidase enzyme, ASAH1, mRNA level significantly increased upon WT PTEN expression compared to empty vector ($p<0.001$). Meanwhile mRNA level of Cerk gene, which encodes the enzyme that catalyzes production of Ceramide-1-P from ceramide, significantly downregulated upon WT PTEN expression compared to empty vector ($p<0.05$). These RT-qPCR experiments revealed that mRNA levels of genes that encode key enzymes for ceramide biosynthesis increased and it pointed out that upon WT PTEN expression, cells were tend to increase anti-survival ceramide accumulation and decrease pro-survival S1P.

3.6. Changes in the cholesterol metabolism of C4-2 cells upon expression of PTEN and its variants

Cholesterol Esters

A

Metabolites	C4-2			
	WT PTEN	Y138L PTEN	G129E PTEN	C124S PTEN
CE(22:5)	0.33	0.45	n.s	n.s
CE(22:6)	0.43	0.49	n.s	n.s
CE(20:5)	0.44	n.s	n.s	n.s

B

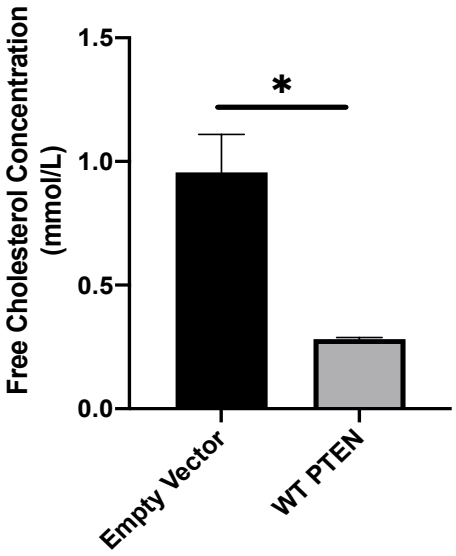

Figure 3.9. WT PTEN and Y138L PTEN expression impaired the cholesterol metabolism of C4-2 cells. A) Quantifications of targeted metabolomics data for selected cholesterol ester metabolites of C4-2 cells upon WT PTEN and mutants-PTEN expression. Table depicts metabolic changes of C4-2 cells for each PTEN variants and fold change (FC) values relative to empty vector metabolite levels. Colored cells indicate significant differences (FC>1.5 and $p<0.05$). Blue represents the downregulation of metabolite, and n.s. represents non-significant (below 1.5 FC threshold) fold changes of metabolites compared to empty vector. Each sample has at least three biological replicates. **B)** Free cholesterol concentration of C4-2 cells upon empty vector and WT PTEN expressions. (n=2 *$p<0.05$)

Cholesterol esters are important biological molecules and they are synthesized through esterification reactions of free cholesterols in the cell. Our targeted metabolomics approach revealed quantifications of certain of cholesterol esters in C4-2 cells upon WT PTEN and mutants PTEN expressions. Both of CE (22:5) and CE (22:6) had significantly downregulated levels (FC>1.5 and $p<0.05$) upon WT PTEN and Y138L PTEN expression compared to empty vector, whereas G129E PTEN and C124S PTEN expressions did not affect levels of these two cholesterol esters in C4-2 cells **(Figure 3.9-A)** This suggests that lipid phosphatase function of PTEN regulates the cholesterol ester levels in C4-2 cells. Additionally, supporting the changes in CE (22:5) and CE (22:6), CE (20:5) level significantly decreased (FC>1.5 and $p<0.05$) upon WT PTEN expression and other PTEN mutants did not affect its level **(Figure 3.9-A)**. Changes observed in the levels of these three cholesterol esters upon WT and Y138L PTEN expression indicates that cholesterol ester level in the cells are affected by the lipid phosphatase function of PTEN. Since cholesterol esters are product of free cholesterols in the cells, we also wanted to see if PTEN expression affects free cholesterol biosynthesis in the cells. Thus, C4-2 cells were induced with doxycycline for expression of empty vector and WT PTEN and free cholesterol assay was performed to quantify and compare free cholesterol concentration of empty vector and WT PTEN expressing C4-2 cells. Free cholesterol assay results revealed that WT PTEN expression significantly decreased the free cholesterol concentration of C4-2 cells ($p<0.05$), compared to empty vector **(Figure 3.9-B)**. Empty vector expressing cells had 0.95 mmol/L concentration of free cholesterol, whereas WT PTEN expressing cells had 0.28 mmol/L of free cholesterol which accounts for 70% decrease in free cholesterol concentration.

Thus, our all three experiments regarding cholesterol metabolism of C4-2 cells; targeted metabolomics, immunoblotting and free cholesterol assay results enlighten that loss of lipid phosphatase function of PTEN causes metabolic rewiring of C4-2 cells for cholesterol biosynthesis.

Since we observed significantly impaired cholesterol metabolism in C4-2 cells upon WT and Y138L PTEN expressions, we aimed to investigate the mRNA expression levels of key genes involved in cholesterol biosynthesis pathways to see if there is a regulation in the transcriptional level. WT PTEN C4-2 cells and Empty Vector C4-2 cells were induced with doxycycline for three days and RT-qPCR experiment was performed. According to RT-qPCR result, except for MVK gene, mRNA expression levels all other genes had an increasing trend compared to empty vector. However, none of the genes gave significant mRNA expression level differences compared to empty vector **(Figure 3.10-A)**.

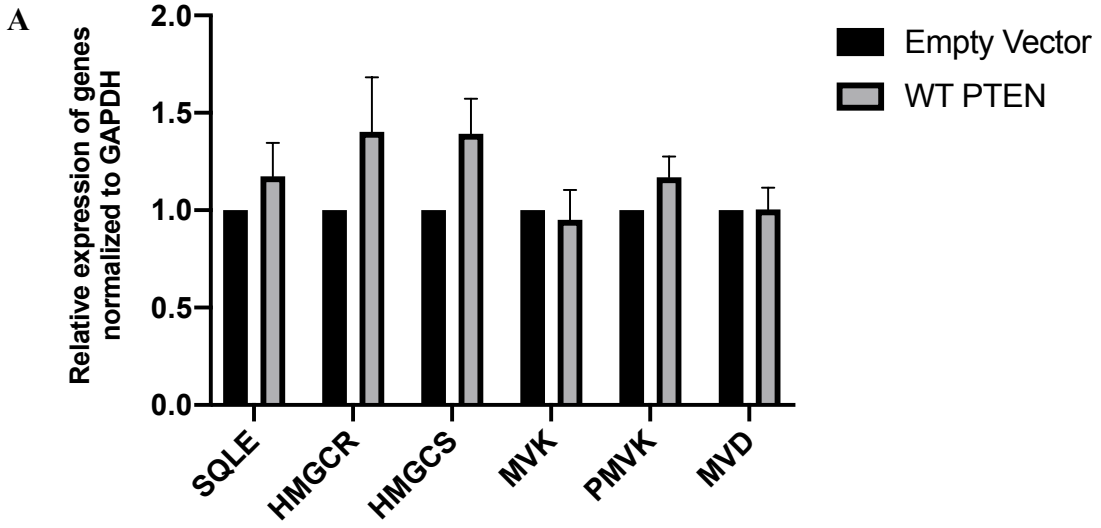

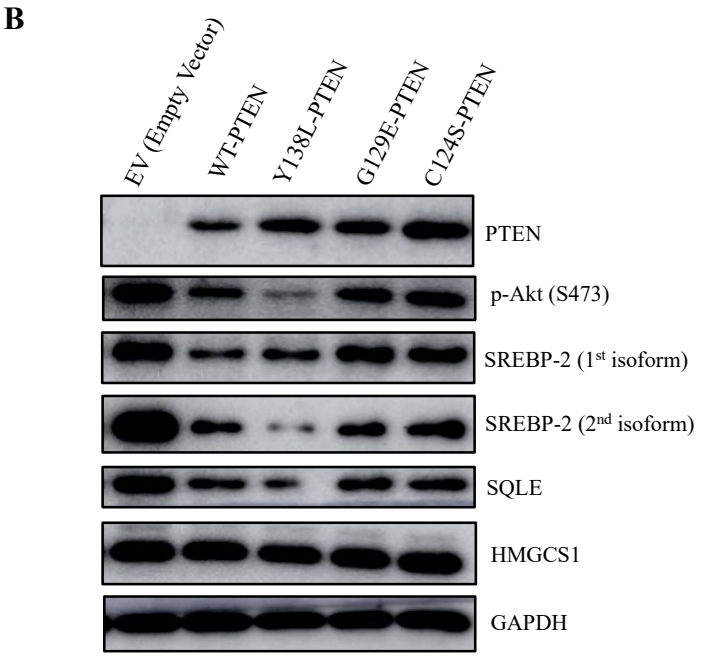

Figure 3.10. mRNA and protein expression levels of genes involved in cholesterol metabolism upon WT PTEN expression. A) RT-qPCR experiment was performed following three days of doxycycline induction of C4-2 cells and fold differences of genes were quantified compared to empty vector. GAPDH was used as a housekeeping gene. n=3, Error bars display SEM. **B)** Immunoblotting of C4-2 cells after treatment with 0.02 - 1 μg/mL range of doxycycline for 72 hours. Cells were harvested and immunoblotting was performed with indicated antibodies. GAPDH was used as a loading control.

We also profiled protein expression levels of key genes involved in cholesterol biosynthesis in order to see if there is a regulation in the protein level. Again, we induced C4-2 cells with doxycycline for 72 hours and immunoblotting was performed to investigate expression levels of key enzymes involved in cholesterol biosynthesis **(Figure 3.10-B)**. SREBP-2 is a master transcription factors and cholesterol biosynthesis are tightly regulated by action of SREBP-2 in the cell. Immunoblotting results showed that upon WT PTEN and Y138L PTEN expression,

SREBP-2 expression level decreased compared to empty vector and also compared to levels of G129E and C124S PTEN expressing C4-2 cells.

In addition to SREBP-2, expression level of SQLE, rate-limiting enzyme of cholesterol biosynthesis pathway, downregulated by expression of WT PTEN and Y138L PTEN compared to empty vector **(Figure 3.10-B)**. However, protein level of HMGCS which catalyzes the first reaction in synthesis of cholesterol, did not change by expression of PTEN. Thus, as concordant with targeted metabolomics data which revealed that cholesterol esters level in C4-2 cells downregulated by lipid phosphatase function of PTEN,and free cholesterol assay data, expression level of key proteins of cholesterol biosynthesis pathway also decreased by WT PTEN and Y138L PTEN, and expression of G129E PTEN and C124S PTEN did not cause any significant changes on them.

3.7. IC_{20} and IC_{50} calculation for inhibitors of determined metabolic pathways

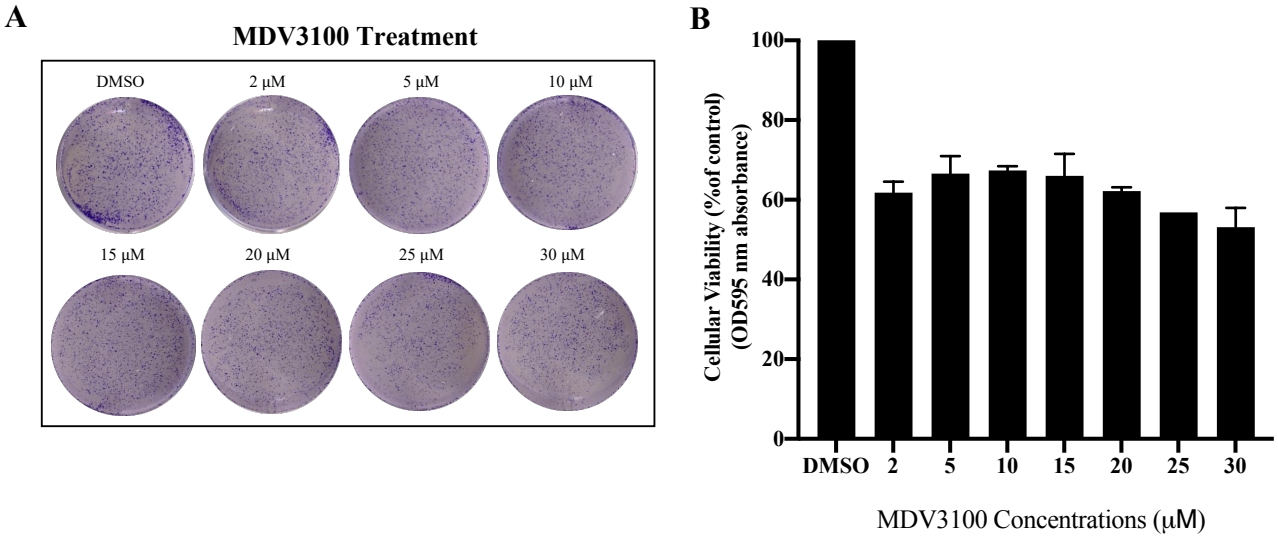

Figure 3.11. Cellular viability of C4-2 cells treated with increasing concentration of AR antagonist, MDV3100. A) Representative image of crystal violet cellular viability assays of C4-2 cells after treatment with different concentrations of MDV3100, B) Quantification of crystal violet stain. n=2, error bars display S.D.

Androgen deprivation therapy (ADT) in which castration and androgen agonist drugs are combined, currently is the most effective treatment for prostate cancers. Although ADT prolongs the overall survival of patients with advanced prostate cancers, emergence of CRPC eliminates ADT, makes disease incurable and resistant to therapy [8]. MDV3100 (Enzalutamide) is a recent, second-generation pharmacological inhibitor of the androgen receptor (AR). It inhibits the activation of AR signaling by blocking binding of androgen to the AR and thus the translocation of AR to the nucleus as well as recruitment of some co-activators [7,8]. C4-2 cells have been derived from metastatic, castration-resistant and androgen-independent human prostate cancer cells. They are inherently resistant to androgen deprivation therapy and also to MDV3100 due to

their ability of androgen-independent growth and it has been reported that MDV3100 has more of a cytostatic effect on C4-2 cells in short-term treatments than a cytotoxic effect and they are resistant to MDV3100 treatment for long-term treatments [74]. We revealed the metabolic vulnerabilities in cholesterol and sphingolipid metabolisms of these cells that are caused by re-expression of PTEN by our metabolomics data and we wanted to sensitize C4-2 cells to MDV3100 by targeting the determined metabolic pathways in combination with MDV3100 treatment. Hence, first we wanted to confirm effects of MDV3100 on C4-2 cell line by crystal violet cellular viability assay. C4-2 cells were treated with increasing concentrations of MDV3100 (up to 30 μM) for 5 days and stained with crystal violet **(Figure 3.11-A)**. In line with previous reports, C4-2 cells showed 40% initial growth inhibition but they did not response further to MDV3100 treatments. From 2 μM to 30 μM, cells showed similar growth inhibition and MDV3100 exhibited cytostatic effects on C4-2 cells growth **(Figure 3.11-B).**

Our metabolomics results signified that enrichment in sphingolipid biosynthesis of C4-2 cells upon PTEN expression. RT-qPCR experiments also showed that PTEN expressions resulted in upregulation mRNA levels of the genes involved in sphingolipid biosynthesis pathways and changes in the mRNA levels pointed out that cells were in tendency to increase anti-survival ceramide level and decrease pro-survival S1P level upon WT PTEN expression. With the light of these results, we wanted to target sphingolipid metabolism of C4-2 cells with pharmalogical inhibitors that lead to accumulation of ceramides and combine these inhibitors with MDV3100 to observe if combination of two drugs lead to synergistic effect. Thus, we employed two inhibitors for that purpose which are ABC294640 (Opaganib) and ARN14988.

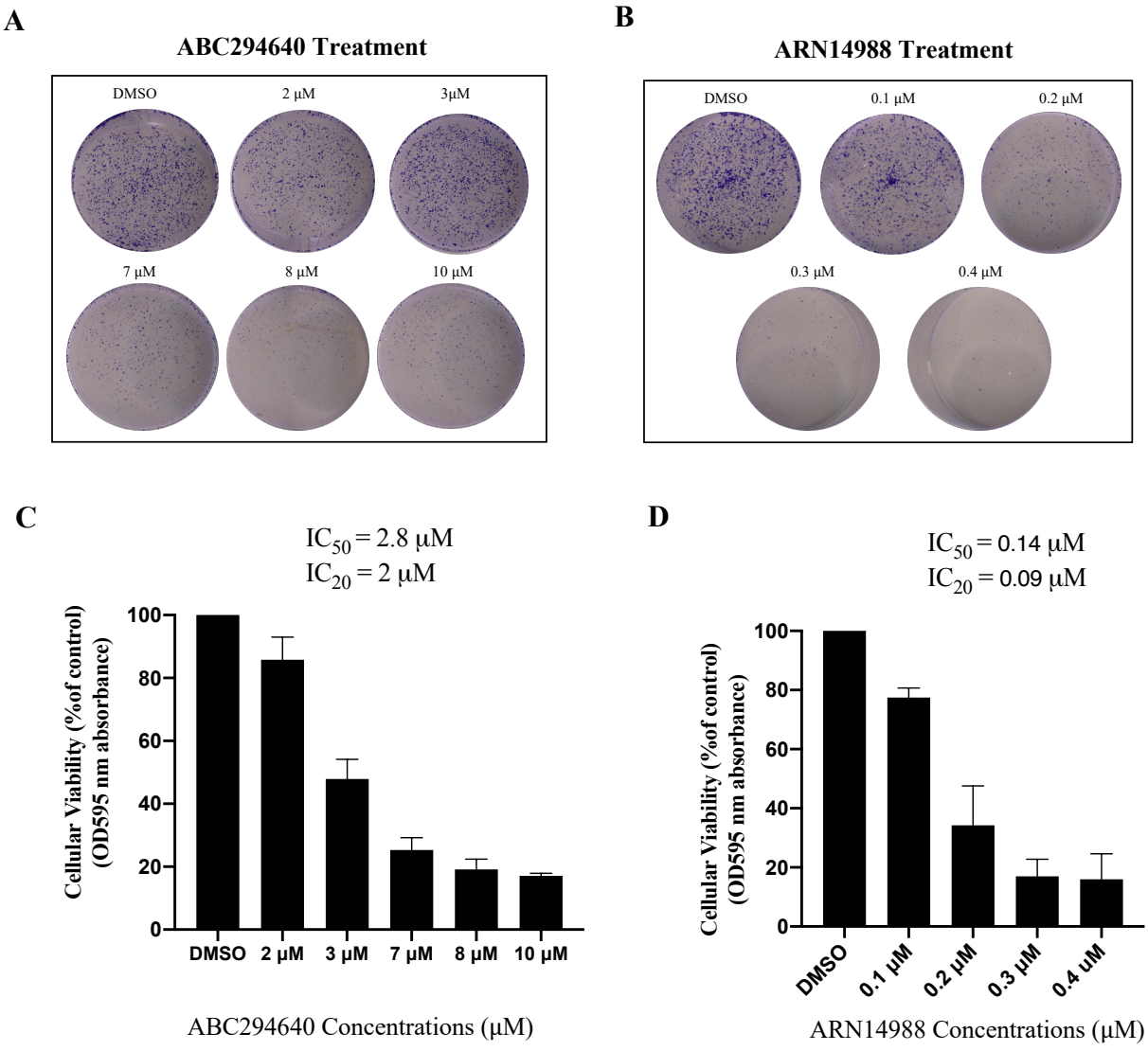

Figure 3.12. Cellular viability of C4-2 cells treated with increasing concentration sphingolipid metabolism inhibitors; ABC294640 and ARN14988. Representative images of crystal violet cellular viability assays of C4-2 cells after treatment with different concentrations of inhibitors; **A)** ABC294640, **B)** ARN1988. Quantifications of crystal violet stain and IC values of inhibitors; **C)** ABC294640, **D)** ARN1988. n=2, error bars display S.D.

ABC294640 (Opaganib) is a SK2 inhibitor so that it inhibits production of S1P and leads to accumulation of anti-proliferative ceramide in cells [74] ARN14988 is an inhibitor of acid ceramidase, ASAH1 and it prevents hydrolysis of ceramides to produce sphingosine, as a result sphingosine synthesis and following S1P synthesis are compromised. Thus, both ABC294640 and ARN14988 inhibitors target sphingolipid metabolism in order to prevent production S1P and increase ceramide levels in tumor cells. [75,76]. In order to perform combinatorial treatments first, we performed crystal violet cellular viability assay to determine IC_{50} and IC_{20} values of the aforementioned sphingolipid metabolism inhibitors on C4-2 cells. To that end, we treated C4-2 cells with increasing doses of inhibitors for 5 days and stained with crystal violet **(Figure 3.12-A&B)**. Quantification of crystal violet assay showed the respective cellular viabilities of the treatment groups **(Figure 3.12-C&D)**. C4-2 cells have IC_{50} value of 2.8 μM and IC_{20} value of 2 μM for ABC294640, SK2 inhibitor **(Figure 3.12-C)** and IC_{50} value of 0.14 μM and IC_{20} value of 0.09 μM for ARN14988, ASAH1 (acid ceramidase) inhibitor **(Figure 3.12-D)**.

According to targeted metabolomics results some cholesterol esters as well as levels of key proteins involved in cholesterol biosynthesis were significantly decreased upon expression of WT PTEN and Y138L PTEN. Simvastatin is an HMG-CoA reductase inhibitor which is one of the first enzymes that catalyzes conversion of HMG-CoA to mevalonate and it is also first late-limiting enzyme of the pathway. It is a widely used cholesterol-lowering agent especially in the treatment of cardiovascular diseases and recent studies have demonstrated that in many cancer types statins have significant impacts in prevention of cancer angiogenesis [62]. Hence, we wanted to target the cholesterol metabolism of C4-2 cells with simvastatin and possibly combine cholesterol synthesis inhibition with MDV3100.

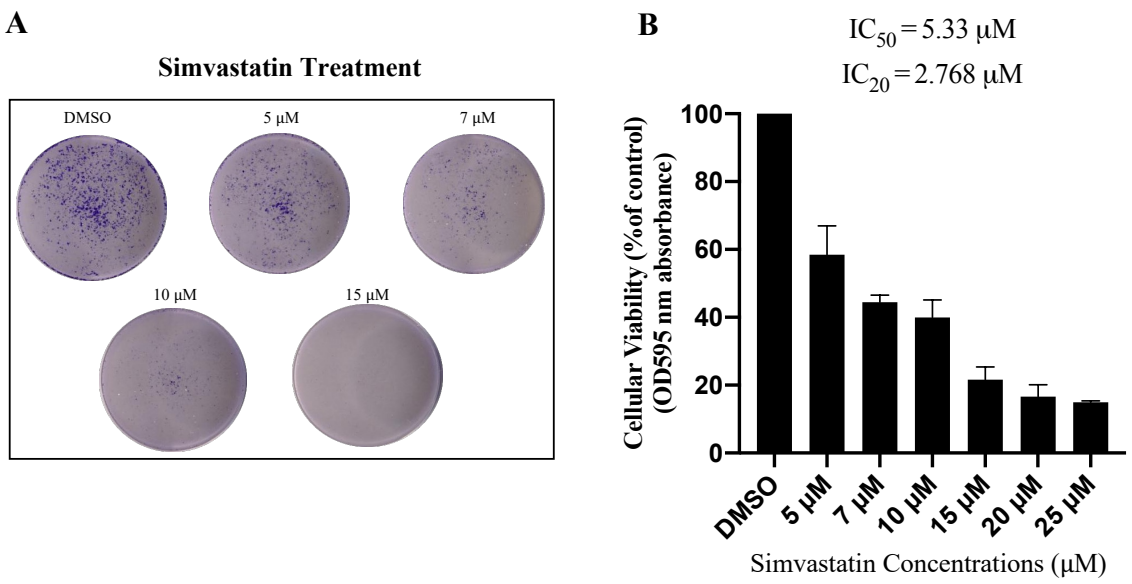

Figure 3.13. Cellular viability of C4-2 cells treated with increasing concentration HMG-CoA reductase inhibitor, simvastatin. A) Representative images of crystal violet cellular viability assays of C4-2 cells after treatment with different concentrations of simvastatin. **B)** Quantifications of crystal violet stain and IC values of simvastatin. n=2, error bars display S.D.

First, we investigated the effects of simvastatin on cellular viability of C4-2 cells by treating them with increasing dose of simvastatin and calculated IC_{20} and IC_{50} values to be used for further combinatorial treatments. C4-2 cells treated within a range of 5 µM to 25 µM for 5 days and then they were stained with crystal violet **(Figure 3.13-A)**. Quantification of the crystal violet cellular viability assay showed that C4-2 cells have IC_{20} value of 2.768 µM and IC_{50} value of 5.33 for simvastatin and after 15 µM concentration of simvastatin cells almost completely died **(Figure 3.13-B)**.

3.8. Combinatorial drug treatments of C4-2 cells with MDV3100-sphingolipid metabolism inhibitors and MDV3100-cholesterol metabolism inhibitor.

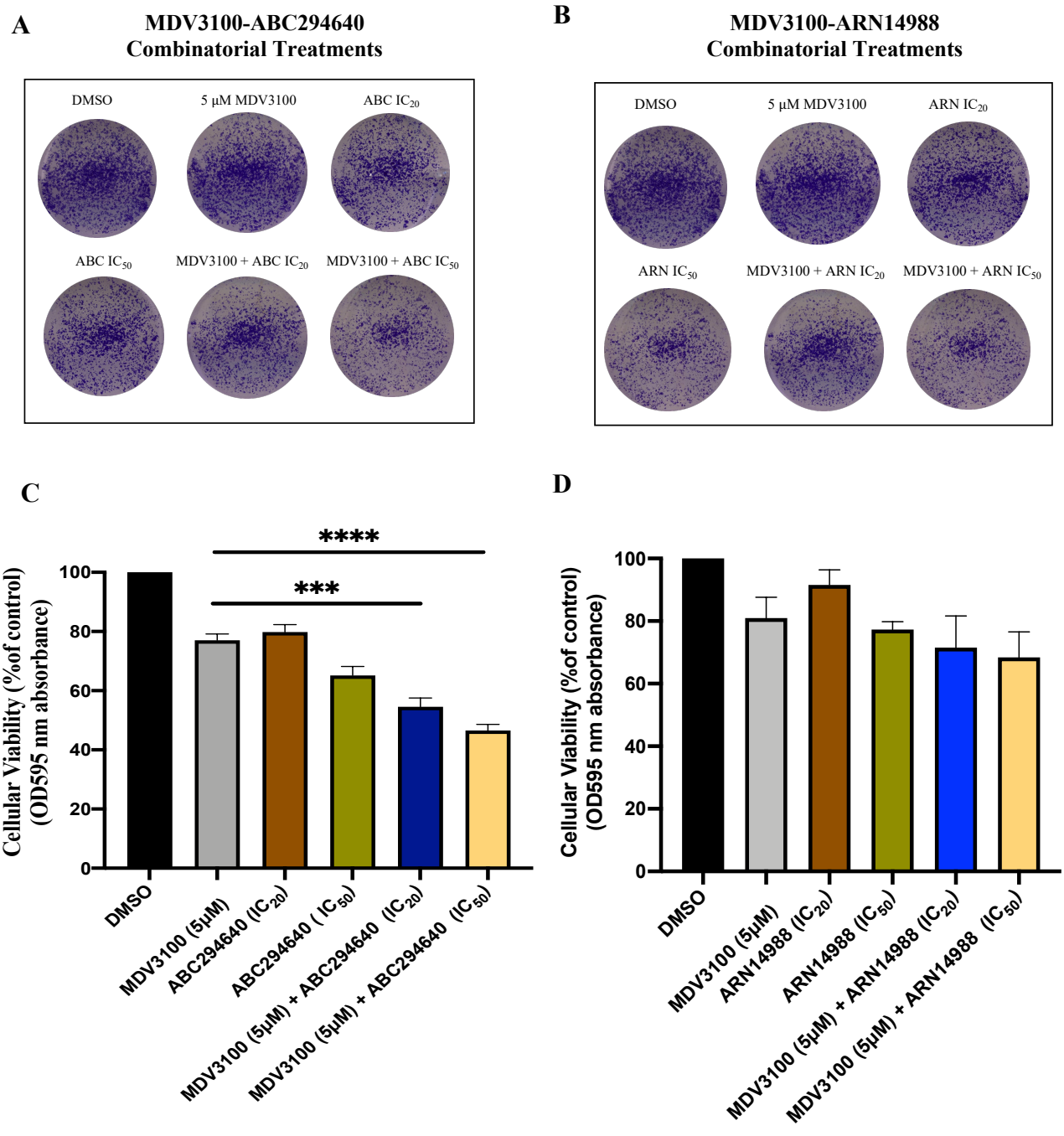

Figure 3.14. Combinatorial drug treatments of C4-2 cells with MDV3100-ABC294640 and MDV3100-ARN14988. Representative images of crystal violet cellular viability assays of C4-2 cells after for **A)** MDV3100-ABC294640 and **B)** MDV3100-ARN14988 combinatorial treatments. Quantifications of crystal violet stain and cellular viabilities of C4-2 cells upon combinatorial treatments with **C)** MDV3100-ABC294640 and **D)** MDV3100-ARN14988. n=3, error bars display S.D. ***p<0.001, ****p<0.0001.

Next, we aimed to investigate the possible synergistic effects of combining MDV3100 with sphingolipid metabolism inhibitors. For combinatorial treatments, 5 μM MDV3100 was combined with either IC_{20} and IC_{50} doses of inhibitors and cells were treated for 5 days for each concentration and stained with crystal violet **(Figure 3.14-A&B)**. In ABC294640 combinations experiment, C4-2 cells had 77% viability after 5 μM MDV3100 treatment alone and their viabilities decreased to 55% and 47% by combining 5 μM MDV3100 with IC_{20} and IC_{50} doses of ABC294640 respectively. We also calculated the Coefficient of Drug Combinations (CDI) values for MDV3100-ABC294640 drug combinations. CDI values smaller than 1 shows synergism of two drugs and if it is smaller than 0.7, it means two drugs result in significant synergistic effect [90]. For the combination of 5 μM MDV3100 with IC_{20} dose of ABC294640, we obtained CDI value as 0.93 and for 5 μM MDV3100 combination with IC_{50} dose of ABC294640 CDI value was calculated as 0.9. CDI values of combinatorial treatments are close 1 so that indicates these combinations are weakly synergistic. Although, cellular viability significantly decreased upon combination of two drugs compared to MDV3100 only treatment group, effects were more additive rather than a complete synergistic **(Figure 3.14-C)**.

In ARN14988 combinations experiment, C4-2 cells had 80% viability after 5 μM MDV3100 treatment alone and their viabilities decreased to 71% and 68% by combining 5 μM MDV3100 with IC_{20} and IC_{50} doses of ARN14988 respectively **(Figure 3.14-D)**. ARN14988 showed less effects on viability of C4-2 cells compared to ABC294640 and it also had an additive effect on viability of C4-2 cells. Thus, both of sphingolipid metabolism inhibitors displayed additive effect of cellular viability when they were combined with MDV3100.

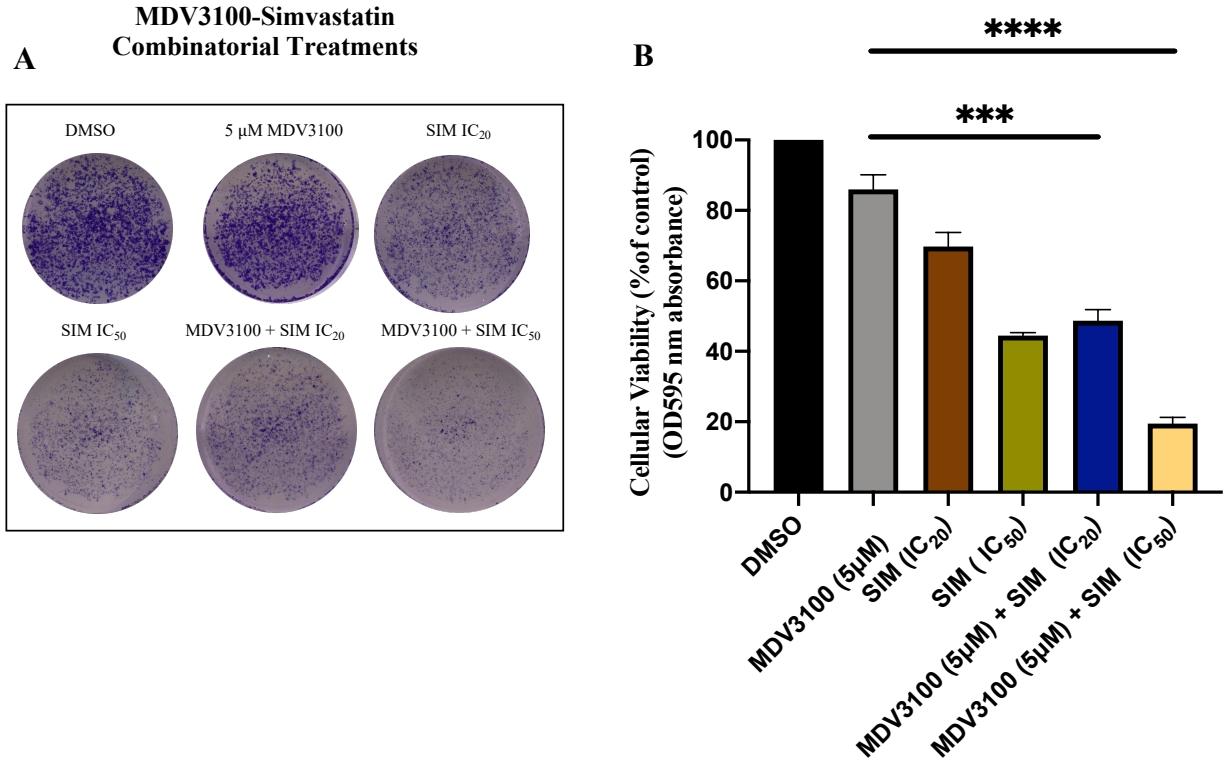

Figure 3.15. Combinatorial drug treatments of C4-2 cells with MDV3100 and Simvastatin. **A)** Representative images of crystal violet cellular viability assays of C4-2 cells after for each treatment. **B)** Quantifications of crystal violet stain and cellular viabilities of C4-2 cells upon treatments. (n=3, ***p<0.001, ****p<0.0001) Error bars display S.D.

Combinatorial treatments were performed with simvastatin in addition to sphingolipid metabolism inhibitors. Same experimental setup, as we did for sphingolipid and MDV3100 combinations, was followed for simvastatin and MDV3100 combinations. Cells were treated with drugs for 5 days and stained with crystal violet **(Figure 3.15-A)**. 5 µM of MDV3100 treatment decreased viability of C4-2 cells to 85% and IC_{20} and IC_{50} doses of simvastatin decreased viability of cells to 70% and 44% respectively. Combination treatment of cells with 5 µM MDV3100 and either with IC_{20}

and IC_{50} doses of simvastatin resulted 48% and 19% cellular viabilities respectively **(Figure 3.15-B)**. Statistical analysis showed that comparison between viabilities only 5 μM MDV3100 treated and 5 μM MDV3100-Sim IC_{20} treated cells and only 5 μM MDV3100 treated and 5 μM MDV3100-Sim IC_{50} treated cells resulted in significantly decreased viabilities where $p<0.001$ and $p<0.0001$ respectively **(Figure 3.15-B)**.

For the combination of 5 μM MDV3100 with IC_{20} dose of simvastatin, CDI values were calculated as 0.81 and for 5 μM MDV3100 combination with IC_{50} dose of simvastatin CDI value was calculated as 0.5, which indicate that these combinations of MDV3100 with IC_{20} and IC_{50} doses of simvastatin resulted in synergistic effect and for the latter combination it resulted in significant synergistic effect on C4-2 cells. Therefore, combinations of two drugs, simvastatin and MDV3100, showed synergistic effects on cellular viability of C4-2 cells.

CHAPTER 4

4. DISCUSSION

Prostate cancer is the second most diagnosed type of cancer after lung cancer in males worldwide. Despite significant research studies and efforts in last few decades to elucidate molecular mechanism and factors contributing to prostate cancer angiogenesis, among males it is still second frequent malignancy. [77]. Currently, there are many different treatments for prostate cancer including chemotherapy, surgery and hormonal therapies, however, all these methods come with many different adverse effects on patients without significant responses. [78]. Androgen signaling is a key mediator of prostate cancer development and progression, which is why androgen depletion therapies, either with surgery (castration) and/or with androgen antagonist drugs, was considered as a promising therapeutic way for prevention of prostate cancer progression. However, ability of prostate cancers to develop resistance mechanisms to androgen-depletion and other therapies and to transform themselves into castration-resistant and androgen independent growth state completely destroys effectiveness of androgen deprivation therapies and leave this disease without any effective treatments [79]. Thus, elucidation of the molecular mechanisms that contribute to progression and development of resistance mechanisms against therapeutics is crucial to understand nature of prostate cancers and contribute to efforts for development of novel treatments.

Amongst many different hallmarks of cancer cells, metabolic reprogramming is considered as early and one of the most significant hallmarks, since it enables uncontrolled growth, survival, metastasis and development of resistance mechanisms to treatments of cancer cells by providing energy and necessary intermediate molecules to support high demand of energy need and

biosynthesis of macromolecules. [80]. PI3K pathway has central a role in regulating cellular growth, metabolism and survival of cells. This pathway is mainly overactivated due to some oncogenic mutations in crucial pathway components in cancers including prostate cancers and many other cancer types. PTEN is a tumor suppressor and the negative regulator of PI3K pathway and it is a dual phosphatase by having enzymatic activity to dephosphorylate both its protein and lipid phosphatases. It antagonizes the PI3K pathway by dephosphorylating its lipid substrate PIP_3 and converting it to PIP_2 so that PTEN tightly controls the PI3K pathway. Loss of function mutations in PTEN is a very frequent and early event in many cancer types including prostate cancers. Large chromosomal deletions or point mutations in PTEN gene have been detected in many cancer types which results in oncogenic activation of PI3K/Akt/mTOR axis and contribute carcinogenesis [33]. Recent studies have been demonstrated that loss of PTEN had significant impacts in metabolic reprogramming for example, loss of PTEN leaded to overexpression in some enzymes involved in fatty acid biosynthesis in prostate cancer and promoted Warburg effect. In addition to that, in transgenic mice models, overexpression of PTEN suppressed the Warburg effect by increasing oxidative phosphorylation and decrease in glucose uptake and mice exhibited healthier metabolisms compared to PTEN-loss counterparts [38]. All these studies indicate that PTEN-loss is a driver for metabolic reprogramming of cancer cells. Thus, in this study, we revealed consequences of PTEN-loss on metabolome of metastatic and castration-resistant prostate cancers which are advanced stage of prostate cancers with PTEN-null background and without any effective treatments currently.

PTEN expression was established in C4-2 and PC-3 prostate cancer cell lines by utilizing Tet-On gene expression system. Since PTEN is not stably expressed and only expressed after induction with doxycycline, this system allowed us to profile acute and dynamic effects of PTEN expression

on cells. Tet-on system was preferred in our experimental setup because when PTEN expression is stable, cancer cells may become irresponsive after some point by receiving feedbacks from other signaling pathways and adapting them. Along with WT PTEN, we also aimed to investigate lipid phosphatase, protein phosphatase and also phosphatase-independent functions of PTEN on cellular metabolism independently, which why we established Tet-on PTEN expression system with mutant variants of PTEN as well.

First, we investigated the effects of PTEN re-expression on PI3K/Akt/mTOR axis and cellular viabilities. WT PTEN and Y138L PTEN expression resulted in significant decreases in p-Akt (S473) level which is the main effector of the PI3K pathway and G129E PTEN and C124S PTEN expression did not affect p-Akt levels compared to empty vector in C4-2 cells. These findings confirm that lipid phosphatase activity of the PTEN downregulates the PI3K pathway and protein phosphatase and phosphatase-independent functions of PTEN did not affect the pathway (Figure 3.1 A). However, in PC-3 cells WT PTEN expression downregulated the p-Akt (S473) level compared to empty vector p-Akt levels but Y138L PTEN expression did not affect the p-Akt level and also effects of WT PTEN expression are not that much prominent as we observed in C4-2 cells (Figure 3.1 B). Immunofluorescence experiments revealed that WT PTEN expression significantly reduced PIP_3 signal on the membrane and catalytically inactive (C124S) PTEN expression did not affect PIP_3 signal which also indicates lipid phosphatase function of PTEN in antagonizing the PI3K pathway (Figure 3.2). We also investigated PTEN re-expression on cellular viabilities of C4-2 and PC-3 cells. In C4-2 cells, expression of WT PTEN and Y138L PTEN caused significant decrease in cellular viabilities compared to empty vector, whereas G129E PTEN and C124S PTEN did not decrease viabilities. In contrast, none of PTEN expressions affected the viability of PC-3 cells compared to empty vector so PC-3 cells showed resistance to PTEN re-expression (Figure

3.3). Since WT PTEN and Y138L PTEN expressions had impact on viabilities of C4-2 cells and no effect on PC-3 cells, we aimed to characterize these cells in expression profiles of PI3K pathway components following PTEN expressions by immunoblotting. Upon WT PTEN and Y138L PTEN expressions, except for p-S6, C4-2 cells exhibited downregulation in phosphorylation level of key effector proteins of the PI3K pathway including p-Akt (S473 and T308), p-mTOR and p-4EBP1 compared to empty vector protein levels. Although PC-3 cells had some level of downregulation in the levels of p-Akt (S473) and p-Akt (T308) by Y138L PTEN and WT PTEN expressions compared to empty vector, differences were not promising and also effects of PTEN were not reflected in downstream protein components of the pathway. These immunoblotting results explains the cellular viability results where C4-2 cells had significantly decreased viabilities upon WT PTEN and Y138L PTEN expressions, which was due to restraining of PI3K pathway by lipid phosphatase function of PTEN. It also explains the unaffected viabilities of PC-3 cells upon WT and Y138L PTEN expressions, since PI3K pathway effector proteins level did not change dramatically. Higher number of subculturing and baseline leakage expression in PC-3 cells might activate other signaling pathways and feedback signals coming from them could compensate the activity of PTEN in these cells and make the cells irresponsive to PTEN re-expression. That is why, PC-3 cells were not included in further experiments.

Metabolites are essential constituents of cells, since they serve as building blocks for accumulation of biomass and signaling pathways, especially the ones related with growth, are regulated by metabolites. That is why, metabolic reprogramming is a must for cancer progression. Revealing metabolic vulnerabilities of cancer cells and targeting them to develop new therapeutics against cancer cells are an active research area in cancer biology [81].

Hence, we performed targeted metabolomics analysis with metabolomics kit. Our Tet-On gene expression system allowed us to profile dynamic and acute changes in the metabolome of cells right after PTEN expression. Although the kit is designed for robust quantification of volatile metabolites in mostly serum samples which have abundant metabolite concentrations compared to cell samples, we were able to quantify and observe some trends in different classes of metabolites upon WT and mutants PTEN expression in mCRPC cells. Lipid metabolism of C4-2 cells exhibited changes by PTEN expressions in phosphatidylcholines, glycerophosphocholines and sphingomyelins. Some sets of phosphatidylcholines tended to increase upon lipid phosphatase intact (WT and Y138L) PTEN expressions and also catalytically inactive (C124S) PTEN expression, whereas protein phosphatase function of PTEN did not have significant impact on the levels of those metabolites. Also, Y138L PTEN expression resulted in significant decrease in comparison to empty vector control in three sets of phosphatidylcholines whose level did not change by expression of other PTEN mutants. These results indicate that lipid phosphatase function and phosphatase-independent functions of PTEN had impact on biosynthesis of these phosphatidylcholines (Figure 3.6-A). In addition to that, quantification of glycerophosphocholines revealed that lipid phosphatase intact PTEN expression (Y138L PTEN) significantly downregulated the biosynthesis of 7 different glycerophosphocholines and their levels mostly did not change by G129E and C124S PTEN expressions which indicates that biosynthesis of these metabolites were affected by lipid phosphatase intact PTEN expression. On other hand, as a last set of lipid metabolites, sphingomyelins were quantified and we observed that WT and Y138L PTEN expressions significantly increased the level of some sets of sphingomyelins and also some of them decreased by WT PTEN expression and did not get affected by other PTEN expressions. Quantifications of these lipid metabolites unveiled that mostly lipid phosphatase and phosphatase-

independent functions of PTEN influenced biosynthesis of lipid metabolites. Previous reports demonstrated tumor microenvironment had increased lipid metabolism including choline metabolites which are linked to promote cancer cells for metastasis, transformation and other cancerogenic phenotypes especially in hormone-dependent, breast and prostate cancers. [82]. In order to interpret these changes in lipid metabolism of C4-2 cells, we performed metabolite set enrichment analysis (MSEA) to understand which metabolic pathways were altered by changes in the level of these lipid metabolites. Since most of the significant changes correspond to lipid-phosphatase intact PTEN expression compared to empty vector, MSEA were performed between empty vector, WT PTEN and Y138L PTEN expressing cells. This analysis demonstrated that sphingolipid metabolism of these cells significantly altered and enriched ($p<0.05$). After sphingolipid metabolism, arachidonic acid and phospholipid biosynthesis pathways also enriched but they were not statistically significant (Figure 3.7). In addition to lipids, we observed significant changes in cholesterol esters level upon WT PTEN and Y138L PTEN expressions. Lipid phosphatase intact PTEN significantly downregulated three different cholesterol ester molecules, which are synthesized from free cholesterols, and they were not affected by G129E and C124S PTEN expressions which points that lipid phosphatase function of PTEN had significant impacts on biosynthesis of these cholesterol esters (Figure 3.8-A).

After revealing the impaired metabolic pathways, we performed literature search on sphingolipid and cholesterol metabolisms in prostate cancers. Sphingolipids have diverse and context-dependent functions in tumor microenvironment. They are known to be regulating growth and survival of tumor cells as well as angiogenesis. Ceramide, which is the central metabolite in sphingolipid metabolisms, possesses anti-survival functions on tumor cells with interfering apoptotic pathways, whereas sphingosine-1phosphate (S1P) which is further metabolite produced

hydrolysis of ceramides have pro-survival effects on tumor cells as opposed to ceramide. Thus, balancing cellular ceramide: S1P level is crucial for tumor growth [48,50].

Cholesterol metabolism is also associated with many cancer types, especially the hormone-dependent breast and prostate cancers. It has been showed that cholesterol levels are elevated in most of the cancer types. As a result of fast and uncontrolled proliferation, cancer cells have to maintain their membrane biogenesis and cholesterol is an indispensable part of the membrane so increase in cholesterol level supports rapid proliferation of cancer cells. Beside its structural properties, cholesterol has other functions in cells such as it is required for synthesis of steroid hormones which are drivers for hormone-dependent prostate cancers [61,62]. Cholesterol esters are directly produced from free cholesterol via esterification reactions and Yue et. al revealed that PTEN-loss induces the accumulation of cholesterol esters due to activation in the PI3K/Akt pathway which promotes aggressiveness of prostate cancers [68]. Thus, as consistent with our targeted metabolomics results and literature findings, both of sphingolipid and cholesterol metabolisms have alterations upon PTEN-loss in cancer cells and they have significant impacts on tumor development and progression.

Next, we aimed to investigate these metabolic pathways more detailed in C4-2 cells. First, we checked and compared the mRNA expression level of the key genes involved in sphingolipid biosynthesis pathway, between empty vector and WT PTEN expressing cells. Most of the genes had increased mRNA expression upon WT PTEN expression, except for Cerk gene. mRNA expression of Cerk gene, which encodes an enzyme catalyzing ceramide to ceramide-1-P reaction, was significantly downregulated upon WT PTEN expression compared to empty vector. Also, mRNA level of ASAH1 gene had significant increase upon WT PTEN expression. This enzyme is known as an acid ceramidase which hydrolysis ceramide and produce S1P. However, ASAH1

enzyme can work in both direction in the pathway according to subcellular localization of the enzyme and also pH of the tumor microenvironment [83]. Thus, these increasing trend in mRNA levels of enzymes catalyzing biosynthesis of ceramide and decreasing in the mRNA levels Cerk whose activity reduces the ceramide level in cells, indicate that WT PTEN expression resulted changes in sphingolipid metabolism to increase anti-survival ceramide levels by changing mRNA expression levels of the key enzymes involved in the pathway. These results also shed light into how PTEN-loss contribute cancer cells growth. It suggests that loss-of PTEN in C4-2 cells cause metabolic reprogramming in sphingolipid metabolism to decrease anti-survival ceramide which support their growth and proliferation.

In cholesterol metabolism aspect, we first checked the free cholesterol concentration of C4-2 cells upon WT PTEN expressions. Since cholesterol esters are produced from free cholesterols, downregulation in cholesterol esters levels might be due to changes in free cholesterol levels and we observed that upon WT PTEN expressions, free cholesterol concentration of C4-2 cells significantly decreased compared to empty vectors (Figure 3.9-B). These results showed that there are significant decreases in cholesterol esters and free cholesterol levels of C4-2 cells upon WT PTEN expressions which directed us to investigate mRNA and protein expression level of key enzymes involved in cholesterol biosynthesis. Since WT PTEN expression had significant impact on cholesterol levels, regulation of key enzymes might also be altered. To that end, we first analyzed the mRNA expression levels of genes encoding those enzymes. However, we did not observe any significant differences in the mRNA level of these genes in comparison between WT PTEN and empty vector expressing cells. All genes, except for MVK, had an increasing trend in their mRNA levels but none of these differences were significant (Figure 3.10-A) Then, we criticized that three days doxycycline induction of C4-2 cells to re-express PTEN might not be

sufficient duration to observe some changes in the mRNA level and/or there might be post-translational modifications on the protein level of these genes. In order to see if the latter reason is the case, we performed immunoblotting after three days doxycycline induction in all PTEN variants C4-2 cells and checked the expression levels of key proteins regulating cholesterol biosynthesis (Figure 3.10-B). Protein levels of SREBP-2, master transcription factor for cholesterol biosynthesis, and SQLE, rate-limiting enzyme of the pathway, were downregulated upon WT and Y138L PTEN expression compared to empty vector and their levels did not change by G129E and C124S PTEN expressions (Figure 3.10-B). This immunoblotting result suggests that there is a protein-level regulation in cholesterol biosynthesis upon lipid phosphatase intact PTEN expressions.

Currently, the most effective therapy against prostate cancer is androgen-deprivation therapies by surgery and medicines in order to block androgen signaling and prevent progression of prostate tumor cells [84]. Although androgen-deprivation therapy is effective to suppress tumor growth at the first line and prolongs overall survival of patients, emergence of CRPC completely destroys efficacy of androgen-deprivation therapies. MDV3100 (Enzalutamide) is an androgen receptor antagonist and it is the most frequently prescribed FDA-approved drug in treatment of prostate cancers as an androgen-deprivation therapy. It is a second-generation inhibitor of androgen receptor and comparing its counterparts e.g., bicalutamide, binding affinity of MDV3100 to androgen receptor is much higher and also it inhibits androgen signaling with three different ways. It can block androgen receptor by binding, interfere with nuclear translocation of androgen receptor and recruitment of co-activators [85]. Thus, it is currently most effective androgen antagonist.

C4-2 cells are metastatic, castration-resistant prostate cancer cell line and they are able to grow in an androgen-independent state and these properties make C4-2 cells extremely lethal and incurable. With the light of all these information, our initial aim was to reveal metabolic vulnerabilities of C4-2 cells caused by loss-of PTEN and targeting their metabolic vulnerabilities along with MDV3100 treatment to sensitize C4-2 cells to MDV3100 and determine possible synergistic effects. Re-expression of PTEN resulted significant changes on the sphingolipid and cholesterol metabolisms of C4-2 cells so that we wanted to target these metabolic pathways. Our analysis showed that PTEN expressions caused trends in sphingolipid metabolisms of C4-2 cells which was to increase their ceramide levels to suppresses survival of cancer cells. Meanwhile, we also revealed C4-2 cells exhibited significantly increased cholesterol metabolism upon PTEN-loss in order to support their fast growth. Thus, we selected inhibitors of sphingolipid and cholesterol biosynthesis pathways and wanted to combine these inhibitors with MDV3100.

First, we wanted to see response of C4-2 parental cells to MDV3100 and determine MDV3100 concentration to be used in further drug combinations experiments. Cells were treated with increasing dose of MDV3100. C4-2 cells exhibited initial response to MDV3100 at 2 μM which resulted in 40% decrease in cell viability compared to DMSO control. However, cells did not further respond to MDV3100 treatment up to 30 μM and they showed resistance to growth inhibition by MDV3100 (Figure 3.11). Since C4-2 cells are able to grow in an androgen-independent state, MDV3100 did not have cytotoxic effects on growth of these cells. Effects of MDV3100 is cytostatic on C4-2 cells rather than cytotoxic. We decided to continue combination experiments with 5 μM dose of MDV3100. These cells gain resistance to MDV3100 treatment (androgen-deprivation therapy) by sustaining their androgen signaling via different mechanisms including activation of mutant androgen receptors, binding of different ligands to androgen

receptor which are not able to bind and initiate signaling under normal physiological conditions also splice variants of androgen receptors. All these adaptations help prostate cancer cells to maintain their growth under androgen-deprived conditions [9,11].

Second, we investigated the effects of inhibitors of sphingolipid and cholesterol biosynthesis pathways and determined IC_{50} and IC_{20} doses of inhibitors in C4-2 parental cells. For sphingolipid metabolism, as PTEN expression resulted changes towards accumulation of ceramide, we wanted to follow same strategy in our combinatorial treatments. Hence, we selected ARN14988 and ABC294640 inhibitors for targeting the sphingolipid metabolism of C4-2 cells. ARN14988 is an inhibitor of acid ceramidase enzyme, named ASAH1. Under normal physiological conditions, acid ceramidase prevents hydrolysis of ceramide to produce sphingosine which is used as a precursor to synthesize pro-survival signaling molecule for cancer cells; Sphingosine-1-Phosphate (S1P). ABC294640 is a Sphingosine Kinase-2 inhibitor which is the enzyme catalyzing reaction to synthesize pro-survival S1P from sphingosine. Basically, by using these inhibitors we aimed to decrease pro-survival S1P accumulation and increase anti-survival ceramide accumulation. Also, for targeting the cholesterol metabolism, we selected HMG-CoA reductase inhibitor named simvastatin. Simvastatin is commonly prescribed cholesterol-lowering drugs especially for cardiovascular diseases and it has been reported by number of different studies that proliferation of various cancer types was compromised by simvastatin [62]. It inhibits cholesterol biosynthesis from very beginning of the pathway by preventing formation of mevalonate from HMG-CoA so it is a suitable inhibitor to reveal PTEN-loss and cholesterol metabolism relationship in prostate cancers. C4-2 parental cells were treated with increasing doses of simvastatin and IC values were determined. To that end we determined IC_{50} and IC_{20} values of each inhibitor by cellular viability assays (Figure 3.12 & Figure 3.13).

In the last part, we performed combinatorial drug treatments of C4-2 parental cells by combining MDV3100 with inhibitors from determined metabolic pathways; sphingolipid and cholesterol metabolisms. Due to high heterogenicity and adaptation capacity to develop resistance against therapies, monotherapies in prostate cancers could not be effective to combat disease in a full extent, which is why combinatorial therapies exhibited higher rate of success in suppressing or eliminating the disease [86]. Thus, we combined sphingolipid and cholesterol metabolism inhibitors with MDV3100 (Figure 3.14). Combination of sphingolipid inhibitors with MDV3100 resulted in more of additive effects in viabilities of C4-2 cells rather than synergistic effect. Although ABC294640 combination with MDV3100 had CDI value close to 1 and resulted in significant decreases on cellular growth compared to MDV3100-only treatment group, it did not lead to complete synergisms and it exhibited weak synergism. Also, ARN14988 combination with MDV3100 did not reduce the cellular viability significantly compared to MDV3100-only treatment and this combination did not lead any synergism. We performed 5 days, short term, treatments on C4-2 cells with these inhibitors and these short-term treatments might not be as effective as long-term treatments. These inhibitors affect sphingolipid pathways to support accumulation of ceramide and metabolites are not abundant molecules in cells so more time might be required to allow accumulation of ceramide and observe its effects on cellular growth. In addition to that, prostate cancers have high heterogenicity and these 2D culture treatments might not reflect behavior of these cells as in the tumor microenvironment. It has been shown that 3D such as spheroids cell culture treatments are more successful to imitate *in vivo* responses of cancer cells especially in drug responses [88,89].

Meanwhile combinatorial treatment experiments were performed with MDV3100 and simvastatin. This combination resulted in synergism of two drugs on inhibiting growth of C4-2 cells (Figure

3.15). Combination of IC_{20} dose of simvastatin with MDV3100 had CDI value of 0.81 which points synergism of two drugs and also compared to single MDV3100 treatment, simvastatin (IC_{20}) – MDV3100 resulted in significant decrease on cellular viabilities of C4-2 cells. Additionally, Combination of IC_{50} dose of simvastatin with MDV3100 had CDI value of 0.5 which indicates significant synergism of two drugs in suppressing cellular growth and again compared to single MDV3100 treatment, simvastatin (IC_{50}) – MDV3100 resulted in significant decrease on cellular viabilities of C4-2 cells. Since simvastatin inhibits cholesterol biosynthesis pathway from initial stage of the pathway, its effect in cholesterol biosynthesis shows up rapidly. That is why, we observed synergism of simvastatin-MDV3100 combination even in the short-term treatments.

All in all, we first time showed that PTEN-loss causes metabolic reprogramming in sphingolipid and cholesterol biosynthesis of mCRPC. Targeting these pathways in combination with MDV3100 resulted significant decreases in cellular viabilities. Especially, compromising cholesterol biosynthesis pathway with simvastatin resulted in synergistic drug combination and sensitized C4-2 cells to MDV3100. Thus, targeting cholesterol pathway in combination with androgen-deprivation therapy would be a promising approach to develop new combinatorial therapies and combat mCRPCs.

CHAPTER 5

5. CONCLUSIONS AND FUTURE PERSPECTIVES

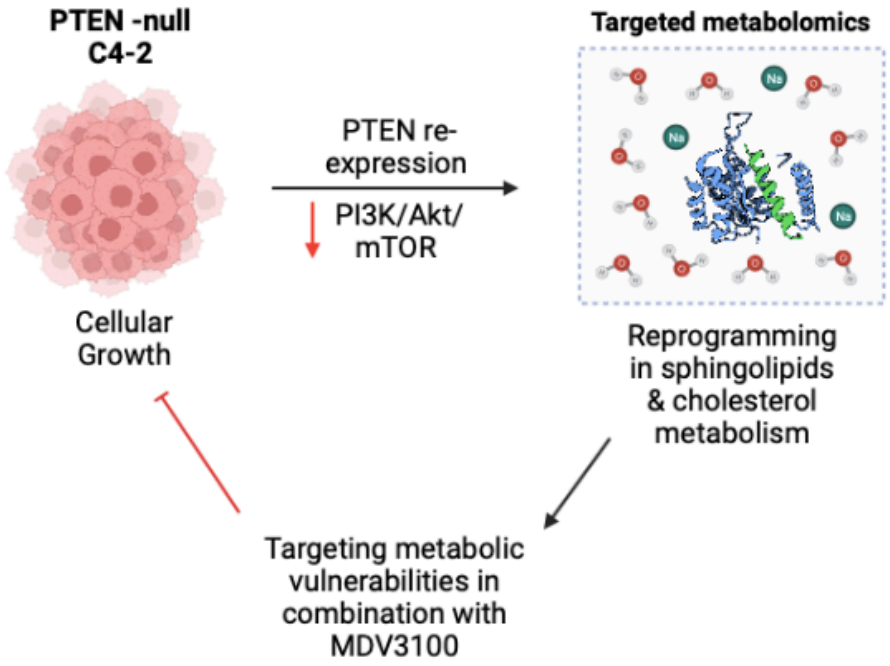

Graphical abstract of the study

In this study, we investigated the effects of PTEN-loss on metabolome of metastatic and castration-resistant prostate cancers. By re-expression of WT PTEN and mutant variants of PTEN, we inspected effects of lipid phosphatase, protein phosphatase and phosphatase-independent individually. Re-expression of lipid phosphatase intact PTEN expressions downregulate PI3K/Akt/mTOR axis and decreased survival of cells significantly. Then, we observed effects of WT and mutants PTEN re-expression on metabolome of mCRPC cells by targeted metabolomics. According to metabolomics data, we revealed that loss-of PTEN caused reprogramming in sphingolipid and cholesterol metabolism of mCRPC cells which boost their rapid and uncontrolled

cell division. Targeting these metabolic vulnerabilities of cells in combination with MDV3100, which is ineffective in treatment of mCRPC patients, resulted in significant decreases in cellular growth and targeting cholesterol biosynthesis pathway in combination with MDV3100 showed synergistic effects in suppressing the cellular growth. Complex heterogenicity and evolutions of gaining resistance against treatments of prostate cancers eliminate treatment options and significantly reduce the efficacy of monotherapies, which is why identifying and targeting vulnerabilities of prostate cancers in combination with other treatments could increase efficacy of therapies. Thus, cholesterol biosynthesis pathway would be a promising target to be used in combinatorial treatments in prostate cancer patients.

Targeted metabolomics approach with commercial kit was not able to quantify all the cellular metabolites. Since kit is mostly designed for measuring metabolite levels in metabolite-abundant serum samples, it was not fully successful in determining low abundant metabolites in the cells. Thus, as one of the future perspectives, total ceramide levels would be quantified in these cells after PTEN re-expressions which might give more insight about metabolic reprogramming in sphingolipid pathway and tendency of cells to accumulate anti-survival ceramide levels following PTEN re-expression. In addition to that, 2D drug treatments may not reflect *in vivo* effects of the drugs for each case and prostate cancers have high heterogenicity and dynamic tumor microenvironment, which is why performing drug combination experiments in 3D cell cultures such as spheroids might give better insight about effects of drug combinations on cellular growth. Lastly, for sphingolipid metabolism part, protein expression levels of genes involved in the pathway would be investigated after PTEN re-expression in order to gain more insight on mechanism about cellular tendency for accumulation of ceramide.

BIBLIOGRAPHY

[1] Rebello, R., Oing, C., Knudsen, K., Loeb, S., Johnson, D., & Reiter, R. et al. (2021). Prostate cancer. *Nature Reviews Disease Primers*, *7*(1). doi: 10.1038/s41572-020-00243-0

[2] Rawla, P. (2019). Epidemiology of Prostate Cancer. *World Journal Of Oncology*, *10*(2), 63-89. doi: 10.14740/wjon1191

[3] Sandhu, S., Moore, C., Chiong, E., Beltran, H., Bristow, R., & Williams, S. (2021). Prostate cancer. *The Lancet*, *398*(10305), 1075-1090. doi: 10.1016/s0140-6736(21)00950-8

[4] Sumanasuriya, S., & De Bono, J. (2017). Treatment of Advanced Prostate Cancer—A Review of Current Therapies and Future Promise. *Cold Spring Harbor Perspectives In Medicine*, *8*(6), a030635. doi: 10.1101/cshperspect.a030635

[5] Dai, C., Heemers, H., & Sharifi, N. (2017). Androgen Signaling in Prostate Cancer. *Cold Spring Harbor Perspectives In Medicine*, *7*(9), a030452. doi: 10.1101/cshperspect.a030452

[6] Fujita, K., & Nonomura, N. (2019). Role of Androgen Receptor in Prostate Cancer: A Review. *The World Journal Of Men's Health*, *37*(3), 288. doi: 10.5534/wjmh.180040

[7] Shafi, A., Yen, A., & Weigel, N. (2013). Androgen receptors in hormone-dependent and castration-resistant prostate cancer. *Pharmacology &Amp; Therapeutics*, *140*(3), 223-238. doi: 10.1016/j.pharmthera.2013.07.003

[8] Zhou, Y., Bolton, E., & Jones, J. (2014). Androgens and androgen receptor signaling in prostate tumorigenesis. *Journal Of Molecular Endocrinology*, *54*(1), R15-R29. doi: 10.1530/jme-14-0203

[9] Huang, Y., Jiang, X., Liang, X., & Jiang, G. (2018). Molecular and cellular mechanisms of castration resistant prostate cancer (Review). *Oncology Letters*. doi: 10.3892/ol.2018.8123

[10] Coutinho, I., Day, T., Tilley, W., & Selth, L. (2016). Androgen receptor signaling in castration-resistant prostate cancer: a lesson in persistence. *Endocrine-Related Cancer*, *23*(12), T179-T197. doi: 10.1530/erc-16-0422

[11] Schalken, J., & Fitzpatrick, J. (2015). Enzalutamide: targeting the androgen signalling pathway in metastatic castration-resistant prostate cancer. *BJU International*, *117*(2), 215-225. doi: 10.1111/bju.13123

[12] Vander Ark, A., Cao, J., & Li, X. (2018). Mechanisms and Approaches for Overcoming Enzalutamide Resistance in Prostate Cancer. *Frontiers In Oncology*, *8*. doi: 10.3389/fonc.2018.00180

[13] Hemmings, B., & Restuccia, D. (2012). PI3K-PKB/Akt Pathway. *Cold Spring Harbor Perspectives In Biology*, *4*(9), a011189-a011189. doi: 10.1101/cshperspect.a011189

[14] Durrant, T., & Hers, I. (2020). PI3K inhibitors in thrombosis and cardiovascular disease. *Clinical And Translational Medicine*, *9*(1). doi: 10.1186/s40169-020-0261-6

[15] Thorpe, L., Yuzugullu, H., & Zhao, J. (2014). PI3K in cancer: divergent roles of isoforms, modes of activation and therapeutic targeting. *Nature Reviews Cancer*, *15*(1), 7-24. doi: 10.1038/nrc3860

[16] Lien, E. C., Dibble, C. C., & Toker, A. (2017). PI3K signaling in cancer: beyond AKT. *Current opinion in cell biology*, *45*, 62–71. https://doi.org/10.1016/j.ceb.2017.02.007
[17] Yang, J., Nie, J., Ma, X., Wei, Y., Peng, Y., & Wei, X. (2019). Targeting PI3K in cancer: mechanisms and advances in clinical trials. *Molecular Cancer*, *18*(1). doi: 10.1186/s12943-019-0954-x
[18] Fruman, D., Chiu, H., Hopkins, B., Bagrodia, S., Cantley, L., & Abraham, R. (2017). The PI3K Pathway in Human Disease. *Cell*, *170*(4), 605-635. doi: 10.1016/j.cell.2017.07.029
[19] Meng, Y., Wang, W., Kang, J., Wang, X., & Sun, L. (2017). Role of the PI3K/AKT signalling pathway in apoptotic cell death in the cerebral cortex of streptozotocin-induced diabetic rats. *Experimental And Therapeutic Medicine*, *13*(5), 2417-2422. doi: 10.3892/etm.2017.4259
[20] Lee, Y., Chen, M., & Pandolfi, P. (2018). The functions and regulation of the PTEN tumour suppressor: new modes and prospects. *Nature Reviews Molecular Cell Biology*, *19*(9), 547-562. doi: 10.1038/s41580-018-0015-0
[21] Milella, M., Falcone, I., Conciatori, F., Cesta Incani, U., Del Curatolo, A., & Inzerilli, N. et al. (2015). PTEN: Multiple Functions in Human Malignant Tumors. *Frontiers In Oncology*, *5*. doi: 10.3389/fonc.2015.00024
[22] Cantley, L., & Neel, B. (1999). New insights into tumor suppression: PTEN suppresses tumor formation by restraining the phosphoinositide 3-kinase/AKT pathway. *Proceedings Of The National Academy Of Sciences*, *96*(8), 4240-4245. doi: 10.1073/pnas.96.8.4240
[23] Lee, J., Yang, H., Georgescu, M., Di Cristofano, A., Maehama, T., & Shi, Y. et al. (1999). Crystal Structure of the PTEN Tumor Suppressor. *Cell*, *99*(3), 323-334. doi: 10.1016/s0092-8674(00)81663-3
[24] Carracedo, A., & Pandolfi, P. (2008). The PTEN–PI3K pathway: of feedbacks and cross-talks. *Oncogene*, *27*(41), 5527-5541. doi: 10.1038/onc.2008.247
[25] LESLIE, N., & DOWNES, C. (2004). PTEN function: how normal cells control it and tumour cells lose it. *Biochemical Journal*, *382*(1), 1-11. doi: 10.1042/bj20040825
[26] Bazzichetto, C., Conciatori, F., Pallocca, M., Falcone, I., Fanciulli, M., & Cognetti, F. et al. (2019). PTEN as a Prognostic/Predictive Biomarker in Cancer: An Unfulfilled Promise?. *Cancers*, *11*(4), 435. doi: 10.3390/cancers11040435
[27] Yehia, L., Keel, E., & Eng, C. (2020). The Clinical Spectrum of PTEN Mutations. *Annual Review Of Medicine*, *71*(1), 103-116. doi: 10.1146/annurev-med-052218-125823
[28] Yin, Y., & Shen, W. (2008). PTEN: a new guardian of the genome. *Oncogene*, *27*(41), 5443-5453. doi: 10.1038/onc.2008.241
[29] Dragoo, D., Taher, A., Wong, V., Elsaiey, A., Consul, N., & Mahmoud, H. et al. (2021). PTEN Hamartoma Tumor Syndrome/Cowden Syndrome: Genomics, Oncogenesis, and Imaging Review for Associated Lesions and Malignancy. *Cancers*, *13*(13), 3120. doi: 10.3390/cancers13133120

[30] Papa, A., Wan, L., Bonora, M., Salmena, L., Song, M., & Hobbs, R. et al. (2014). Cancer-Associated PTEN Mutants Act in a Dominant-Negative Manner to Suppress PTEN Protein Function. *Cell*, *157*(3), 595-610. doi: 10.1016/j.cell.2014.03.027
[31] Faubert, B., Solmonson, A., & DeBerardinis, R. (2020). Metabolic reprogramming and cancer progression. *Science*, *368*(6487). doi: 10.1126/science.aaw5473
[32] Liberti, M., & Locasale, J. (2016). The Warburg Effect: How Does it Benefit Cancer Cells?. *Trends In Biochemical Sciences*, *41*(3), 211-218. doi: 10.1016/j.tibs.2015.12.001
[33] Hoxhaj, G., & Manning, B. (2019). The PI3K–AKT network at the interface of oncogenic signalling and cancer metabolism. *Nature Reviews Cancer*, *20*(2), 74-88. doi: 10.1038/s41568-019-0216-7
[34] Chen, C., Chen, J., He, L., & Stiles, B. (2018). PTEN: Tumor Suppressor and Metabolic Regulator. *Frontiers In Endocrinology*, *9*. doi: 10.3389/fendo.2018.00338
[35] Aquila, S., Santoro, M., Caputo, A., Panno, M., Pezzi, V., & De Amicis, F. (2020). The Tumor Suppressor PTEN as Molecular Switch Node Regulating Cell Metabolism and Autophagy: Implications in Immune System and Tumor Microenvironment. *Cells*, *9*(7), 1725. doi: 10.3390/cells9071725
[36] Wang, L., Xiong, H., Wu, F., Zhang, Y., Wang, J., & Zhao, L. et al. (2014). Hexokinase 2-Mediated Warburg Effect Is Required for PTEN- and p53-Deficiency-Driven Prostate Cancer Growth. *Cell Reports*, *8*(5), 1461-1474. doi: 10.1016/j.celrep.2014.07.053
[37] Fusco, N., Sajjadi, E., Venetis, K., Gaudioso, G., Lopez, G., & Corti, C. et al. (2020). PTEN Alterations and Their Role in Cancer Management: Are We Making Headway on Precision Medicine?. *Genes*, *11*(7), 719. doi: 10.3390/genes11070719
[38] Zhou, X., Yang, X., Sun, X., Xu, X., Li, X., & Guo, Y. et al. (2019). Effect of PTEN loss on metabolic reprogramming in prostate cancer cells. *Oncology Letters*. doi: 10.3892/ol.2019.9932
[39] Garcia-Cao, I., Song, M., Hobbs, R., Laurent, G., Giorgi, C., & de Boer, V. et al. (2012). Systemic Elevation of PTEN Induces a Tumor-Suppressive Metabolic State. *Cell*, *149*(1), 49-62. doi: 10.1016/j.cell.2012.02.030
[40] Hannun, Y., & Obeid, L. (2008). Principles of bioactive lipid signalling: lessons from sphingolipids. *Nature Reviews Molecular Cell Biology*, *9*(2), 139-150. doi: 10.1038/nrm2329
[41] Ogretmen, B. (2017). Sphingolipid metabolism in cancer signalling and therapy. *Nature Reviews Cancer*, *18*(1), 33-50. doi: 10.1038/nrc.2017.96
[42] Hanada, K. (2003). Serine palmitoyltransferase, a key enzyme of sphingolipid metabolism. *Biochimica Et Biophysica Acta (BBA) - Molecular And Cell Biology Of Lipids*, *1632*(1-3), 16-30. doi: 10.1016/s1388-1981(03)00059-3
[43] Pralhada Rao, R., Vaidyanathan, N., Rengasamy, M., Mammen Oommen, A., Somaiya, N., & Jagannath, M. (2013). Sphingolipid Metabolic Pathway: An Overview of Major Roles Played in Human Diseases. *Journal Of Lipids*, *2013*, 1-12. doi: 10.1155/2013/178910

[44] Rao, R., & Acharya, J. (2008). Sphingolipids and membrane biology as determined from genetic models. *Prostaglandins &Amp; Other Lipid Mediators*, *85*(1-2), 1-16. doi: 10.1016/j.prostaglandins.2007.10.002
[45] Wigger, D., Gulbins, E., Kleuser, B., & Schumacher, F. (2019). Monitoring the Sphingolipid de novo Synthesis by Stable-Isotope Labeling and Liquid Chromatography-Mass Spectrometry. *Frontiers In Cell And Developmental Biology*, *7*. doi: 10.3389/fcell.2019.00210
[46] Ponnusamy, S., Meyers-Needham, M., Senkal, C., Saddoughi, S., Sentelle, D., & Selvam, S. et al. (2010). Sphingolipids and cancer: ceramide and sphingosine-1-phosphate in the regulation of cell death and drug resistance. *Future Oncology*, *6*(10), 1603-1624. doi: 10.2217/fon.10.116
[47] Hannun, Y., & Obeid, L. (2017). Sphingolipids and their metabolism in physiology and disease. *Nature Reviews Molecular Cell Biology*, *19*(3), 175-191. doi: 10.1038/nrm.2017.107
[48] Morad, S., Levin, J., Shanmugavelandy, S., Kester, M., Fabrias, G., Bedia, C., & Cabot, M. (2012). Ceramide–Antiestrogen Nanoliposomal Combinations—Novel Impact of Hormonal Therapy in Hormone-Insensitive Breast Cancer. *Molecular Cancer Therapeutics*, *11*(11), 2352-2361. doi: 10.1158/1535-7163.mct-12-0594
[49] Guenther, G., Peralta, E., Rosales, K., Wong, S., Siskind, L., & Edinger, A. (2008). Ceramide starves cells to death by downregulating nutrient transporter proteins. *Proceedings Of The National Academy Of Sciences*, *105*(45), 17402-17407. doi: 10.1073/pnas.0802781105
[50] Rutherford, C., Childs, S., Ohotski, J., McGlynn, L., Riddick, M., & MacFarlane, S. et al. (2013). Regulation of cell survival by sphingosine-1-phosphate receptor S1P1 via reciprocal ERK-dependent suppression of Bim and PI-3-kinase/protein kinase C-mediated upregulation of Mcl-1. *Cell Death &Amp; Disease*, *4*(11), e927-e927. doi: 10.1038/cddis.2013.455
[51] Van Brocklyn, J. (2010). Regulation of cancer cell migration and invasion by sphingosine-1-phosphate. *World Journal Of Biological Chemistry*, *1*(10), 307. doi: 10.4331/wjbc.v1.i10.307
[52] Voelkel-Johnson, C., Norris, J., & White-Gilbertson, S. (2018). Interdiction of Sphingolipid Metabolism Revisited: Focus on Prostate Cancer. *Advances In Cancer Research*, 265-293. doi: 10.1016/bs.acr.2018.04.014
[53] Costa-Pinheiro, P., Heher, A., Raymond, M., Jividen, K., Shaw, J., & Paschal, B. et al. (2020). Role of SPTSSB-Regulated de Novo Sphingolipid Synthesis in Prostate Cancer Depends on Androgen Receptor Signaling. *Iscience*, *23*(12), 101855. doi: 10.1016/j.isci.2020.101855
[54] Ryland, L., Fox, T., Liu, X., Loughran, T., & Kester, M. (2011). Dysregulation of sphingolipid metabolism in cancer. *Cancer Biology &Amp; Therapy*, *11*(2), 138-149. doi: 10.4161/cbt.11.2.14624
[55] Cerqueira, N., Oliveira, E., Gesto, D., Santos-Martins, D., Moreira, C., & Moorthy, H. et al. (2016). Cholesterol Biosynthesis: A Mechanistic Overview. *Biochemistry*, *55*(39), 5483-5506. doi: 10.1021/acs.biochem.6b00342
[56] Ikonen, E. (2008). Cellular cholesterol trafficking and compartmentalization. *Nature Reviews Molecular Cell Biology*, *9*(2), 125-138. doi: 10.1038/nrm2336

[57] Möbius, W., Van Donselaar, E., Ohno-Iwashita, Y., Shimada, Y., Heijnen, H., Slot, J., & Geuze, H. (2003). Recycling Compartments and the Internal Vesicles of Multivesicular Bodies Harbor Most of the Cholesterol Found in the Endocytic Pathway. *Traffic*, *4*(4), 222-231. doi: 10.1034/j.1600-0854.2003.00072.x
[58] Huang, B., Song, B., & Xu, C. (2020). Cholesterol metabolism in cancer: mechanisms and therapeutic opportunities. *Nature Metabolism*, *2*(2), 132-141. doi: 10.1038/s42255-020-0174-0
[59] Berndt, N., Hamilton, A., & Sebti, S. (2011). Targeting protein prenylation for cancer therapy. *Nature Reviews Cancer*, *11*(11), 775-791. doi: 10.1038/nrc3151
[60] Finlay-Schultz, J., & Sartorius, C. (2015). Steroid Hormones, Steroid Receptors, and Breast Cancer Stem Cells. *Journal Of Mammary Gland Biology And Neoplasia*, *20*(1-2), 39-50. doi: 10.1007/s10911-015-9340-5
[61] Chimento, A., Casaburi, I., Avena, P., Trotta, F., De Luca, A., & Rago, V. et al. (2019). Cholesterol and Its Metabolites in Tumor Growth: Therapeutic Potential of Statins in Cancer Treatment. *Frontiers In Endocrinology*, *9*. doi: 10.3389/fendo.2018.00807
[62] Cruz, P., Mo, H., McConathy, W., Sabnis, N., & Lacko, A. (2013). The role of cholesterol metabolism and cholesterol transport in carcinogenesis: a review of scientific findings, relevant to future cancer therapeutics. *Frontiers In Pharmacology*, *4*. doi: 10.3389/fphar.2013.00119
[63] Brown, M., Radhakrishnan, A., & Goldstein, J. (2018). Retrospective on Cholesterol Homeostasis: The Central Role of Scap. *Annual Review Of Biochemistry*, *87*(1), 783-807. doi: 10.1146/annurev-biochem-062917-011852
[64] Theesfeld, C., Pourmand, D., Davis, T., Garza, R., & Hampton, R. (2011). The Sterol-sensing Domain (SSD) Directly Mediates Signal-regulated Endoplasmic Reticulum-associated Degradation (ERAD) of 3-Hydroxy-3-methylglutaryl (HMG)-CoA Reductase Isozyme Hmg2. *Journal Of Biological Chemistry*, *286*(30), 26298-26307. doi: 10.1074/jbc.m111.244798
[65] Krycer, J., & Brown, A. (2013). Cholesterol accumulation in prostate cancer: A classic observation from a modern perspective. *Biochimica Et Biophysica Acta (BBA) - Reviews On Cancer*, *1835*(2), 219-229. doi: 10.1016/j.bbcan.2013.01.002
[66] Xue, L., Qi, H., Zhang, H., Ding, L., Huang, Q., & Zhao, D. et al. (2020). Targeting SREBP-2-Regulated Mevalonate Metabolism for Cancer Therapy. *Frontiers In Oncology*, *10*. doi: 10.3389/fonc.2020.01510
[67] Longo, J., Mullen, P., Yu, R., van Leeuwen, J., Masoomian, M., & Woon, D. et al. (2019). An actionable sterol-regulated feedback loop modulates statin sensitivity in prostate cancer. *Molecular Metabolism*, *25*, 119-130. doi: 10.1016/j.molmet.2019.04.003
[68] Yue, S., Li, J., Lee, S., Lee, H., Shao, T., & Song, B. et al. (2014). Cholesteryl Ester Accumulation Induced by PTEN Loss and PI3K/AKT Activation Underlies Human Prostate Cancer Aggressiveness. *Cell Metabolism*, *19*(3), 393-406. doi: 10.1016/j.cmet.2014.01.019
[69] T. Das, A., Tenenbaum, L., & Berkhout, B. (2016). Tet-On Systems For Doxycycline-inducible Gene Expression. *Current Gene Therapy*, *16*(3), 156-167. doi: 10.2174/1566523216666160524144041

[70] Várnai, P., & Balla, T. (1998). Visualization of Phosphoinositides That Bind Pleckstrin Homology Domains: Calcium- and Agonist-induced Dynamic Changes and Relationship to Myo-[3H]inositol-labeled Phosphoinositide Pools. *Journal Of Cell Biology*, *143*(2), 501-510. doi: 10.1083/jcb.143.2.501
[71] Law, S. H., Chan, M. L., Marathe, G. K., Parveen, F., Chen, C. H., & Ke, L. Y. (2019). An Updated Review of Lysophosphatidylcholine Metabolism in Human Diseases. *International journal of molecular sciences*, *20*(5), 1149. https://doi.org/10.3390/ijms20051149
[72] Britten, C., Garrett-Mayer, E., Chin, S., Shirai, K., Ogretmen, B., & Bentz, T. et al. (2017). A Phase I Study of ABC294640, a First-in-Class Sphingosine Kinase-2 Inhibitor, in Patients with Advanced Solid Tumors. *Clinical Cancer Research*, *23*(16), 4642-4650. doi: 10.1158/1078-0432.ccr-16-2363
[73] Scher, H., Beer, T., Higano, C., Anand, A., Taplin, M., & Efstathiou, E. et al. (2010). Antitumour activity of MDV3100 in castration-resistant prostate cancer: a phase 1–2 study. *The Lancet*, *375*(9724), 1437-1446. doi: 10.1016/s0140-6736(10)60172-9
[74] Mukherji, D., Pezaro, C., & De-Bono, J. (2012). MDV3100 for the treatment of prostate cancer. *Expert Opinion On Investigational Drugs*, *21*(2), 227-233. doi: 10.1517/13543784.2012.651125
[75] Doan, N., Alhajala, H., Al-Gizawiy, M., Mueller, W., Rand, S., & Connelly, J. et al. (2017). Acid ceramidase and its inhibitors: a de novo drug target and a new class of drugs for killing glioblastoma cancer stem cells with high efficiency. *Oncotarget*, *8*(68), 112662-112674. doi: 10.18632/oncotarget.22637
[76] French, K., Zhuang, Y., Maines, L., Gao, P., Wang, W., & Beljanski, V. et al. (2010). Pharmacology and Antitumor Activity of ABC294640, a Selective Inhibitor of Sphingosine Kinase-2. *Journal Of Pharmacology And Experimental Therapeutics*, *333*(1), 129-139. doi: 10.1124/jpet.109.163444
[77] Rawla, P. (2019). Epidemiology of Prostate Cancer. *World Journal Of Oncology*, *10*(2), 63-89. doi: 10.14740/wjon1191
[78] Chen, F., & Zhao, X. (2013). Prostate Cancer: Current Treatment and Prevention Strategies. *Iranian Red Crescent Medical Journal*, *15*(4), 279-284. doi: 10.5812/ircmj.6499
[79] Dai, C., Heemers, H., & Sharifi, N. (2017). Androgen Signaling in Prostate Cancer. *Cold Spring Harbor Perspectives In Medicine*, *7*(9), a030452. doi: 10.1101/cshperspect.a030452
[80] Phan, L., Yeung, S., & Lee, M. (2014). Cancer metabolic reprogramming: importance, main features, and potentials for precise targeted anti-cancer therapies. *Cancer Biology & Medicine*, *11*(1), 1.
[81] Figlia, G., Willnow, P., & Teleman, A. (2020). Metabolites Regulate Cell Signaling and Growth via Covalent Modification of Proteins. *Developmental Cell*, *54*(2), 156-170. doi: 10.1016/j.devcel.2020.06.036

[82] Mori, N., Wildes, F., Takagi, T., Glunde, K., & Bhujwalla, Z. (2016). The Tumor Microenvironment Modulates Choline and Lipid Metabolism. *Frontiers In Oncology*, *6*. doi: 10.3389/fonc.2016.00262
[83] Zhou, J., Tawk, M., Tiziano, F., Veillet, J., Bayes, M., & Nolent, F. et al. (2012). Spinal Muscular Atrophy Associated with Progressive Myoclonic Epilepsy Is Caused by Mutations in ASAH1. *The American Journal Of Human Genetics*, *91*(1), 5-14. doi: 10.1016/j.ajhg.2012.05.001
[84] Zhao, J., Zhao, Y., Wang, L., Zhang, J., Karnes, R., & Kohli, M. et al. (2016). Alterations of androgen receptor-regulated enhancer RNAs (eRNAs) contribute to enzalutamide resistance in castration-resistant prostate cancer. *Oncotarget*, *7*(25), 38551-38565. doi: 10.18632/oncotarget.9535
[85] Merseburger, A. S., Hammerer, P., Rozet, F., Roumeguère, T., Caffo, O., da Silva, F. C., & Alcaraz, A. (2015). Androgen deprivation therapy in castrate-resistant prostate cancer: how important is GnRH agonist backbone therapy?. *World journal of urology*, *33*(8), 1079–1085. https://doi.org/10.1007/s00345-014-1406-2
[86] Bhatia, K., Bhumika, & Das, A. (2020). Combinatorial drug therapy in cancer - New insights. *Life Sciences*, *258*, 118134. doi: 10.1016/j.lfs.2020.118134
[87] Melissaridou, S., Wiechec, E., Magan, M., Jain, M., Chung, M., Farnebo, L., & Roberg, K. (2019). The effect of 2D and 3D cell cultures on treatment response, EMT profile and stem cell features in head and neck cancer. *Cancer Cell International*, *19*(1). doi: 10.1186/s12935-019-0733-1
[88] Mills, I. Maintaining and reprogramming genomic androgen receptor activity in prostate cancer. *Nat Rev Cancer* **14,** 187–198 (2014). https://doi.org/10.1038/nrc3678
[89] Melissaridou, S., Wiechec, E., Magan, M., Jain, M. V., Chung, M. K., Farnebo, L., & Roberg, K. (2019). The effect of 2D and 3D cell cultures on treatment response, EMT profile and stem cell features in head and neck cancer. *Cancer cell international*, *19*, 16. https://doi.org/10.1186/s12935-019-0733-1
[90] HAO, Ji-qing; LI, Qi; XU, Shu-ping; SHEN, Yu-xian; SUN, Gen-yun Effect of lumiracoxib on proliferation and apoptosis of human nonsmall cell lung cancer cellsin vitro, Chinese Medical Journal: April 2008 - Volume 121 - Issue 7 - p 602-607
[91] Keppler-Noreuil, KM, Parker, VE, Darling, TN, Martinez-Agosto, JA. 2016. Somatic overgrowth disorders of the PI3K/AKT/mTOR pathway & therapeutic strategies. *Am J Med Genet Part C Semin Med Genet* 172C: 402– 421.

APPENDIX

Copyright permissions

SPRINGER NATURE LICENSE
TERMS AND CONDITIONS

Jun 11, 2022

This Agreement between Mr. Taha Bugra Güngül ("You") and Springer Nature ("Springer Nature") consists of your license details and the terms and conditions provided by Springer Nature and Copyright Clearance Center.

License Number	5325990988809
License date	Jun 11, 2022
Licensed Content Publisher	Springer Nature
Licensed Content Publication	Nature Reviews Cancer
Licensed Content Title	Maintaining and reprogramming genomic androgen receptor activity in prostate cancer
Licensed Content Author	Ian G. Mills
Licensed Content Date	Feb 24, 2014
Type of Use	Thesis/Dissertation
Requestor type	academic/university or research institute
Format	print and electronic
Portion	figures/tables/illustrations
Number of figures/tables/illustrations	1
High-res required	no

JOHN WILEY AND SONS LICENSE
TERMS AND CONDITIONS

Jun 11, 2022

This Agreement between Mr. Taha Bugra Güngül ("You") and John Wiley and Sons ("John Wiley and Sons") consists of your license details and the terms and conditions provided by John Wiley and Sons and Copyright Clearance Center.

License Number	5325980895572
License date	Jun 11, 2022
Licensed Content Publisher	John Wiley and Sons
Licensed Content Publication	American Journal of Medical Genetics Part A
Licensed Content Title	Somatic overgrowth disorders of the PI3K/AKT/mTOR pathway & therapeutic strategies
Licensed Content Author	Julian A. Martinez−Agosto, Thomas N. Darling, Victoria E.R. Parker, et al
Licensed Content Date	Nov 18, 2016
Licensed Content Volume	172
Licensed Content Issue	4
Licensed Content	20

SPRINGER NATURE LICENSE
TERMS AND CONDITIONS

Jun 11, 2022

This Agreement between Mr. Taha Bugra Güngül ("You") and Springer Nature ("Springer Nature") consists of your license details and the terms and conditions provided by Springer Nature and Copyright Clearance Center.

License Number	5325981110794
License date	Jun 11, 2022
Licensed Content Publisher	Springer Nature
Licensed Content Publication	Nature Reviews Molecular Cell Biology
Licensed Content Title	The functions and regulation of the PTEN tumour suppressor: new modes and prospects
Licensed Content Author	Yu-Ru Lee et al
Licensed Content Date	Jun 1, 2018
Type of Use	Thesis/Dissertation
Requestor type	academic/university or research institute
Format	print and electronic
Portion	figures/tables/illustrations
Number of figures/tables/illustrations	1
High-res required	no

SPRINGER NATURE LICENSE
TERMS AND CONDITIONS

Jun 11, 2022

This Agreement between Mr. Taha Bugra Güngül ("You") and Springer Nature ("Springer Nature") consists of your license details and the terms and conditions provided by Springer Nature and Copyright Clearance Center.

License Number	5325981331624
License date	Jun 11, 2022
Licensed Content Publisher	Springer Nature
Licensed Content Publication	Nature Reviews Cancer
Licensed Content Title	Sphingolipid metabolism in cancer signalling and therapy
Licensed Content Author	Besim Ogretmen
Licensed Content Date	Nov 17, 2017
Type of Use	Thesis/Dissertation
Requestor type	academic/university or research institute
Format	print and electronic
Portion	figures/tables/illustrations
Number of figures/tables/illustrations	1
High-res required	no

SPRINGER NATURE LICENSE
TERMS AND CONDITIONS

Jun 11, 2022

This Agreement between Mr. Taha Bugra Güngül ("You") and Springer Nature ("Springer Nature") consists of your license details and the terms and conditions provided by Springer Nature and Copyright Clearance Center.

License Number	5325990116550
License date	Jun 11, 2022
Licensed Content Publisher	Springer Nature
Licensed Content Publication	Nature Metabolism
Licensed Content Title	Cholesterol metabolism in cancer: mechanisms and therapeutic opportunities
Licensed Content Author	Binlu Huang et al
Licensed Content Date	Feb 10, 2020
Type of Use	Thesis/Dissertation
Requestor type	academic/university or research institute
Format	print and electronic
Portion	figures/tables/illustrations
Number of figures/tables/illustrations	1
Will you be translating?	no